KERNFORSCHUNGSANLAGE JÜLICH
GESELLSCHAFT MIT BESCHRÄNKTER HAFTUNG
Institut für Festkörperforschung

Dynamical Diffraction Theory

by

Peter H. Dederichs

Jül - 797 - FF
September 1971

Als Manuskript gedruckt

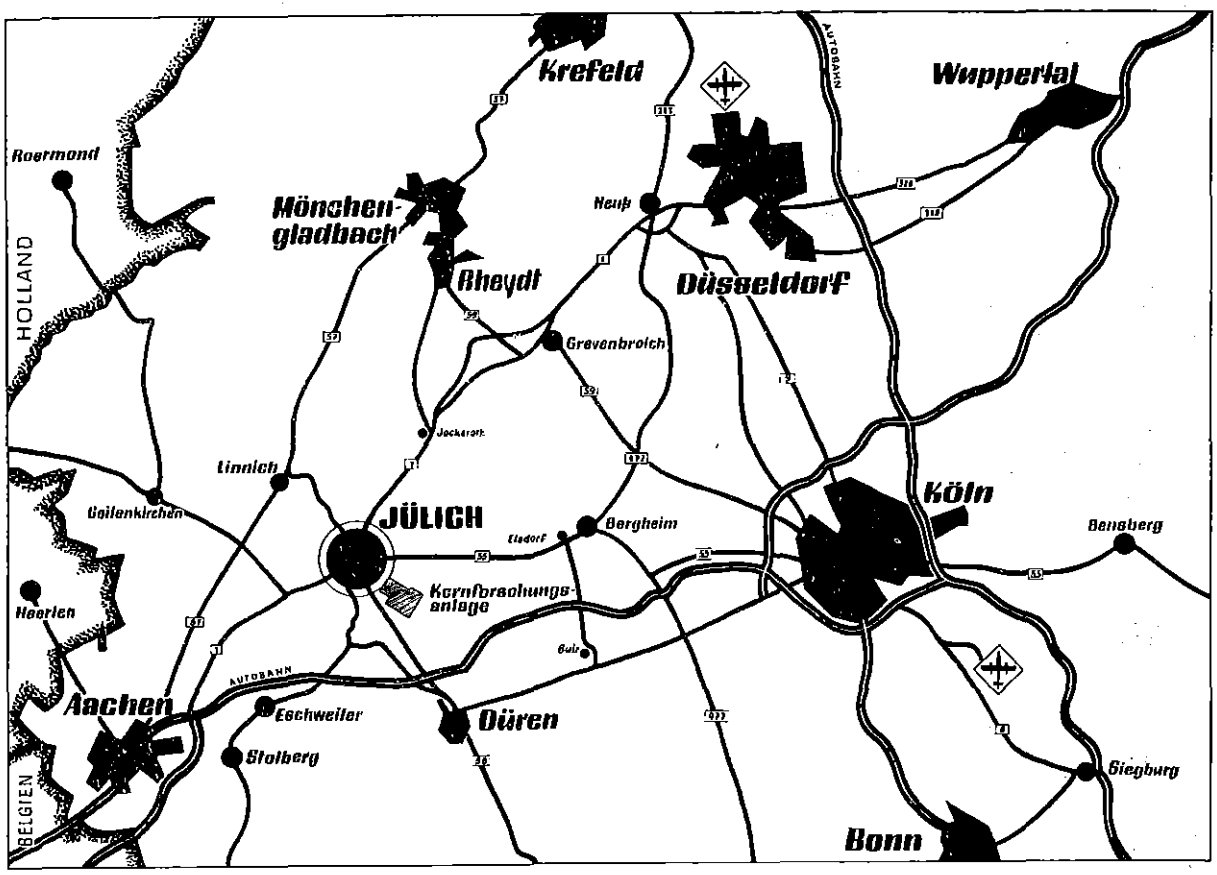

Berichte der Kernforschungsanlage Jülich – Nr. 797
Institut für Festkörperforschung Jül - 797 - FF

Dok.: Electron Diffraction - Theory
Neutron Diffraction - Theory
X-Ray Diffraction - Theory
Leed
Defects - Distribution, Statistical

Im Tausch zu beziehen durch: ZENTRALBIBLIOTHEK der Kernforschungsanlage Jülich GmbH,
Jülich, Bundesrepublik Deutschland

Dynamical Diffraction Theory

by

Peter H. Dederichs

Contents

1. Introduction

Two theories are widely used to describe the intensities observed in electron or X-ray diffraction by crystals. The "kinematical theory" treats the crystal as perturbation and is therefore valid only for sufficiently small crystals. For larger crystals one has to take into account the multiple scattering of the incident wave. This problem, which is simplified substantially by the periodicity of the crystal, has been dealt with first by Darwin in 1914 [1]. More fundamentally the problem has been treated in a series of papers by Ewald in 1917 [2] and later on by von Laue [3]. These papers form the basis of the so-called "dynamical theory", which has been extended further by Bethe [4] for the case of electron diffraction.

The dynamical theory for X-ray diffraction is summarized in the books of von Laue [5], Zachariasen [6] and James [7] as well as in two more recent review articles of Batterman and Cole [8] and James [9]. For electron diffraction we refer to the books of von Laue [10], Heidenreich [11] and Hirsch et al. [12].

In the last twenty years there has been a renewed and steadily increasing interest in dynamical diffraction of X-rays and electrons, which is due partly to the availability of large, perfect crystals and to the development of the electron microscope. New branches

have evolved, such as low-energy-electron-diffraction (LEED), channelling of high energy electrons and positrons or dynamical scattering of Moessbauer-quanta. Also the dynamical theory has made considerable progress. For instance starting with the papers of Molière [13] and Yoshioka [14], the theory for the elastic or "coherent" wave could be sufficiently generalized to take into account the effects of inelastic waves, thermal motion or statistical defects.

In this report we review the conventional form of the dynamical theory. We will emphasise not so much the two beam case or special wave fields or special applications of the theory, but present the basic principles in a self-contained way, including some new methods such as the band structure for complex wave vectors or the t-matrix method. Moreover we parallelly develope the theory for electron-, X-ray- and neutron-diffraction and discuss the similarities and differences. A condensed version of this report will be published as the first part of a review article in SOLID STATE PHYSICS. The second part of that review, being referred to as "Part II" in this report, deals with the theory of the coherent wave and the effects of inelastic waves, thermal motion, and statistically distributed defects, both for electron and X-ray diffraction.

Since this is a purely theoretical article, we will not give any long list of tables of atomic form factors, wavelengths etc. Nevertheless we feel obliged to give the reader, being not familiar with dynamical

diffraction, an idea of the order of magnitude of the most important quantities. Therefore the following table gives some typical values of the energy E, etc. for the cases of neutron-, X-ray-, electron-, and low-energy-electron-diffraction, being abreaviated by the symbols n, X, e and LEED. The most important quantity for diffraction is the extinction length, which is essentially the thickness of the crystal for which the kinematical theory breaks down. For neutrons and LEED, the extinction lengths differ by a factor 10^5, meaning that the dynamical theory is absolutely necessary for LEED, but that most experiments with neutrons and X-rays are well described by kinematical theory. For electrons and X-rays the absorption length $\frac{1}{\mu}$, given in the fourth line, is roughly a factor 10 larger than the extinction length. Here neutrons are an exception, since they are practically not absorbed. The last quantity $\frac{1}{\Delta\mu}$ is the absorption length for the case that a Bragg reflection is excited (anomalous transmission). For X-rays the absorption is then reduced by a factor $\approx$30, which is known as the Bormann effect, whereas the absorption of electrons is only slightly reduced.

	n	X	e	LEED
energy E	10 meV	10 keV	100 keV	100 eV
wave length λ	1 Å	1 Å	0.05 Å	1 Å
extinction length d_{ext}	10^5 Å	10^4 Å	10^2-10^3 Å	5 Å
absorption length $\frac{1}{\mu}$	10^8 Å	10^5 Å	10^3-10^4 Å	10 Å
$\frac{1}{\Delta\mu}$	$>10^8$ Å	$30 \cdot 10^5$ Å	$3 \cdot (10^3$-$10^4)$ Å	10 Å

2. Electrons in Periodic Potentials

In this section we will review the basic facts and theorems about the bandtheory of electrons in ideal crystals as far as they are important for diffraction. For more details we refer to the literature. [15]

2. 1. The Crystal Potential

The motion of the electron is described by the Schrödingerequation for the wavefunction ϕ:

$$(1) \quad H\phi = \left\{ -\frac{\hbar^2}{2m} \nabla_{\underline{r}}^2 + V(\underline{r}) \right\} \phi(\underline{r}) = E\,\phi(\underline{r})$$

where E is the energy and $V(\underline{r})$ the crystal potential. In an infinite periodic crystal the potential $V(\underline{r})$ is periodic, too. Therefore we have for all lattice vectors $\underline{R}$: $V(\underline{r}) = V(\underline{r} + \underline{R})$. Furthermore $V(\underline{r})$ can be split up into contributions from the different unit cells of the crystal. Therefore we have

$$(2) \quad V(\underline{r}) = V(\underline{r} + \underline{R}) = \sum_{\underline{R}} v(\underline{r} - \underline{R})$$

where $v(\underline{r})$, the potential of the Wigner-Seitz-cell, is directly connected with the charge distribution. For a primitive lattice we have:

$$(3) \quad v(\underline{r}) = -\frac{Ze^2}{r} + \int_{V_c} d\underline{r}' \, \frac{e^2 \varrho(\underline{r}')}{|\underline{r} - \underline{r}'|} \quad \text{with} \int_{V_c} d\underline{r}' \, \varrho(\underline{r}') = Z$$

The first term represents the attractive interaction with the nucleus of charge number Z, the second one the repulsive interaction with the electron density $\varrho(\underline{r})$ in the first cell (V_c = volume of the unitcell). Because of electric neutrality the volume integral of $\varrho(\underline{r})$ over one unit cell is equal to Z.

$V(\underline{r})$ can be expanded in a Fourier series.

$$(4) \qquad V(\underline{r}) = \sum_{\underline{h}} V_{\underline{h}} \, e^{i\underline{h}\underline{r}}$$

Due to the periodicity of $V(\underline{r})$ we have to sum only over reciprocal lattice vectors $\underline{h}$ because only these vectors fulfill the periodicity condition $e^{i\underline{h}\underline{R}} = 1$ for all $\underline{R}$. By considering

$$(5) \qquad \frac{1}{V_c} \int_{V_c} d\underline{r} \, e^{i(\underline{h} - \underline{h}')\underline{r}} = \delta_{\underline{h},\underline{h}'}$$

we get for $V_{\underline{h}}$

$$(6) \qquad V_{\underline{h}} = \frac{1}{V_c} \int_{V_c} e^{-i\underline{h}\underline{r}} V(\underline{r}) d\underline{r} = \frac{1}{V_c} \int_{-\infty}^{+\infty} e^{-i\underline{h}\underline{r}} v(\underline{r}) d\underline{r}$$

where we have used equ. (5) and transformed the sum over the different unit cells into an integral over the whole space. Substituting (3) into (6) we get finally

$$(7) \qquad V_{\underline{h}} = -\frac{4\pi e^2}{V_c} \frac{1}{h^2} (Z - f_{\underline{h}}) \quad \text{with}$$

$$f_{\underline{h}} = \int_{V_c} d\underline{r} \, e^{-i\underline{h}\underline{r}} \, \varrho(\underline{r})$$

Here $f_{\underline{h}}$ is the "atomic scattering factor for X-rays", being smaller than or equal to $f_o = Z$ for all $\underline{h}$. Therefore all coefficients $V_{\underline{h}}$ are negative. For large $\underline{h}$ only the first term, i.e. the interaction with the nucleus, remains. For small $\underline{h}$, $V_{\underline{h}}$ approaches a constant. By expanding $e^{i\underline{h}\underline{r}}$ in (7) in powers of $\underline{h}$, the first and second terms cancel ($\varrho(\underline{r}) = \varrho(-\underline{r})$) and the third one gives, assuming cubic symmetry or a radially symmetric charge

density

$$(8) \qquad V_o = -\frac{2\pi e^2 Z}{3V_c} \langle \underline{r}^2 \rangle \quad \text{with} \quad \langle \underline{r}^2 \rangle = \frac{1}{Z} \int_{V_c} d\underline{r}\, r^2\, \varrho(\underline{r})$$

As a simple analytic example we can calculate $V_{\underline{h}}$ for a free H-atom. Here we have

$$(9) \qquad \varrho(\underline{r}) = \frac{1}{\pi a_B^3} e^{-\frac{2r}{a_B}} \; ; \; v(\underline{r}) = -\frac{e^2}{r} e^{-\frac{2r}{a_B}} \left(1 + \frac{r}{a_B}\right)$$

$$(10) \qquad V_{\underline{h}} = -\frac{\pi e^2 a_B^2}{V_c} \cdot \frac{2 + \left(\frac{a_B h}{2}\right)^2}{\left\{1 + \left(\frac{a_B h}{2}\right)^2\right\}^2}$$

Whereas for small r the Coulomb attraction of the nucleus dominates, the potential $v(\underline{r})$ decreases exponentially for large r.
For many elements the coefficients $V_{\underline{h}}$, the scattering amplitudes for electrons, have been calculated numerically [12].
Due to the reality of $V(\underline{r})$ we obtain from (6)

$$(11) \qquad V_{\underline{h}} = V^*_{-\underline{h}}$$

Furthermore, if S is a symmetry operation of the lattice then we have $V(\underline{r}) = V(S\underline{r})$ and $S\underline{R}$ is again a lattice vector. Therefore we get for $V_{\underline{h}}$, since $\underline{r}\cdot\underline{h} = (S\underline{r})\cdot(S\underline{h})$

$$(12) \qquad V_{\underline{h}} = V_{S\underline{h}}$$

For instance, if S is the inversion ($S\underline{r} = -\underline{r}$), this means together with (11)

$$(13) \qquad V_{\underline{h}} = V_{-\underline{h}} = V^*_{\underline{h}}$$

The modifications for nonprimitive lattices are abvious. In this case the potentials $v(\underline{r})$ is a sum of the potentials $v_\mu(\underline{r} - \underline{R}^\mu)$ of the atoms μ at the positions $\underline{R}^\mu$ in the

first cell, Therefore we have for $V_{\underline{h}}$ instead of (7)

$$(14) \quad V_{\underline{h}} = - \frac{4\pi e^2}{V_c} \frac{1}{h^2} \cdot \sum_{\mu} \left(z_{\mu} - f_{\underline{h}}^{\mu} \right) e^{-i\underline{h}\underline{R}^{\mu}}$$

where $f_{\underline{h}}^{\mu}$ is the atomic scattering factor for X-rays of the atom μ.

2.2. Blochwaves

The periodicity of the potential has important consequences for the eigenfunctions ϕ and for the allowed eigenenergies. To see this we introduce the translation operator $T_{\underline{R}}$,which shifts every function $f(\underline{r})$ by a vector $\underline{R}$ being a lattice vector in the following.

$$(15) \quad T_{\underline{R}} \; f(\underline{r}) = f(\underline{r} + \underline{R}) \quad \text{with} \quad T_{\underline{R}} = e^{\underline{R} \cdot \nabla_{\underline{r}}} = e^{\frac{i}{\hbar} \underline{R} \cdot \underline{p}}$$

Due to this representation $T_{\underline{R}}$ commutes with the kinetic energy. But because of the periodicity, $T_{\underline{R}}$ also commutes with $V(\underline{r})$ and consequentlywith H.

$$(16) \quad T_{\underline{R}} \, V(\underline{r}) = V(\underline{r} + \underline{R}) \, T_{\underline{R}} = V(\underline{r}) \, T_{\underline{R}} \quad \text{or} \left[T_{\underline{R}} \, , H \right] = 0$$

Therefore the eigenfunctions $\phi \, (\underline{r})$ of H can be choosen so that they are simultaneously eigenfunctions of $T_{\underline{R}}$. By denoting $\hbar\underline{k}$ as the eigenvalues of the operator $\underline{p}$, the eigenvalues of $T_{\underline{R}}$ are $e^{i\underline{k}\underline{R}}$. Thus the simultaneous eigenfunction $\phi \, (\underline{r})$, indexed now by $\underline{k}$, obeys the equations

$$(17) \quad T_{\underline{R}} \, \phi_{\underline{k}}(\underline{r}) = e^{i\underline{k}\underline{R}} \, \phi_{\underline{k}}(\underline{r}) \quad \text{and} \quad H \, \phi_{\underline{k}}(\underline{r}) = E_{\underline{k}} \, \phi_{\underline{k}}(\underline{r})$$

Due to $e^{i\underline{h}\underline{R}} = 1$ one obtains the same eigenvalue $e^{i\underline{k}\underline{R}}$ if one replaces $\underline{k}$ by $\underline{k} + \underline{h}$. Therefore the index $\underline{k}$ is

only determined up to a reciprocal lattice vector and only the "reduced" value of $\underline{k}$ is important.For instance, $\underline{k}$ can be restricted to the first Brillouin-zone.
By making an ansatz of the form

$$(18) \quad \phi_{\underline{k}}(\underline{r}) = e^{i\underline{k}\underline{r}}\, u_{\underline{k}}(\underline{r})$$

one verifies directly by applying $T_{\underline{R}}$ on $\phi_{\underline{k}}$ that $u_{\underline{k}}(\underline{r})$ is a periodic function in $\underline{r}$.

$$(19) \quad u_{\underline{k}}(\underline{r}) = u_{\underline{k}}(\underline{r} + \underline{R})$$

Therefore $\phi_{\underline{k}}(\underline{r})$ is essentially a plane wave $e^{i\underline{k}\underline{r}}$ modulated by a periodic function $u(\underline{r})$ and is called a "Blochwave", whereas $u_{\underline{k}}(\underline{r})$ is often refered to as "Blochfunction".
Due to its periodicity $u_{\underline{k}}(\underline{r})$ can be expanded in plane waves $e^{i\underline{h}\underline{r}}$ analogously to (4). Therefore we have for $\phi_{\underline{k}}(\underline{r})$

$$(20) \quad \phi_{\underline{k}}(\underline{r}) = \sum_{\underline{h}} C_{\underline{h}}(\underline{k})\; e^{i(\underline{k} + \underline{h})\underline{r}}$$

The coefficents $C_{\underline{h}}$ can be determined by introducing (20) into the Schrödingerequation (1). Considering the orthogonality of the different plane waves $e^{i\underline{h}\underline{r}}$ (5), this results in an infinite system of linear homogeneous equations for the $C_{\underline{h}}(\underline{k})$.

$$(21) \quad \left\{ E_{\underline{k}} - \frac{\hbar^2}{2m} (\underline{k} + \underline{h})^2 \right\} C_{\underline{h}}(\underline{k}) = \sum_{\underline{h}'} V_{\underline{h}-\underline{h}'}\, C_{\underline{h}'}(\underline{k})$$

This system has only a solution, if its determinant vanishes.

$$(22) \quad \det \left\| \left\{ E_{\underline{k}} - \frac{\hbar^2}{2m} (\underline{k} + \underline{h})^2 \right\} \delta_{\underline{h},\underline{h}'} - V_{\underline{h} - \underline{h}'} \right\| = 0$$

For each $\underline{k}$ the determinant vanishes for an infinite number of energies $E_\nu(\underline{k})$ ($\nu = 1, 2, \ldots$) being compatible with $\underline{k}$. They can, for instance, be ordered according to their magnitude.

$$E_1(\underline{k}) \leq \ldots \leq E_\nu(\underline{k}) \leq E_{\nu+1}(\underline{k}) \leq \ldots$$

All the energies obtained for a given ν by varying $\underline{k}$ in the first Brillouin-zone are called the ν^{th} energy band. If $\underline{k}$ varies in a certain direction, we may get qualitatively the behaviour of E as a function of $\underline{k}$ as shown in fig. 1. The energy E_1, being lower than all energies of the first band, is forbidden. For $E = E_2$ we get just one $\underline{k}$ vector. Between the first and second band there is an energy gap so that E_3 is not allowed. For $E = E_4$ we have a band overlap. We get as solutions $\underline{k}$-vectors belonging to different bands.

The orthonormalization condition for the Bloch waves is

$$(23) \quad \int_{-\infty}^{+\infty} \frac{d\underline{r}}{(2\pi)^3} \; \phi^*_{\underline{k}',\nu'}(\underline{r}) \, \phi_{\underline{k},\nu}(\underline{r}) = \delta(\underline{k} - \underline{k}') \, \delta_{\nu,\nu'}$$

for all $\underline{k}$ and $\underline{k}'$ in the first Brillouin zone. We have choosen the factor $(2\pi)^3$ to get the same condition as for plane waves.

By introducing the ansatz (18) into (23) we get for the Bloch functions

$$(24) \quad \frac{1}{V_c} \int_{V_c} d\underline{r} \; u^*_{\underline{k},\nu'}(\underline{r}) \, u_{\underline{k},\nu}(\underline{r}) = \delta_{\nu,\nu'}$$

where we have taken into account that

$$(25)\qquad \sum_{\underline{R}} e^{i(\underline{k}-\underline{k}')\underline{R}} = \frac{(2\pi)^3}{V_c}\cdot\delta(\underline{k}-\underline{k}')$$

for $\underline{k},\underline{k}'$ in 1. Br.zone.

Analogously we get for the coefficients $C_{\underline{h}}(\underline{k},\nu)$ using (5)

$$(26)\qquad \sum_{\underline{h}} C^{*}_{\underline{h}}(\underline{k},\nu')\, C_{\underline{h}}(\underline{k},\nu) = \delta_{\nu,\nu'}$$

The system of Blochwaves is also complete,

$$(27)\qquad \sum_{\nu}\int \frac{d\underline{k}}{(2\pi)^3}\, \phi^{*}_{\underline{k},\nu}(\underline{r}')\, \phi_{\underline{k},\nu}(\underline{r}) = \delta(\underline{r}-\underline{r}')$$

yielding for the coefficients $C_{\underline{h}}$

$$(28)\qquad \sum_{\nu} C^{*}_{\underline{h}'}(\underline{k},\nu)\, C_{\underline{h}}(\underline{k},\nu) = \delta_{\underline{h},\underline{h}'}$$

The equations (26) and (28) mean that the matrix $M_{\nu,\underline{h}} = c_{\underline{h}}(\underline{k},\nu)$ is unitary ($M^{-1} = M^{+}$). M represents just the transformation from all the planes waves $e^{i(\underline{k}+\underline{h})\underline{r}}$ with the same reduced $\underline{k}$-vector to the Blochwaves $\phi_{\underline{k},\nu}$ with the same $\underline{k}$, as can be seen from equation (20).

An important quantity is the current density of a Blochwave, being periodically in space because of the translation properties of $\phi_{\underline{k},\nu}$

$$(29)\qquad \underline{j}_{\underline{k},\nu}(\underline{r}) = \frac{\hbar}{2mi}\left\{\phi^{*}_{\underline{k},\nu}(\underline{r})\,\partial_{\underline{r}}\,\phi_{\underline{k},\nu}(\underline{r}) - \phi_{\underline{k},\nu}\,\partial_{\underline{r}}\,\phi^{*}_{\underline{k},\nu}\right\}$$

$$= \underline{j}_{\underline{k},\nu}(\underline{r}+\underline{R})$$

Using the plane-wave-expansion (20) and averaging over a

unit cell, we obtain for the average current density by using equ. (5):

$$(30)\qquad \left\langle j_{\underline{k},\nu}(\underline{r}) \right\rangle_{V_c} = \frac{\hbar}{m} \sum_{\underline{h}} (\underline{k} + \underline{h}) \left| C_{\underline{h}} \right|^2$$

Therefore the currents of the different plane waves add incoherently. This result can be simplified further by using the Schroedinger equation (21) for the $C_{\underline{h}}$. Multiplying (21) by $C^*_{\underline{h}}(\underline{k},\nu)$, summing over $\underline{h}$ and differentiating with respect to $\underline{hk}$, one gets

$$(31)\qquad \sum_{\underline{h}} \left\{ \frac{1}{\hbar} \frac{\partial E}{\partial \underline{k}} - \frac{\hbar}{m} (\underline{k} + \underline{h}) \right\} \left| C_{\underline{h}} \right|^2$$
$$+ \sum_{\underline{h}} \left\{ \left(E - \frac{\hbar^2}{2m} (\underline{k} + \underline{h})^2 \right) C_{\underline{h}} - \sum_{\underline{h}'} V_{\underline{h}} - \underline{h}', C_{\underline{h}'} \right\} \frac{1}{\hbar} \partial_{\underline{k}} C^*_{\underline{h}}$$
$$+ \sum_{\underline{h}'} \left\{ \left(E - \frac{\hbar^2}{2m} (\underline{k} + \underline{h})^2 \right) C^*_{\underline{h}'} - \sum_{\underline{h}} V_{\underline{h}} - \underline{h}', C^*_{\underline{h}} \right\} \frac{1}{\hbar} \partial_{\underline{k}} C_{\underline{h}'} = 0$$

Obviously the second line vanishes and by considering equ. (11) the third one, too. Further according to (26) we have $\sum_{\underline{h}} \left| C_{\underline{h}} \right|^2 = 1$ and so we get

$$(32)\qquad \left\langle j_{\underline{k},\nu}(\underline{r}) \right\rangle_{V_c} = \frac{1}{\hbar} \frac{\partial E_\nu(\underline{k})}{\partial \underline{k}}$$

Therefore the current is always perpendicular to the two dimensional surfaces $E_\nu(\underline{k})$ = constant, which are called dispersion surfaces.

2.3. Complex $\underline{k}$, E and Symmetries of $E_\nu(\underline{k})$

Up to here we have tacitly assumed, that the eigenvalues $\underline{k}$ and E are real. However this has not necessarily to be so, because the determinant (22) has formal solutions also for complex $\underline{k}$ and E. For instance, the eigensolutions $\phi_{\underline{k}}$ for complex $\underline{k}$ are damped waves, decreasing in one direction and increasing in the opposite. But

they are also eigenfunctions of $T_{\underline{R}}$ and H as (17); the only, but very important difference is that the scalar product (23) diverges due to the exponential increase.

In an infinite ideal crystal and for stationary problems such eigenfunctions for complex $\underline{k}$ and E are only of pathological interest, since all the Blochfunctions for real $\underline{k}$ and E form already a complete set (27). However scattering of electrons by a finite crystal produces "damped" Blochwaves (with real E) quite naturally, as will be seen in section 3. Furthermore for a finite crystal there are no divergence difficulties for the scalar product because the volume of integration is finite. Similary by considering time dependent problems, e. g. initial value problems, complex E's can occur as decay constants. Therefore in the following we will allow E and $\underline{k}$ to have complex values and will consider the symmetries of the function $E_\nu(\underline{k})$ in the complex E,$\underline{k}$ space.

First we see from the determinant (22) after replacing $\underline{k}$ by $\underline{k}+\underline{h}"$ and then introducing $\underline{h}+\underline{h}"$ and $\underline{h}'+\underline{h}"$ as new summation indices, that for $\underline{k}+\underline{h}$ we have the same manifold of allowed energies $E_1, E_2, \ldots$ as for the Bloch vector $\underline{k}$. Therefore we obtain

$$(33) \quad E_\gamma(\underline{k}) = E_\gamma(\underline{k}+\underline{h})$$

as long as $\underline{k}$ and $\underline{k}+\underline{h}$ refer to the same band (i.e. belong to the same Riemann's sheet; see below)

Because the Blochwaves $\underline{k}$ and $\underline{k} + \underline{h}$ also have the same eigenvalue $e^{i\underline{k}\underline{R}}$ for the translationoperator $T_{\underline{R}}$, they can be choosen as periodic in $\underline{k}$.

$$(34) \quad \phi_{\underline{k},\nu}(\underline{r}) = \phi_{\underline{k}+\underline{h},\nu}(\underline{r})$$

Further if S is a symmetry operation of the crystal, then we have $V(\underline{r}) = V(S\underline{r})$ and together with $\underline{h}$ also $S\underline{h}$

is a reciprocal lattice vector. Using (12) and by substituting in (22) $S\underline{h}$ and $S\underline{h}'$ as new summation indices, we get the same manifold of solutions E_γ for the wave vectors $\underline{k}$ and $S\underline{k}$, so that

$$(35) \quad E_\gamma(\underline{k}) = E_\gamma(S\underline{k})$$

if $\underline{k}$ and $S\underline{k}$ belong to the same band. Therefore E has the same symmetry as the potential.
Especially for the inversion this means:

$$(35a) \quad E_\nu(\underline{k}) = E_\nu(-\underline{k})$$

A special consequence of the inversion symmetry is that for $\underline{k} \to 0$ we get

$$(35b) \quad \left.\frac{\partial E_\nu(\underline{k})}{\partial \underline{k}}\right|_{\underline{k} \to 0} = 0$$

On the other hand, if there is a reflection symmetry around a plane, then we have for all $\underline{k}$ on this plane

$$(35c) \quad \underline{n} \cdot \frac{\partial E_\nu(\underline{k})}{\partial \underline{k}} = 0$$

where $\underline{n}$ is perpendicular to the plane.

Further, since $V(\underline{r})$ is a local potential, the matrix-element of $V(\underline{r})$ in the determinant depends only on the difference $\underline{h} - \underline{h}'$. Because the first term in (22) is symmetrical in $\underline{h}$ and $\underline{h}'$ one has

$$(36) \quad E_\nu(\underline{k}) = E_\nu(-\underline{k})$$

independent of the existence of the inversion as a symmetry operation, as one sees by interchanging $\underline{h}$ and $\underline{h}'$ in (22).

Due to the reality of $V(\underline{r})$ we obtained in (12) $V_{\underline{h}} = V^{*}_{-\underline{h}}$. Therefore by forming the complex conjugate of the determinant we must have

$$(37) \quad E(\underline{k}) = E^{*}(\underline{k}^{*})$$

where $E(\underline{k})$ and $E^{*}(\underline{k}^{*})$ will refer to the same band ν mostly, but not necessarily. This result is important for the subsequent discussion.

Combining the symmetry relations (35), (36) and (37) we have

$$(38) \quad E_{\nu}(\underline{k}) = E_{\nu}(S\underline{k}) = E_{\nu}(-\underline{k}) = E^{*}_{\nu}(\underline{k}^{*})$$

From the following identities for the eigenvalues of the translationoperator $T_{\underline{R}}$

$$(39) \quad e^{i\underline{k}\underline{R}} = e^{i(S\underline{k})(S\underline{R})} = e^{i(-\underline{k})(-\underline{R})} = \left(e^{-i\underline{k}^{*}\underline{R}}\right)^{*}$$

we see that in the absence of degeneracies the corresponding Blochwaves are equal apart from phasefactors.

$$(40) \quad \phi_{\underline{k},\nu}(\underline{r}) = \lambda \cdot \phi_{S\underline{k},\nu}(S\underline{r}) = \lambda' \cdot \phi_{-\underline{k},\nu}(-\underline{r}) = \lambda'' \cdot \phi^{*}_{\underline{k}^{*},\nu}(-\underline{r})$$

For special choices of the phasefactors we refer to the literature [15] .

So far we only considered purely elastic scattering by the potential $V(\underline{r})$ of section 2.1. However this is a poor approach because inelastic effects often are very important and cannot be neglected. In part II of this review we will see that some of the effects of inelastic scattering can be taken into account in a relatively simple way by considering only the coherent wave. For this coherent wave inelastic effects lead to an apparent absorption, which can be described by a socalled "optical potential". However this "optical potential"

is no longer such a simple potential as $V(\underline{r})$ of section 2.1., as will be discussed in detail in part II. For instance, it is a nonlocal potential, i. e. an integral operator

$$(41) \quad U\,\phi(\underline{r}) = \int d\underline{r}'\, U(\underline{r},\underline{r}')\,\phi(\underline{r}') \qquad *)$$

Moreover, it es nonhermitian: $U \neq U^{\dagger}$. Most important, however, is the fact that in an infinite crystal the optical potential U is periodic.

$$(42) \quad U(\underline{r},\underline{r}') = U(\underline{r} + \underline{R},\ \underline{r}' + \underline{R})$$

Therefore Bloch's theorem and the equation (15) - (22) of section 2.2.remain valid. For instance, for the dispersion condition(22) we get for such a potential

$$(43) \quad \det \left\| \left\{ E - \frac{\hbar^2}{2m} (\underline{k} + \underline{h})^2 \right\} \delta_{\underline{h},\underline{h}'} - U_{\underline{k} + \underline{h},\ \underline{k} + \underline{h}'} \right\| = 0$$

with

$$(44) \quad U_{\underline{k} + \underline{h},\underline{k} + \underline{h}'} = \frac{1}{V_c} \int_{V_c} d\underline{r} \int_{-\infty}^{\infty} d\underline{r}' e^{-i(\underline{k} + \underline{h})\underline{r}} \cdot U(\underline{r},\underline{r}')\, e^{i(\underline{k} + \underline{h}')\underline{r}'}$$

The regions of integration for $\underline{r}$ and $\underline{r}'$ can also be interchanged due to the periodicity of U.

Now we will discuss the symmetries of $E_\nu(\underline{k})$ for the optical potential U.First we note, that the periodicity of $E_\nu(\underline{k})$ (33) and $\phi_{\underline{k},\nu}(\underline{r})$ (34) in $\underline{k}$ space remains because this is a direct consequence of the periodicity of the potential. Similarly the symmetry (35) due to symmetry operations S does not change either. However,

---

*) It is interesting to see, that a nonlocal potential $U(\underline{r},\underline{r}')$ can always be represented by a local, but "velocity" dependent potential

$$V(\underline{r},\underline{p}) = \int d\underline{R}\, U(\underline{r},\underline{r} + \underline{R})\, e^{\frac{i}{\hbar}\underline{p}\cdot\underline{R}}$$

Here $\underline{p} = \frac{\hbar}{i} \partial_{\underline{r}}$ is the impulsoperator, and $e^{\frac{i}{\hbar}\underline{p}\underline{R}}$ is the translation operator for a translation $\underline{R}$.

the relations (36) and (37) will change.

According to (44) we get the following identities for the matrixelements of U

$$(45) \qquad U_{\underline{k}+\underline{h},\underline{k}+\underline{h}'} = (\hat{U})_{-\underline{k}-\underline{h}',-\underline{k}-\underline{h}} = (U^{\dagger})_{\underline{k}+\underline{h}',\underline{k}+\underline{h}}$$

where $\hat{U}$ is the transpose of U and $U^{\dagger}$ the hermitian adjoint. Making the anologous substitutions as in (36) (37) we get a relation connecting the band structure of the potentials U, $\hat{U}$ and $U^{\dagger}$:

$$(46) \qquad E^{\{U\}}_{\nu}(\underline{k}) = E^{\{\hat{U}\}}_{\nu}(-\underline{k}) = \left\{ E^{\{U^{\dagger}\}}_{\nu}(\underline{k}^*) \right\}^*$$

For the special cases that $U = \hat{U}$ or $U = U^{\dagger}$ we get symmetry relations for $E_{\nu}(\underline{k})$

$$(47a) \qquad E_{\nu}(\underline{k}) = E_{\nu}(-\underline{k}) \quad \text{for} \quad U = \hat{U}$$

$$(47b) \qquad E_{\nu}(\underline{k}) = E^*_{\nu}(\underline{k}^*) \quad \text{for} \quad U = U^{\dagger}$$

$$(47c) \qquad E_{\nu}(\underline{k}) = E^*_{\nu}(-\underline{k}^*) \quad \text{for} \quad U^{\dagger} = \hat{U} \quad (U(\underline{r},\underline{r}') \text{ real}) \quad *)$$

These relations are in agreement with the special relations (36) (37) for local potential. For instance, equ. (36) immediately follows from (47a) because a local potential $V(\underline{r})$ is always symmetric as can be seen by writing it in the nonlocal form $V(\underline{r})\,\delta(\underline{r} - \underline{r}')$. Similarly equ. (37) follows from (47b) because a local, but hermitian potential is real. As is shown in part II, the optical potential $U(\underline{r},\underline{r}')$ is symmetrical. Therefore the inversion symmetry $E_{\nu}(\underline{k}) = E_{\nu}(-\underline{k})$ is always valid.

The Bloch waves for complex $\underline{k}$ will in general be no more orthogonal as (23), simply because these integrals

*) A real potential $U(\underline{r},\underline{r}')$ is invariant with respect to time inversion. Note however that the optical potential is not real.

diverge for complex $\underline{k}$. However, one can still give an orthogonality relation for the eigenfunctions ϕ of U and $U^\dagger$ for the same $\underline{k}$-vectors by the following identity:

$$(48)\quad 0 = \left(\phi^{\{U^\dagger\}}_{\underline{k}^*,\nu'} , H\, \phi^{\{U\}}_{\underline{k},\nu} \right) - \left(H^\dagger \phi^{\{U^\dagger\}}_{\underline{k}^*,\nu'} , \phi^{\{U\}}_{\underline{k},\nu} \right)$$
$$= \left(E^{\{U\}}_{\nu}(\underline{k}) - \left(E^{\{U^\dagger\}}_{\nu'}(\underline{k}^*) \right)^* \right) \left(\phi^{\{U^\dagger\}}_{\underline{k}^*,\nu'} , \phi^{\{U\}}_{\underline{k},\nu} \right)$$

Due to (46) the scalar product has to vanish for $\nu \neq \nu'$. Therefore we get for the Blochfunction $u_{\underline{k},\nu}(\underline{r})$ (the exponential factors $e^{i\underline{k}\underline{r}}$ in (48) cancel each other so that there is no divergence!):

$$(49)\quad \frac{1}{V_c} \int_{V_c} d\underline{r}\; u^{*\{U^\dagger\}}_{\underline{k}^*,\nu'}(\underline{r})\, u^{\{U\}}_{\underline{k},\nu}(\underline{r}) = \delta_{\nu,\nu'}$$

This is a generalization of (24) for nonhermitian potentials and complex $\underline{k}$. Especially for hermitian potentials but complex $\underline{k}$ we have

$$(50)\quad \frac{1}{V_c} \int_{V_c} d\underline{r}\; u^{*}_{\underline{k}^*,\nu'}(\underline{r})\; u_{\underline{k},\nu}(\underline{r}) = \delta_{\nu,\nu'}$$

Thus one can see, that due to these orthogonality relations and due to the divergence of the scalar product for different $\underline{k}$ and $\underline{k}'$ one has to be somewhat careful by operating with "damped" Blochwaves. However, many relations and methods familiar from "normal" Blochwaves can be used for damped ones as well.

2.4. Bandstructure for Complex k (one dimension).

For the scattering of electrons by a crystal, the energy E is real, of course. For the representation of the wave function in the crystal we therefore need only

those Blochwaves which, wether oscillating or damped, all have the same given energy E, as will be discussed in section 3 in detail.

Moreover we consider only the scattering at crystals being infinite in two directions (x and y) and limited in the other (z), i.e. we consider only the scattering by a crystal filling the half space $z \geq 0$ or by a crystal slab filling the space with $0 \leq z \leq t$. For these crystals the periodicity of the crystal potential in x and y direction is not perturbed by the crystal surfaces because the potential in the vacuum $V(\underline{r}) = 0$ fulfills every periodicity condition. Therefore the potential in the whole space has the x-y periodicity of the crystal potential. Accordingly, the x-y components $\underline{\tilde{k}}$ of the incident plane wave $\underline{K} = (\underline{\tilde{k}}, K_z)$ are good quantum numbers, meaning that all allowed Blochwaves in the crystal must have the same reduced x-y-component $\underline{\tilde{k}}$, which is also real.

Therefore only the z-component k_z of the Blochvector $\underline{k} = (\underline{\tilde{k}}, k_z)$ can be complex and we are interested in the band structure $E_\nu(k_z)$ as a complex function E of the complex z-component k_z, with $\underline{k}_{x,y} = \underline{\tilde{k}}$ being given and real. Especially we have to know those complex k_z values being compatible with real energies $E_\nu(k_z)$. These k_z values ly on lines in the two dimensional k_z-plane named "real lines" by Heine [16] . On his work the following section is based.

First we want to discuss the <u>one dimensional band structure.</u> We start with the symmetry relations for $E_\nu(k)$ which are for a local and real potential according to (36) (37) (33) :

$$(51) \quad E(k) = E(-k) = E^*(k^*) = E\left(k + n\frac{2\pi}{a}\right)$$

for $n = 0, \pm 1, \pm 2, \ldots$

One sees immediately that for $k = k^*$ we have $E_\nu(k) = E^*_\nu(k)$, i.e. the real axis $k = k^*$ is a real line $E = E^*$. Moreover the lines $k = n\frac{\pi}{a} + ik''$ with real k'' can be real lines, too, being perpendicular to the real axis. For we get from (51)

$$(52) \quad E\left(n\tfrac{\pi}{a} + ik''\right) = E\left(-n\tfrac{\pi}{a} - ik''\right) = E^*\left(-n\tfrac{\pi}{a} + ik''\right) = E^*\left(n\tfrac{\pi}{a} + ik''\right)$$

Therefore E is either real, if the energies on both sides refer to the same band $\left(E_\nu(n\,\pi/a + ik'') = E^*_\nu\right)$, or there are two bands with complex conjugate energies $\left(E_\nu(n\,\pi/a + ik'') = E^*_{\nu'}(n\,\pi/a + ik'')\right)$.

As will be shown later, these are already all the real lines in the one dimensional case, namely the real axis, the imaginary axis and the Brillouin-zone boundary $k = \pm\frac{\pi}{a} + ik''$. Further we have on these lines $E_\nu(k) = E_\nu(-k) = E_\nu(k^*)$. Therefore the whole band structure is specularly symmetrical with respect to the real and the imaginary axis.

The Schroedinger equation in one dimension with a periodic potential $V(x) = V(x + a)$ is an ordinary second order differential equation having two linear independent solutions for each energy. From this it follows simply that the function $\mu(E) = \cos ka$ is an entire function of the complex variable E as has been shown by Kohn [17] Hence the inverse $E(\mu)$ of the entire function $\mu(E)$ is an analytic function of μ except where $d\mu/dE = 0$. In the vicinity of such a point μ_μ we have

$$\mu = \mu_\mu + \frac{1}{2}\mu''_\mu (E - E)^2 \quad \text{or} \quad E = E_\mu + \sqrt{\frac{2}{\mu''_\mu}(\mu - \mu_\mu)}$$

As a function of k this means

$$(53) \qquad E = E_\nu + c\sqrt{(k - k_\nu)}$$

Therefore E is an analytic function of k in the whole k plane with the exception of the branch points k_ν.

Above we have seen that the real axis also is a real line and that at the points $k_o = n\frac{\pi}{a}$ real lines leave the real axis going into the complex plane. At what points k_o on the real axis can this occur generally? In order to see this we expand E(k) and $E(k^*)$ in the vicinity of k_o.

$$(54) \qquad E(k) = E(k_o) + E'(k_o)\delta k + \tfrac{1}{2}E''(k_o)(\delta k)^2 + \cdots$$

$$\text{with} \qquad \delta k = k - k_o$$

$$E(k^*) = E(k_o) + E'(k_o)\delta k^* + \tfrac{1}{2}E''(k_o)(\delta k^*)^2 + \ldots$$

Because for a real line we have $E(k) = E(k^*)$ and because k should be complex we find

$$(55) \qquad E'(k_o) = 0 \qquad \text{and} \qquad \delta k = i\delta k'' \quad \text{with real } \delta k''$$

Therefore real lines can leave the real axis only at extrema of $E_\nu(k)$ and only at right angles (Fig. 2). Moreover such an extremum k_o is a saddle point, i.e. either a maximum on the real axis $\left((\delta k)^2 \geq 0\right)$ and a minimum on the perpendicular real line with $(\delta k)^2 = -(\delta k'')^2 \leq 0$ or vice versa.

In the one dimensional case we have extrema at the

positions $k_o = 0$ and $k_o = \pm \pi/a$ (or $n\pi/a$) which follows directly from $E_\nu(k) = E_\nu(-k)$ and $E_\nu(\frac{\pi}{a} + k) = E_\nu(\frac{\pi}{a} - k)$. No other extrema can occur because this would automatically lead to more than two linear independent solutions, which is a contradiction. (Fig. 3) Moreover the real lines, leaving the real axis at $k_o = n\frac{\pi}{a}$, are straight lines, as has been shown by (52).

The behaviour of the real lines in the vicinity of a saddlepoint also can be studied by the following contour integral around a contour $\mathcal{L}$ surrounding k_o close enough to include no branch point (Fig.2, [16]). By a well known theorem we have

$$(56) \qquad I = \int_{\mathcal{L}} dk \, \frac{d}{dk}\{\ln f(k)\} = 2\pi i (Z - P)$$

where Z and P are the number of zeros and poles, respectively, enclosed by the contour and counted according to their multiplicity. Putting $f(k) = E(k) - E(k_o)$ we have due to the saddle point at k_o: $Z = 2$ and $P = 0$ and consequently

$$(57) \qquad I = 4\pi i = \left\{ \ln|E(k)-E(k_o)| + i\arg\{E(k)-E(k_o)\} \right\}_{\mathcal{L}}$$

Here the bracket with the index $\mathcal{L}$ means the change of the bracket by going around the contour. Because the ln gives no contribution, the argument of $E(k) - E(k_o)$ increases from 0 to 4π on going around the contour. Therefore, there are four points k on the contour with real E(k), namely the k values belonging to $\arg[E(k)-E(k_o)] = 0, \pi, 2\pi$ and 3π which are the crossing points of the real lines with the contour $\mathcal{L}$ (points A, B, C, D in Fig 2). From this simple theorem it follows directly that real lines cannot simply terminate.

For we get the result $I = 4\pi i$ for every closed contour surrounding k_o. For the same reason they cannot branch. Moreover the energy varies monotonically along the real line exept at the saddle points k_o, because every point with $\frac{dE}{dk} = 0$ has to be a crossing point of real lines (56).

Because the argument (56) (57) holds always as long the contour $\mathcal{C}$ does not enclose a branch point k_μ, there are only two possibilities for the real line in the complex plane (line BD in Fig. 2). Either it reaches a branch point k_μ or it does not. If it reaches a branch point then it behaves in the vicinity of k_μ as (53), namely the real line runs around the branch point into another Riemann sheet of the complex k plane, from where it will loop back to the real axis, running on the same line in k-space, but on the other edge of the branch cut in the next Riemann sheet. All along the energy varies monotonically until the next saddle point k_o' on the real axis in the next Riemann sheet is reached where the line crosses the real line on the real axis.

On the other hand, if the real line encloses no branch point, then the line has to run to infinity while the energy always varies monotonically. However, then the k-value gets extremely large :

$\left|\frac{h^2k^2}{2m}\right| \gg V(r)$ and the band structure can be calculated by neglecting V(r). But for free electrons we have

$$(58a) \quad E(k) = \left(k + n\frac{2\pi}{a}\right)^2 \frac{\hbar^2}{2m} \quad , n = 0, \pm 1, \pm 2, \ldots$$

Or with $k = k' + ik''$ and $-\frac{\pi}{a} < k' \leq \frac{\pi}{a}$ we obtain

$$(58b)\quad \frac{2m}{\hbar^2} E_\nu(k) = \left(k' + n\frac{2\pi}{a}\right)^2 + 2ik''\cdot\left(k' + n\frac{2\pi}{a}\right) - k''^2$$

and only get a real line for $k' = 0$ and $n = 0$. This is the imaginary axis along which E decreases to $-\infty$ for increasing $|k''|$. Therefore the imaginary axis is the only real line running to infinity, all other ones reach a branch point and loop back to the real axis.

Therefore in the one dimensional case we can summarize the result as follows. The whole band structure is specularly symmetric to the real and the imaginary axis. For large negative energies we have purely imaginary k values (Fig. 4 and 5, point A). By moving along the imaginary axis to $k = 0$ the energy increases to the lowest values of the first band (point B). Then moving along the real axis the energy, continuously increasing, assumes all the values of the first allowed band until one reaches the saddle point C at the Brillouin zone boundary. Here the real line again enters the complex plane and moves to the branch point k_1, the energy increasing to D. There the real line leaves the first Riemann sheet and moves in the second one back from k_1 to the real axis, where the energy reaches the bottom of the second band (point E). From here on the energy assumes all the values of the second allowed energy band, whereas the real lines run to $k = 0$ in the second sheet (F). By going around the branch point k_2 (G) we get into the third Riemann sheet and to the third band on the real axis (H), etc.

2.5. Band Structure for Complex $\underline{k}$ (3 dimensions and $V \neq V^{\dagger}$)

For the three dimensional case many results of the one dimensional band structure remain valid. First we want to define the appropriate basis vectors of the lattice for the scattering at a given crystal surface lying in the x-y plane. We choose the two shortest (non-parallel) translation vectors $\underline{a}_1$ and $\underline{a}_2$ in the crystal surface. Then the total potential in the crystal and in the vacuum is invariant under a surface translation $\underline{R}^{\underline{n}} = n_1\underline{a}_1 + n_2\underline{a}_2$. Further the third basis vector $\underline{a}_3$ is perpendicular to both $\underline{a}_1$ and $\underline{a}_2$ and gives the shortest periodicity in z-direction. As an example we have plotted in Fig. 6 the basis vectors $\underline{a}_1$ $\underline{a}_2$ and $\underline{a}_3$ for the (100) surface of a f.c.c. crystal. This is a non-primitive description of a primitive lattice, with each unit cell containing two atoms. Analogously $\underline{b}_1$ and $\underline{b}_2$ are the reciprocal lattice vectors of the surface net, lying in the x-y plane, and $\underline{b}_3$ points in z-direction.

Then according to the last section the reduced x-y component $\underline{\kappa}$ (in the surface mesh $(\underline{b}_1 , \underline{b}_2)$) of the Blochvector $\underline{k} = (\underline{\kappa}, k_z)$ is determined by the incident plane wave and real. Assuming the surface plane to be a reflection plane, we have for the energy $E(\underline{\kappa}, k_z)$ as a function of k_z for a given real $\underline{\kappa}$ the following symmetries:

$$(59) \qquad E(k_z) = E(-k_z) = E^{*}(k_z^{*}) = E(k_z + n\frac{\pi}{a_3})$$

Therefore the real axis $k_z = k_z^{*}$ is again a real line. Further the whole bandstructure is specularly symmetrical with respect to the real and the imaginary axis. Blount[18] has shown that $E(k_z)$ is an analytic function of k_z everywhere in the complex plane with the exceptions of branch points of the type (53), which are the only

singularities. However, in disagreement to the one dimensional case extrema do not only occur at

$k_z = 0 \quad \text{or} \pm \frac{\pi}{a_3}$.

Analogously to (54) a real line can leave the real axis only at saddle points k_o and at right angles (Fig. 2). However, these real lines have not necessarily to be straight lines. They only are straight due to the inversion symmetry for $k_o = 0$ and $k_o = \pm \pi / a_3$. Further the real lines cannot terminate and cannot branch as can be shown by the Z-P-theorem (56) (57). In principle they can cross, for instance in k_o on the real axis. But a crossing point for complex k_z would be highly accidental. For according to (56) we have $\frac{\partial E}{\partial k_z} = 0$ at a crossing point. As Herring [19] points out this would be vanishingly probable because the slightest perturbation would destroy E being real and $\frac{\partial E}{\partial k} = 0$ at the same point(exept for the crossing points on the real axis, being a real line for symmetry reasons). Therefore along the real lines the energy varies monotonically, exept at the saddle points on the real axis.

Again there are only two possibilities for a real line leaving the real axis at a saddle point. Either it can enclose a branch point of the type (53), enters there into a new Riemann sheet and loops in this sheet back to another saddle point on the real axis coming so to the adjacent allowed energy band. Or it has to run to infinity with monotonically varying energy. Because the k_z vector on these lines gets arbitrarily large, the occurence of these lines can already be seen in the free electrons approximation. For each reciprocal lattice

vector $\underline{h} = (\underline{\varkappa}, h_z)$ with x-y component $\underline{\varkappa}$ we get

$$(60) \quad \frac{2m}{\hbar^2} E(k_z) = (\underline{k} + \underline{h})^2 = (\underline{\kappa} + \underline{\varkappa})^2 + (k_z + h_z)^2$$

$$= (\underline{\kappa} + \underline{\varkappa})^2 + (k_z' + h_z)^2 + 2ik_z''(k_z' + h_z') - k_z''^2$$

where we need only the section of the parabola $(k_z + h_z)^2$ which falls into the "first Brillouin zone" $-\frac{\pi}{a_3} < k_z' \leq \frac{\pi}{a_3}$. We see that for $k_z' = -h_z$ we get a real line running to $k_z'' \to \pm\infty$, i.e. we get a real line for all reciprocal lattice vectors $\underline{h}$ with $-\frac{\pi}{a_3} < h_z \leq \frac{\pi}{a_3}$. Therefore in three dimensions we get ∞^2 real lines running to infinity, contrary to the one dimensional case with one line only.

Qualitatively we have therefore a situation as shown in Fig. 7. We start with the parabola of $\underline{h}_{1,0} = (\underline{\varkappa}_1, 0)$ at the energy $\frac{\hbar^2}{2m}(\underline{\kappa} + \underline{\varkappa}_1)^2$. The reversed parabola $(\underline{\kappa} + \underline{\varkappa}_1)^2 - k_z''^2$ belonges to a real line running to infinity. If we add to this the parabolas belonging to the reciprocal lattice vectors $\underline{h}_{1,n} = (\underline{\varkappa}_1, n\frac{2\pi}{a_3})$ then we have a typical free electron bandstructure in one dimension. However, we have a lot of other parabolas in three dimensions, for instance the one of $\underline{h}_{2,0} = (\underline{\varkappa}_2, 0)$ and the sections of the parabolas $\underline{h}_{2,n} = (\underline{\varkappa}_2, n\frac{2\pi}{a})$ which again look like another typical one dimensional bandstructure with an additional real line going to infinity. Thus we had to superimpose an infinite number of one dimensional band-

structures with one real "infinite" line each.

Now by switching on the potential $V(\underline{r})$, the degeneracies at the crossing of the different parabolas is removed and the bands split up (Fig. 8). The extrema (saddle points!) on the adjacent bands are connected by a loop due to a real line going into the complex plane around a branch point. Whereas the real lines for $k' = 0$ and $k' = \pm \frac{\pi}{a}$ are straight lines for symmetry reasons, the "additional" real lines inside the Brillouin zone are not straight. Moreover one sees that for a given energy one gets only a finite number of "allowed" Blochwaves with real $\underline{k}$ (in Fig. 8 at most 4), but always an infinite number of "damped" Blochwaves with complex k_z. The whole bandstructure is symmetrical with respect to the real and imaginary axis.

Nonhermitian potentials: The basic assumptions for the foregoing discussion of the bandstructure are the symmetry relations (51), (59), especially the equation $E_\nu(k_z) = E_\nu^*(k_z^*)$ resulting in the real axis being a real line. However the optical potential is in general a nonhermitian potential, for which this symmetry relation is not valid. Instead we have the relation (46), namely $E_\nu^{\{U\}}(k_z) = \left(E_\nu^{\{U^\dagger\}}(k_z^*)\right)^*$. Consequently the real lines for the potential U and the ones for $U^\dagger$ lie symmetrically to each other with respect to the real axis, which is no more a real line (Fig. 9.)(exept again for $U = U^\dagger$, where both lines coincide on the real axis). Therefore all the general predictions for the band structure are no more valid. If however the optical potential is only weakly nonhermitian, we can study its band structure by means of perturbation theory, starting from a hermitian

potential, as will be done in the following.

Splitting the potential U up into an hermitian part U' and an antihermitian part iU"

$$(61) \quad U = U' + iU'' \text{ with } U' = \frac{U+U^\dagger}{2} = U'^\dagger; \; U'' = \frac{U-U^\dagger}{2i} = U''^\dagger$$

we treat U" as a perturbation. The eigenfunctions $\phi^{(o)}_{\underline{k},\nu}$ for hermitian potential U' are defined by

$$(62) \quad (H_o + U') \, \phi^{(o)}_{\underline{k},\nu} = E^{(o)}_\nu(\underline{k}) \, \phi^{(o)}_{\underline{k},\nu}$$

To obtain the Blochwave $\phi_{\underline{k},\nu}(\underline{r})$ for the potential U for a given energy E and a given x-y-component $\underline{\kappa}$ of $\underline{k} = \{\underline{\kappa}, k_z\}$ we make the ansatz for $\phi_{\underline{k},\nu}$:

$$(63) \quad \phi_{\underline{k},\nu}(\underline{r}) = \sum_{\nu'} C_{\nu'} \, \phi^{(o)}_{\underline{k},\nu'}(\underline{r})$$

This is really an ansatz for the Blochfunction $u_{\underline{k},\nu}$ in terms of the $u^{(o)}_{\underline{k},\nu'}$'s, building a complete system for real $\underline{k}$ (27,28).
Encouraged by the orthogonality (50), we assume also completeness for complex $\underline{k}$. Then we have for the coefficients C_ν

$$(64) \quad \left(E^{(o)}_\nu(\underline{k}) - E\right) C_\nu + i \sum_{\nu'} U''_{\nu\nu'}(\underline{k}) \, C_{\nu'} = 0$$

with

$$U''_{\nu\nu'}(\underline{k}) = \frac{1}{V_c} \int_{V_c} d\underline{r} \int_{-\infty}^{\infty} d\underline{r}' e^{-i\underline{k}\underline{r}} u^{(o)*}_{\underline{k}^*,\nu}(\underline{r}) \cdot U''(\underline{r},\underline{r}') u^{(o)}_{\underline{k},\nu'}(\underline{r}') e^{i\underline{k}\underline{r}'}$$

Now in 0^{th} order we have $E = E^{(o)}_\nu(\underline{k}_o)$ with $\underline{k}_o = (\underline{\kappa}, k_{oz})$; in first order $\underline{k} = \underline{k}_o + \delta\underline{k}$ is determined by

$$(65) \quad E^{(o)}_\nu(\underline{k}_o + \delta\underline{k}) - E^{(o)}_\nu(\underline{k}_o) = -i \, U''_{\nu\nu}(\underline{k}_o)$$

Expanding up to linear terms in $\delta\underline{k} = (0,\delta k_z)$ we get

$$(66) \qquad \delta k_z = - i \frac{U''_{\nu\nu}(\underline{k}_o)}{\frac{\partial E_\nu^{(0)}(\underline{k}_o)}{\partial k_{oz}}}$$

and by using the plane wave expansion (20)

$$(67) \qquad \delta k_z = - i \frac{1}{\frac{\partial E_\nu^{(0)}(\underline{k}_o)}{\partial k_{oz}}} \sum_{\underline{h},\underline{h}'} c_{\underline{h}}^*(\underline{k}_o^*,\nu)\, c_{\underline{h}'}(\underline{k}_o,\nu)\, U''_{\underline{h}-\underline{h}'}$$

where for a local potential $U''(\underline{r},\underline{r}') = U''(\underline{r})\ \delta(\underline{r}-\underline{r}')$ the coefficients $U''_{\underline{h}}$ are given by (6). It is interesting to see that δk_z is a periodic function of $\underline{k}_o$. Further for real $\underline{k}_o$ in the allowed energy bands δk_z is purely imaginary representing the absorption of the Blochwave. Moreover it is inversely proportional to the z-component of the group velocity which is plausible from a classical point of view. For $\frac{\partial E}{\partial k_{oz}} \approx 0$ equation (66) is no more valid and in (65) we have to take the quadratic terms in δk_z into account. Due to dispersion this leads to finite values of δk_z even at the extrema $\partial E / \partial k_{zo} = 0$ (instead of ∞ according to (66)).

$$(68) \qquad \delta k_z = \frac{1 \pm i}{\sqrt{2}} \left\{ \left| \frac{U''_{\nu\nu}(\underline{k}_o)}{\frac{1}{2} \frac{\partial^2 E(\underline{k}_o)}{\partial k_{oz}^2}} \right| \right\}^{1/2}$$

Therefore δk_z, being proportional to $\sqrt{U''}$ at the extrema, is especially large and the absorption is very effective at these points. For the wave function we get in first order:

$$(69)\quad \phi_{\underline{k},\nu}(\underline{r}) = e^{i(\underline{k}_o+\delta\underline{k})\underline{r}} \left\{ u_{\underline{k}_o+\delta\underline{k},\nu}(\underline{r}) + \right.$$

$$\left. + \sum_{\nu'\neq\nu} \frac{i\,U''_{\nu\nu'}(\underline{k}_o)}{E_\nu(\underline{k}_o)-E_{\nu'}(\underline{k}_o)}\, u^{(o)}_{\underline{k}_o,\nu'}(\underline{r}) \right\}$$

where the most important term for real $\underline{k}_o$ is the damping factor $e^{i\delta k_z z}$ (δk_z imaginary).

Near the branching points k_+ where the energies of different bands are equal one has to apply degenerate perturbation theory. The results are somewhat lengthy and will not be given here.

In Fig. 9 we have plotted the real lines for the nonhermitian potential U according to the present perturbation theory. For simplicity we have choosen the linear case. Further $U=\hat{U}$ is assumed to be symmetric, as it is always the case for the optical potential, leading to the inversion symmetry (47a) in the complex k_z-plane. The upper figure shows $E^{(o)}_\nu(k_o)$ in the expanded zone scheme, whereas the lower shows the real lines in the different sheets. The real lines of the potential $U^\dagger$ (dahed lines) are obtained from the real lines of U by reflection at the real axis. Further the crossing points disappeared, being very sensitive to the perturbation (68).

2.6 The Two Beam Case [5-12]

For electron diffraction the calculations of the Bloch waves and the band structures is simplified very much since the energy is much larger than the potential. Therefore one can apply perturbation theory. For $V(\underline{r}) = 0$, i.e. in the free

electron case, we get for the $C_{\underline{h}}$'s (21)

$$(70) \quad \left\{K^2 - (\underline{k}+\underline{h})^2\right\} C_{\underline{h}} = 0 \quad \text{with} \quad E = \frac{h^2}{2m} K^2$$

For given energy and given $\underline{k}$ the expression in brackets will in general not vanish for all $\underline{h}$ and there are no allowed waves. However for certain $\underline{k}$ it may happen that $K^2 = (\underline{k}+\underline{h})^2$ for one $\underline{h}$, say for $\underline{h} = 0$. Then $C_{\underline{h}} = \delta_{\underline{h},0}$ and the plane wave $e^{i\underline{k}\underline{r}}$ is allowed. For $V \neq 0$ equation (21) gives

$$(71) \quad \left\{ K_o^2 - (\underline{k}+\underline{h})^2 \right\} C_{\underline{h}} = \sum_{\underline{h}' (\neq \underline{h})} v_{\underline{h}-\underline{h}'} \, C_{\underline{h}'}$$

$$\text{with } v_{\underline{h}} = \frac{2m}{\hbar^2} V_{\underline{h}} \quad \text{and} \quad K_o^2 = K^2 - v_o = \frac{2m}{\hbar^2} (E - V_o)$$

Now if $V(\underline{r})$ is small, we get by introducing the plane wave ansatz $C_{\underline{h}} = \delta_{\underline{h},0}$ on the right side of (71) for

$$(72) \quad \underline{h} = 0: \quad (K_o^2 - \underline{k}^2) \, C_o \cong 0$$

$$\underline{h} \neq 0: \qquad C_{\underline{h}} \cong \frac{v_{\underline{h}}}{K_o^2 - (\underline{k}+\underline{h})^2}$$

For small $v_{\underline{h}}$ the denominator will normally be much larger than $v_{\underline{h}}$. Therefore all "secondary waves" $C_{\underline{h}}$ for $\underline{h} \neq 0$ are small and we have only <u>one</u> strong <u>beam</u> $\phi = e^{i\underline{k}\underline{r}}$ with a slightly renormalized $\underline{k}$-value.

However, if the condition $K^2 \cong (\underline{k}+\underline{h})^2$ is fulfilled not only for the "primary wave" $\underline{h} = 0$, but also for

other, secondary waves $\underline{h} \neq 0$, then these waves may also become strong and the perturbation theory (72) breaks down. Graphically this condition means that for certain $\underline{h}$ the vectors $\underline{k}+\underline{h}$ lie on or near the "Ewaldsphere" with radius K (Fig. 10). Because the energies $\frac{\hbar^2}{2m}\,\underline{k}^2$ and $\frac{\hbar^2}{2m}\,(\underline{k}+\underline{h})^2$ are nearly equal in these cases, we have to apply degenerate perturbation theory taking into account all strongly excited plane waves. In this section we restrict ourselves to the two beam case where only two plane waves $\underline{k}$ and $\underline{k}+\underline{h}$ are strong. For this we get from (71)

$$(73)\qquad (K_o^2 - \underline{k}^2)\; C_o = v_{-\underline{h}}\; C_{\underline{h}}$$

$$\left(K_o^2 - (\underline{k}+\underline{h})^2\right) C_{\underline{h}} = v_{\underline{h}}\; C_o$$

By setting the determinant equal to zero, we get the dispersion equation

$$(74)\qquad (K_o^2 - \underline{k}^2)\cdot(K_o^2 - (\underline{k}+\underline{h})^2) = v_{\underline{h}}\cdot v_{-\underline{h}}$$

The allowed $\underline{k}$ vectors for a given energy lie on a dispersion surface consisting of two branches (Fig. 11) For $v_{\underline{h}} = 0$ it degenerates into two spheres with radius K_o, one around the reciprocal lattice vector $\underline{h}$ and the other around the origin. For $v_{\underline{h}} \neq 0$ the spheres split up at the intersecting line, where the Bragg condition $\underline{k}^2 = (\underline{k}+\underline{h})^2$ is fulfilled, and the outer branch 2 completely surrounds the inner branch 1. Exactly in the Bragg condition we have for $\underline{k} = \underline{k}_B$: $\underline{k}_B^2 = (\underline{k}_B+\underline{h})^2$. Near the Bragg spot $\underline{k}_B$ we get from (74) by setting $\underline{k} = \underline{k}_B+\delta\underline{k}$ and neglecting 3rd and 4th order terms in $\delta\underline{k}$:

$$(75)\qquad 4\left(\underline{k}_B\cdot\delta\underline{k}\right)\left((\underline{k}_B+\underline{h})\cdot\delta\underline{k}\right) = v_{\underline{h}}\cdot v_{-\underline{h}}$$

Neglecting the higher order terms in $\delta\underline{k}$ for $v_{\underline{h}} = 0$ is equivalent to replacing the spheres in Fig. 11 by the tangential planes in the point $\underline{k}_B$ (Fig. 12). By decomposing the vectors in (75) in ξ and η components we get with $K_o \sin\theta_B = {}^{h}/_{2}$

$$(76) \qquad \delta k_\xi^2 - \delta k_\eta^2 \, tg^2\theta_B = \frac{|v_{\underline{h}}|^2}{4K_o^2 \cos^2\theta_B}$$

In this approximation the dispersion surfaces are hyperbolas, the asymptotes of which are the tangential planes of the spheres. The smallest separation of the two branches is

$$(77) \qquad \Delta k = \frac{|v_{\underline{h}}|}{K_o \cos\theta_B}$$

The distance $d_{ext} = \frac{2\pi}{\Delta k}$, over which the two Blochwaves on the opposite branches get a phase difference 2π, is called the extinction length.

From the quadratic equation we get for the energy as a function of $\underline{k}$

$$(78) \qquad \frac{2m}{\hbar^2} E(\underline{k}) - v_o = K_o^2 = \frac{1}{2}\left(\underline{k}^2 + (\underline{k}+\underline{h})^2\right) \pm$$

$$\pm \frac{1}{2}\sqrt{\left(\underline{k}^2 - (\underline{k}+\underline{h})^2\right)^2 + 4|v_{\underline{h}}|^2}$$

showing that for $\underline{k}^2 = (\underline{k}+\underline{h})^2$ there is a band gap of the width $\Delta E = 2|V_{\underline{h}}|$. For $\underline{k} = (k_\eta, 0, 0) \| \underline{h}$ we have plotted $E(k_\eta)$ according to (78) in Fig. 13a. For an energy E_1 below the band gap we get four k-values. For this energy the dispersion surface is represented by two nonintersecting spheres. This is shown in Fig. 13b, where the four $\underline{k}$-values $\|$ to $\underline{h}$ are marked by points.

For the energy E_2 in the bandgap the spheres have opened up (Fig. 13c) giving only two k-values in Fig. 13a, whereas for the energy E_3 above the bandgap we get the dispersion surface of Fig 11.

Introducing K_o^2 from (78) into equation (73) we get for the ratio

$$(79) \qquad \frac{C_{\underline{h}}(\underline{k})}{C_o(\underline{k})} = \text{sign}(v_{\underline{h}}) \cdot \left(W \pm \sqrt{1+W^2} \right)$$

$$\text{with} \quad W = \frac{(\underline{k} + \frac{\underline{h}}{2}) \cdot \underline{h}}{|v_{\underline{h}}|} = \frac{\delta \underline{k} \cdot \underline{h}}{|v_{\underline{h}}|}$$

Here and in the following as well as in (78) the upper sign refers to the inner branch 1, the lower to the outer branch 2. By normalizing the $C_{\underline{h}}$'s according to (26) we have

$$(80) \qquad C_o = \frac{1}{\sqrt{2}} \left(1 \mp \frac{W}{\sqrt{1+W^2}} \right)^{1/2}$$

$$C_{\underline{h}} = \mp \text{sign}(v_{\underline{h}}) \cdot \frac{1}{\sqrt{2}} \left(1 \pm \frac{W}{\sqrt{1+W^2}} \right)^{1/2}$$

For $|W| \to \infty$, i.e. if the Bragg condition is not fulfilled, we get for $\underline{k}$ vectors on the sphere around the origin: $C_o = 1$, $C_{\underline{h}} = 0$ and on the sphere around $\underline{h}$ $C_o = 0$ and $C_{\underline{h}} = \mp 1$ (Fig 11).

Exactly in the Bragg condition we have $W = 0$. The two Blochwaves $\phi_{\underline{k}}(\underline{r})$ are in this case

$$(81) \qquad \phi^{I}(\underline{r}) = \frac{1}{\sqrt{2}} e^{i\underline{k}\underline{r}} \left(1 + e^{i\underline{h}\underline{r}} \right) = \sqrt{2}\, e^{i(\underline{k} + \frac{\underline{h}}{2})\underline{r}} \cdot \cos\left(\frac{\underline{h}\cdot\underline{r}}{2}\right)$$

and

$$(82) \qquad \phi^{II}(\underline{r}) = -\sqrt{2}\, i\, e^{i(\underline{k}+\frac{\underline{h}}{2})\underline{r}} \sin\left(\frac{\underline{h}\cdot\underline{r}}{2}\right)$$

For $v_{\underline{h}} < 0$, which is always the case for electron diffraction, the Blochwave ϕ^{I} lies on the outer branch and ϕ^{II} on the inner one. This would be reversed for $v_{\underline{h}} > 0$ (x-ray diffraction!). Characteristic for both waves are the modulation functions $\cos(\frac{\underline{h}\cdot\underline{r}}{2})$ and $\sin(\frac{\underline{h}\cdot\underline{r}}{2})$. Therefore ϕ^{I} is always maximal at the atomic positions on the reflecting planes and vanishes in the middle between the planes (Fig. 14). Contrary, ϕ^{II} has nodal planes at the reflecting planes and is maximal between these planes. Whereas both waves have the same energy, the wave on the outer branch has more kinetic energy due to the fact that $\underline{k}$ and $\underline{k}+\underline{h}$ are larger than on the inner branch. This can also be seen at the form of the wave function ϕ^{I} and ϕ^{II}. E.g. the wave ϕ^{I}, being concentrated at the atomic positions, has a larger (but negative) potential energy than ϕ^{II}, and consequently a larger kinetic energy.

It is noteworthy that the Bloch functions on the different branches 1 and 2 of the dispersion surface, but for the same parameter W, are orthogonal and further we the following relations (see also section 2.8)

$$(83) \qquad c_o^1 c_o^2 + c_{\underline{h}}^1 c_{\underline{h}}^2 = 0 = c_o^1 c_{\underline{h}}^1 + c_o^2 c_{\underline{h}}^2$$

$$c_o^1 c_o^1 + c_o^2 c_o^2 = 1 = c_{\underline{h}}^1 c_{\underline{h}}^1 + c_{\underline{h}}^2 c_{\underline{h}}^2$$

According to (32) the average current is always perpendicular to the dispersion surface. In the two-beam case it is given by

$$(84) \quad \left\langle \underline{j}_{\underline{k}}(\underline{r}) \right\rangle_{V_c} = \frac{\hbar}{m}\left\{ \underline{k}_B + \underline{h}\,\frac{1}{2}\left(1 \pm \frac{W}{\sqrt{1+W^2}}\right)\right\}$$

In the vicinity of the Bragg condition the direction of the current changes by an angle of $2\,\Theta_B$, namely from the direction $\underline{k} \cong \underline{k}_B$ on the sphere around the origin to the direction $\underline{k}+\underline{h} \cong \underline{k}_B+\underline{h}$ on the sphere around $\underline{h}$ (Fig. 12).
Exactly in the Bragg condition (W = 0) the current is parallel to the reflecting planes.

For an absorbing crystal, i.e. for a nonhermitian potential, the $\underline{k}$-vectors are complex (see section 2.5.). It is clear already from Fig. 14 that the absorption of the Blochwaves ϕ^I and ϕ^{II} must be vastly different because the "absorption power" will be concentrated at the atoms. We get a higher than normal absorption for ϕ^I and an anomalously low absorption for the sin-waves ϕ^{II} representing the so-called "anomalous transmission" effect. Quantitatively we have from (67) by assuming a local imaginary potential $iU''(\underline{r})$ with coefficients $U''_{\underline{h}} = U''_{-\underline{h}}$

$$(85) \quad \delta k_z = -\frac{i}{\frac{\partial E}{\partial k_z}}\left(U''_o \pm \operatorname{sign}(v_{\underline{h}})\cdot U''_{\underline{h}}\,\frac{1}{\sqrt{1+W^2}}\right)$$

Here, as in section 2.4., the z-axis is perpendicular to the surface and $\frac{1}{\hbar}\frac{\partial E}{\partial k_z}$ is the z-component of (84). In the symmetrical Laue-case the reflecting planes are perpendicular to the surface, i.e. $\underline{h} = (h,k,0)$ and we get for the absorption $\mu(W) = 2|\delta k_z|$ of the waves I and II:

$$(86) \qquad \mu^{I,II}(W) = \mu_0 \pm \frac{1}{\sqrt{1+W^2}}\,\mu_{\underline{h}}$$

$$\text{with} \qquad \mu_0 = \frac{2mU''_0}{\hbar^2 K\cos\Theta} \quad ; \quad \mu_{\underline{h}} = \frac{2mU''_{\underline{h}}}{\hbar^2 K\cos\underline{\Theta}}$$

where μ_0 is the normal absorption coefficient of a plane wave. $\mu(W)$ is plotted in Fig. 15. For $|W| \gg 1$, i.e. outside the Bragg condition, we get the normal absorption μ_0 whereas in the Bragg condition the absorption of wave II is $\Delta\mu = \mu_0 - \mu_{\underline{h}}$. If the absorption is concentrated at the centers of the atoms, then $U''_0 = U''_{\underline{h}}$ and the absorption for wave field II vanishes This is plausible from Fig. 14 because the sin-function vanishes at the positions of the centers of the atom. By writing $U''(\underline{r})$ analogously to the real potential (2) as $U''(\underline{r}) = \sum_{\underline{R}} u''(\underline{r}-\underline{R})$ and by expanding $\mu_{\underline{h}}$ in powers of $\underline{h}$, we obtain for the anomalous absorption coefficient $\Delta\mu_{\underline{h}}$ assuming radial symmetry for $u''(\underline{r})$:

$$(87) \qquad \Delta\mu_{\underline{h}} = \mu_0 - \mu_{\underline{h}} \cong \mu_0 \frac{1}{6}\langle \underline{r}^2\rangle \underline{h}^2$$

$$\text{with} \qquad \langle \underline{r}^2\rangle = \frac{\int \underline{r}^2 u''(\underline{r})\,d\underline{r}}{\int u''(\underline{r})\,d\underline{r}}$$

Accordingly $\Delta\mu$ varies as $\underline{h}^2$ and is proportional to the 2nd moment of the imaginary potential of the atoms. However due to the large spatial extent of the outer orbitals, this is not a good approximation in electron diffraction, but X-ray diffraction only.

2. 7. Some Multiple Beam Cases

Multiple beam cases are very important in electron diffraction due to the strong interaction and the small wave length. However, unlike the two-beam case multiple-beam cases can no longer be solved analytically. For instance, to obtain the dispersion relation in the three-beam case, one has to solve a cubic equation. Nevertheless, some simple analytical results can be given for special multiple-beam cases, from which a number of properties can be derived.

First we will discuss qualitatively the effect of the socalled systematic reflections [20,12]. These are the secondary reflections $2\underline{h}$, $3\underline{h}$,... and $-\underline{h}$, $-2\underline{h}$,... lying on the same line as the reciprocal lattice point $\underline{h}$ corresponding to strong reflection $(\underline{k}+\underline{h})$ of the two-beam case (Fig. 16). Because the radius K_o of the Ewald sphere is appreciably larger than h, the reciprocal lattice points $n\underline{h}$ lie relatively close to the Ewald sphere and are always excited to some extent. At least qualitatively, their influence can be determined by perturbation theory [4].

Going back to the equation (71) for the $C_{\underline{h}}$, we assume that in addition to the two strong beams $\underline{k}$ and $\underline{k}+\underline{h}$ we have a number of weak beams $\underline{k}+\underline{g}$ with $\underline{g} \neq 0, \underline{h}$, for which we get approximately

$$(88) \qquad C_{\underline{g}} \cong \frac{1}{K_o^2 - (\underline{k}+\underline{g})^2} \left(v_{\underline{g}} C_o + v_{\underline{g}-\underline{h}} C_{\underline{h}} \right)$$

On the right side, we have neglected the coefficients $C_{\underline{g}'}$ of the other weak beams which are assumed to be small. Going back with this result into the exact equations for C_o and $C_{\underline{h}}$, we get the modified two beam equations

$$(89) \qquad \left(K^2 - v^B_{o,o} - \underline{k}^2 \right) C_o = v^B_{o,h} C_{\underline{h}}$$

$$\left(K^2 - v^B_{\underline{h},\underline{h}} - (\underline{k}+\underline{h})^2 \right) C_{\underline{h}} = v^B_{\underline{h},o} C_o$$

where the coefficients $v^B_{\underline{h},\underline{h}'}$, named Bethe potentials, are given by

$$(90) \qquad v^B_{\underline{h},\underline{h}'} = v_{\underline{h}-\underline{h}'} + \sum_{\underline{g}(\neq o,\underline{h})} \frac{v_{\underline{h}-\underline{g}} \, v_{\underline{g}-\underline{h}}}{K_o^2 - (\underline{k}+\underline{g})^2}$$

It is seen that the reciprocal lattice points $\underline{g}$ lying inside the Ewald sphere $(K_o^2 > (\underline{k}+\underline{g})^2)$ give rise to a repulsive potential correction wheras the outer ones give an attractive contribution.

Applying this to the systematic reflections $\underline{g} = n\underline{h}(n = 2,3,\ldots,-1,-2,\ldots)$ of a low order reflection $\underline{h}$, we get for $v_{\underline{h}} = v_{-\underline{h}}$: $v^B_{\underline{h},\underline{h}} = v^B_{o,o}$ and $v^B_{\underline{h},o} = v^B_{o,\underline{h}}$. Further we replace $\underline{k}$ in (90) by the vector $\underline{k}_B$ satisfying the exact Bragg condition $\underline{k}_B^2 = (\underline{k}_B+\underline{h})^2 = K_o^2$. Then we have $K_o^2 - (\underline{k}_B+n\underline{h})^2 = -n(n-1)\underline{h}^2$ and consequently:

$$(91) \qquad v^{B}_{\underline{h},o} = v_{\underline{h}} - \frac{1}{h^2} \sum_{n(\neq 0,1)} \frac{v_{(n-1)\underline{h}}\, v_{n\underline{h}}}{n(n-1)}$$

With this we get for the branch seperation $\Delta k = 2\pi/d_{ext}$

$$(92) \qquad \Delta k = \frac{v^{B}_{\underline{h},o}}{K_o \cos\theta_B} = \frac{1}{K_o \cos\theta_B} \left\{ |v_{\underline{h}}| + \frac{1}{h^2} \left(v_{2\underline{h}}\, v_{\underline{h}} + \frac{1}{3} v_{3\underline{h}}\, v_{\underline{h}} + \ldots \right) \right\}$$

The first term in the bracket represents the two beam expression (77). Therefore the extinction distance decreases due to the systematic reflections.

We may also calculate the influence of the systematic reflections upon the absorption. According to (67,86) the absorption of a Blochwave $\underline{k}$ for a simple imaginary potential $iU'(\underline{r})$ can be written as

$$(93) \qquad \mu = \sum_{\underline{h},\underline{h}'} C^{*}_{\underline{h}}\, C_{\underline{h}'}\, \mu_{\underline{h}-\underline{h}'}$$

From (88) we get for the systematic reflection $n\underline{h}$ $(n \neq 0,1)$

$$(94) \qquad C_{n\underline{h}} \cong - \frac{1}{n(n-1)h^2} \left(v_{n\underline{h}}\, C_o + v_{(n-1)\underline{h}}\, C_{\underline{h}} \right)$$

For instance, we obtain for the absorption of the wave field II (Fig. 14) exactly in the Bragg condition, by taking into account only the linear therm in $C_{n\underline{h}}$

$$(95) \qquad \Delta\mu = \mu_o - \mu_{\underline{h}} + (\mu_{\underline{h}} - \mu_{2\underline{h}}) \cdot \frac{-v_{\underline{h}} + v_{2\underline{h}}}{h^2} +$$

$$+ (\mu_{2\underline{h}} - \mu_{3\underline{h}}) \cdot \frac{-v_{2\underline{h}} + v_{3\underline{h}}}{3h^2} + \ldots$$

Therefore the systematic reflections diminish the anomalous transmission effect ($v_{\underline{h}} < 0$!).

Now we want to discuss situations, where, for symmetry reasons, we get more than two strong waves. A first example is the <u>three-beam case</u> shown in Fig. 17a, for which we get three strong waves $\underline{k}$, $\underline{k}+\underline{h}$, and $\underline{k}+\underline{h}'$. In Fig 17a we have taken $|\underline{h}| = |\underline{h}'|$. Moreover we assume that $v_{\underline{h}} = v_{\underline{h}'} = v_{-\underline{h}}$. Exactly in the Bragg condition we have $\underline{k}^2 = (\underline{k}+\underline{h})^2 = (\underline{k}+\underline{h}')^2$ and by substituting $K_o^2 - \underline{k}^2 = x$ we get for this the matrix equation

$$(96) \qquad \begin{pmatrix} x & -v_{\underline{h}} & -v_{\underline{h}-\underline{h}'} \\ -v_{\underline{h}} & x & -v_{\underline{h}} \\ -v_{\underline{h}-\underline{h}'} & -v_{\underline{h}} & x \end{pmatrix} \cdot \begin{pmatrix} C_{\underline{h}} \\ C_o \\ C_{\underline{h}'} \end{pmatrix} = 0$$

Due to the symmetry of the problem we have one anti-symmetrical solution with $C_o = 0$ and $C_{\underline{h}'} = -C_{\underline{h}}$, for which we get the x-value

$$(97) \qquad x^a = -v_{\underline{h}-\underline{h}'}$$

Further we have two symmetrical solutions with $C_{\underline{h}} = C_{\underline{h}'}$, the x-values of which are

$$(98) \qquad x^s_{1,2} = \frac{1}{2}\left\{ v_{\underline{h}-\underline{h}'} \pm \sqrt{(v_{\underline{h}-\underline{h}'})^2 + 8v_{\underline{h}}^2} \right\};$$

$$\frac{C_{\underline{h}}}{C_o} = \frac{x}{2v_{\underline{h}}}$$

We get an especially interesting case, if the reflection $\underline{h}-\underline{h}'$ is forbidden ($v_{\underline{h}-\underline{h}'} = 0$). In this case there is no direct coupling between the coefficient $C_{\underline{h}}$ and $C_{\underline{h}'}$. Nevertheless by starting with a strong plane wave $\underline{k}+\underline{h}$ (instead of $\underline{k}$ as before) we get a strong wave $\underline{k}+\underline{h}'$, too, which is due to the indirect coupling via the plane wave $\underline{k}$. This effect has long been known as "Umweganregung".

As a second example we discuss the symmetrical <u>four-beam case</u> shown in Fig. 17b. The reciprocal lattice vectors $\underline{h}$ and $\underline{h}'$ form a rectangle with $\underline{h}+\underline{h}'$ and $\underline{h}'-\underline{h}$ as diagonals. Further here we assume $v_{\underline{h}} = v_{-\underline{h}}$, $v_{\underline{h}'} = v_{-\underline{h}'}$ and similarly $v_{\underline{h}+\underline{h}'} = v_{\underline{h}-\underline{h}'}$. The problem is simplified by considering that Fig. 17b is symmetrical with respect to reflections on the plane going through the origin and the line S and on the plane through O and S'. Therefore, if the Bragg conditions $\underline{k}^2 = (\underline{k}+\underline{h})^2 = (\underline{k}+\underline{h}')^2 = (\underline{k}+\underline{h}+\underline{h}')^2$ are exactly fulfilled, the eigenfunctions can be chosen as similtaneous eigenfunctions to the reflections $\underline{\underline{S}}$ and $\underline{\underline{S}}'$. For instance for the reflection $\underline{\underline{S}}$ we have:

$$(99) \qquad \underline{\underline{S}} \cdot \begin{pmatrix} C_o \\ C_{\underline{h}} \\ C_{\underline{h}+\underline{h}'} \\ C_{\underline{h}'} \end{pmatrix} = \begin{pmatrix} C_{\underline{h}} \\ C_o \\ C_{\underline{h}'} \\ C_{\underline{h}+\underline{h}'} \end{pmatrix} = s \cdot \begin{pmatrix} C_o \\ C_{\underline{h}} \\ C_{\underline{h}+\underline{h}'} \\ C_{\underline{h}'} \end{pmatrix}$$

where the eigenvalue s of $\underline{\underline{S}}$ can have the values $s = \pm 1$ only. Thus the four eigensolutions can be ordered according to their eigenvalues s and s' for the reflections S and S', namely (s,s') = (1,1),(1,-1),(-1,1) and (-1,-1). For instance, for the complete symmetrical solution (1,1) we have

$$(100) \qquad (1,1): \quad C_o = C_{\underline{h}} = C_{\underline{h}'} = C_{\underline{h}+\underline{h}'} = \frac{1}{2}$$

and for $x = K_o^2 - \underline{k}^2 = K_o^2 - (\underline{k}+\underline{h})^2 = \ldots$ we get

$$x = v_{\underline{h}} + v_{\underline{h}'} + v_{\underline{h}+\underline{h}'}$$

The corresponding Blochwave has the form

$$(101) \qquad \phi_{\underline{k}}^{(1,1)}(\underline{r}) = e^{i\underline{k}\underline{r}} e^{i\frac{\underline{h}+\underline{h}'}{2}\underline{r}} \; 2 \cos \frac{\underline{h}\cdot\underline{r}}{2} \cdot \cos \frac{\underline{h}'\cdot\underline{r}'}{2}$$

It has two modulation factors of the type I shown in Fig. 14 and vanishes in the middle between the reflecting $\underline{h}$ and $\underline{h}'$ planes, being maximal on these planes. Analogously we get for the other waves

$$(102) \qquad (-1,1): \quad C_o = -C_{\underline{h}} = C_{\underline{h}'} = -C_{\underline{h}+\underline{h}'} = \frac{1}{2}$$

$$(1,-1): \quad C_o = C_{\underline{h}} = -C_{\underline{h}'} = -C_{\underline{h}+\underline{h}'} = \frac{1}{2}$$

$$(-1,-1): \quad C_o = -C_{\underline{h}} = -C_{\underline{h}'} = C_{\underline{h}+\underline{h}'} = \frac{1}{2}$$

Especially interesting is the totally antisymmetrical wave (-1,-1) because it has two sin-modulation factors.

$$(103)\quad \phi_{\underline{k}}^{(-1,-1)}(\underline{r}) = e^{i\underline{k}\underline{r}} \cdot e^{i\frac{\underline{h}+\underline{h}'}{2}\underline{r}} \sin\frac{\underline{h}\cdot\underline{r}}{2} \cdot \sin\frac{\underline{h}'\cdot\underline{r}}{2}$$

It vanishes on both reflecting planes $\underline{h}$ and $\underline{h}'$ and even quadratically at the atomic positions on the intersecting lines of these planes. Therefore this Blochwave has an especially weak absorption, even weaker than the wave ϕ^I of the two beam case. One gets:

$$(104)\quad \Delta\mu = \mu_o - \mu_{\underline{h}} - \mu_{\underline{h}'} + \mu_{\underline{h}+\underline{h}'}$$

By expanding analogously to (87) $\mu_{\underline{h}}$ into powers of h, even the quadratic terms in $\underline{h}$ vanish $(h^2+h'^2 = (\underline{h}+\underline{h}')^2)$ and the expansion starts with h^4 only. This is just due to the fact that unlike to the two beam case the wave field vanishes quadratically at the atomic positions.

2.8 Orthogonality on the Dispersion Surface

In the inttroductory section 2.2 we have seen, that the Bloch functions ($u_{\underline{k}\gamma}(\underline{r})$ for the same $\underline{k}$-vector, but for different bands γ, i.e. energies $E_\gamma(\underline{k})$, are orthogonal (equs. 2.24,26,28). Now we show, that for a special, but very important case we also get an orthogonality relation for Bloch functions $u_{\underline{k}\gamma}(\underline{r})$ on the different branches of the dispersion surface, i.e. for different $\underline{k}$'s, but for the same energy. *)

Let us first consider a simple situation, namely where all reflecting lattice vectors $\underline{h}$ ly in one plane. Of course, this is always true for the 2 and 3 beam case, but also for the 4 beam case of Fig. 17b and for the two-beam case with systematic reflections (Fig. 16). By writing $\underline{k} = \{\underline{\mathfrak{K}}, k_z\}$, where $\underline{\mathfrak{K}}$ is the parallel component of $\underline{k}$ in the plane of the reciprocal lattice vectors, we get from the Schrödinger equation

$$(105) \quad (K^2-k_z^2-(\underline{\mathfrak{K}}+\underline{h})^2)\ C_{\underline{h}} - \sum_{\underline{h}'} v_{\underline{h}-\underline{h}'} = 0$$

For a given normal component $\underline{\mathfrak{K}}$ this represents an eigenvalue problem of the sort

$$(106) \quad \sum_{\underline{h}'} N_{\underline{h},\underline{h}'}\ C_{\underline{h}'} = (K^2-k_z^2)C_{\underline{h}} \quad \text{with} \quad N_{\underline{h}\underline{h}'}=-(\underline{\mathfrak{K}}+\underline{h})^2\delta_{\underline{h}\underline{h}'}-v_{\underline{h}-\underline{h}'}$$

---

*) Note that for different $\underline{k}$-values the Bloch waves $\phi_{\underline{k}\gamma}(\underline{r})=e^{i\underline{k}\underline{r}}u_{\underline{k}\gamma}(\underline{r})$ are automatically orthogonal (equ. 23); however not the Bloch functions $u_{\underline{k}\gamma}(\underline{r})$!

Since $N_{\underline{h},\underline{h}'}$ does not depend on k_z and K, but only on the parallel component $\underline{\kappa}$, the same is true for the eigenvalues $\varepsilon_\nu(\underline{\kappa})$ and eigensolutions $C_{\underline{h}}(\nu)$. Thus the band structure for fixed $\underline{\kappa}$ consists of parabolas

$$K^2 = k_z^2 + \varepsilon_\nu(\underline{\kappa}) \tag{107}$$

being shifted from the origine by the amount $\varepsilon_\nu(\underline{\kappa})$ (Fig. 17c). Further all Bloch functions $u_{k_z\nu}(\underline{r})$ on the same parabola are identical for arbitrary k_z, since the coefficients $C_{\underline{h}}(\nu)$ depend on $\underline{\kappa}$ and $\varepsilon_\nu(\underline{\kappa})$ only. In general, however, according to equ. (2.24) all Bloch functions with the same value of $\underline{k}=\{\underline{\kappa}, k_z\}$, but with different band indices are orthogonal (e.g. the Bloch functions belonging to the points B and C in Fig. 17c). Therefore we conclude, that any two Bloch functions lying on different bands are orthogonal, too (e.g. B and D in Fig. 17c). Especially this is also true for the Bloch functions A and B, which belong to the same energy $E=\frac{\hbar^2}{2m}K^2$. On the dispersion surface E = constant these points ly on the different branches, so that their planar-component $\underline{\kappa}$ is the same. Fig. 17d shows the positions of A and B on the two beam dispersion surface.

Therefore, if we only have reciprocal lattice vectors lying in one plane, all Bloch functions with the same planar component $\underline{\kappa}$, but on the different branches of the dispersion surface, are orthogonal and form a complete set.

$$\sum_{\underline{h}} C_{\underline{h}}^*(\nu')\,C_{\underline{h}}(\nu) = \delta_{\nu\nu'} \quad , \quad \sum_{\nu} C_{\underline{h}'}(\nu)\,C_{\underline{h}}(\nu) = \delta_{\underline{h}\underline{h}'} \tag{109}$$

Let us now consider the more general problem with arbitrary reciprocal lattice vectors $\underline{h}$.

$$(110)\qquad \sum_{\underline{h}'} \left\{ (K^2-(\underline{k}+\underline{h})^2)\delta_{\underline{h}\underline{h}'} - v_{\underline{h}-\underline{h}'} \right\} C_{\underline{h}'} = 0$$

Since $|v_h| \ll K^2$, we write for $\underline{k}$:

$$\underline{k} = \underline{K}+\delta\underline{k} \quad \text{with} \quad \delta k \ll K.$$

Here $\underline{K}$ can be thought as the wave vector in the vacuum ($\underline{K}^2=K^2$), and $\delta\underline{k}$ describes the deviation of the dispersion surface from the free electron dispersion surface. For a given direction $\underline{n}$ of $\delta\underline{k}=\delta k\ \underline{n}$ we obtain by neglecting quadratic terms in δk

$$(111)\qquad (\underline{k}+\underline{h})^2 \cong (\underline{K}+\underline{h})^2 + 2(\underline{K}+\underline{h})\cdot\delta\underline{k} \cong (\underline{K}+\underline{h})^2 + 2K\cos\theta_h \cdot \delta k$$

$$\text{with} \quad \cos\theta_{\underline{h}} = \frac{K+h}{|\underline{K}+\underline{h}|}\cdot\underline{n}$$

From (110) we get then an equation, Which determines the allowed δk-values for a given direction $\underline{n}=\delta\underline{k}/\delta k$.

$$(112)\qquad \sum_{\underline{h}'} M_{\underline{h}\underline{h}'} C_{\underline{h}'} = \delta k \cos\theta_{\underline{h}} C_{\underline{h}}$$

$$\text{with} \quad M_{\underline{h}\underline{h}'} = \frac{1}{2K}\left(K^2-(\underline{K}+\underline{h})^2\right)\delta_{\underline{h}\underline{h}'} - v_{\underline{h}-\underline{h}'}$$

By introducing modified coefficients $\tilde{C}_{\underline{h}} = \sqrt{\cos\theta_{\underline{h}}}\, C_{\underline{h}}$, this can be transformed in the eigenvalue equation

$$(113)\qquad \sum_{\underline{h}'} \tilde{M}_{\underline{h}\underline{h}'} \tilde{C}_{\underline{h}'} = \delta k\, \tilde{C}_{\underline{h}}$$

$$\text{with} \quad \tilde{M}_{\underline{h},\underline{h}'} = \frac{1}{\sqrt{\cos\theta_{\underline{h}}\cdot\cos\theta_{\underline{h}'}}} M_{\underline{h}\underline{h}'}$$

For real potential $V(\underline{r})$, M is a hermitian matrix ($M^{\dagger}=M$). Then $\tilde{M}$ is hermitian, too, if all $\cos\Theta_{\underline{h}} > 0$, all $\sqrt{\cos\Theta_{\underline{h}}}$ real, respectively. Consequently the eigenvalues $\delta k^{(\gamma)}$ are real and the Bloch waves are undamped. Further the eigensolutions $\tilde{C}_{\underline{h}}(\gamma)$ are orthogonal and form a complete set.

$$(114)\quad \sum_{\underline{h}} \tilde{C}^{*}_{\underline{h}}(\gamma')\ \tilde{C}_{\underline{h}}(\gamma) = \delta_{\gamma,\gamma'} \quad ; \quad \sum_{\gamma} \tilde{C}^{*}_{\underline{h}'}(\gamma)\ \tilde{C}_{\underline{h}}(\gamma) = \delta_{\underline{h},\underline{h}'}$$

Note, that this is not an orthogonality condition for the Bloch functions $u_{k\gamma}(\underline{r})$, since it refers to the modified coefficients $\tilde{C}_{\underline{h}} = \sqrt{\cos\Theta_{\underline{h}}}\cdot C_{\underline{h}}$.

However, we obtain such an orthogonality condition for the Bloch functions if all $\cos\Theta_{\underline{h}}$ are equal, since then $\tilde{C}_{\underline{h}}(\gamma)$ and $C_{\underline{h}}(\gamma)$ are equal up to a normalisation constant. For instance, this is the case for the example discussed before, where all $\underline{h}$ lying in one plane perpendicular to $\underline{n}$. Then equation (114) reduces to (109). Further, and more important, this is also the case for high energy electrons, where $K \gg h$ and $\cos\Theta_{\underline{h}} \cong \cos\Theta_{o}$.

Finally we discuss the case $\tilde{M} \neq \tilde{M}^{\dagger}$ occuring if either $M \neq M^{\dagger}$ ($V \neq V^{\dagger}$) or if $\cos\Theta_{\underline{h}} < 0$ for at least one $\underline{h}$. Then the eigenvalues $\delta k^{(\gamma)}$ are complex and the Bloch waves are damped. Further their eigensolution $\tilde{C}^{\{M\}}(\gamma)$ are no longer orthogonal. However, one can show in analogy to (2.49) that

$$(115)\quad \sum_{\underline{h}} \tilde{C}^{\{\tilde{M}^{\dagger}\}*}(\gamma')\ \tilde{C}^{\{\tilde{M}\}}(\gamma) = \delta_{\gamma',\gamma}$$

where $\tilde{C}^{\{\tilde{M}^{\dagger}\}}(\gamma)$ are the eigensolutions of $\tilde{M}^{\dagger}$ with the eigenvalues $\delta k^{(\gamma)*}$.

3. Diffraction of Electrons by Ideal Crystals

3.1. Wavefields in the Vacuum and in the Crystal

We consider now the scattering of an incident electron with impuls $\hbar\underline{K}$ by a finite crystal of volume Ω_{crystal}. For the total potential of the crystal we choose the form

$$(1) \qquad V(\underline{r}) = s_{\Omega}(\underline{r})\, V_{\infty}(\underline{r}) \quad \text{with} \quad s_{\Omega}(\underline{r}) = \begin{cases} 1 & \text{for } \underline{r} \text{ in } \Omega_{\text{cryst.}} \\ 0 & \text{for } \underline{r} \text{ in vacuum} \end{cases}$$

Here $V_{\infty}(\underline{r})$ is the periodic potential of an infinite ideal crystal as it has been discussed in section 2.1. The stepfunction $s_{\Omega}(\underline{r})$ cuts off the potential $V_{\infty}(\underline{r})$ at the crystal surface, so that $V(\underline{r}) = 0$ in the vacuum. With the ansatz (1) we have neglected deviations of the crystal potential from the perfect periodicity in the immediate vicinity of the crystal surface. However due to the large extinction length such surface effects cannot be observed by diffraction (besides in LEED, where approximation (1) is questionable).

In the vacuum we have $V(\underline{r}) = 0$. Therefore in the vacuum the wavefunction $\Psi(\underline{r})$ has to be a sum of plane waves $e^{i\underline{K}_i\underline{r}}$ having the same energy as the incident wave $\underline{K}$. On the other hand, in the crystal, where $V(\underline{r}) = V_{\infty}(\underline{r})$, the wavefunction has to be a sum of Blochwaves $\phi_{\underline{k}_j}(\underline{r})$ with the energy $E_{\nu}(\underline{k}_j) = \frac{\hbar^2 K^2}{2m}$. Both results follow from

the fact that plane waves are the eigenfunctions for $V(\underline{r}) = 0$ and Blochwaves are the eigenfunctions for $V(\underline{r}) = V_\infty(\underline{r})$ and that the energy $E = \frac{\hbar^2 K^2}{2m}$ is given by the incident plane wave. Therefore we have

$$(2)\quad \psi(\underline{r}) = \begin{cases} e^{i\underline{K}\underline{r}} + \sum_i R_i\, e^{i\underline{K}_i\underline{r}} & \text{vacuum} \\ & \text{for } \underline{r} \text{ in the} \\ \sum_j P_j\, \phi_{\underline{k}_j}(\underline{r}) & \text{crystal} \end{cases}$$

$$\text{with } \frac{\hbar^2 \underline{K}^2}{2m} = E = \frac{\hbar \underline{K}_i^{\,2}}{2m} = E_\nu(\underline{k}_j) \text{ for all } \underline{K}_i \text{ and } \underline{k}_j$$

How many and which Blochwaves $\underline{k}_j$ or plane waves $\underline{K}_i$, respectively, are excited, depends very much on the special form of the crystal. The case of a crystal slab and a half crystal will be discussed in the next sections. Knowing the waves $\underline{k}_j$ and $\underline{K}_i$, the coefficients P_j and R_i have to be determined by the boundary conditions for $\psi(\underline{r})$ on the crystal surface. Namely at the surface $\psi(\underline{r})$ has to be continous and the same applies to the current through the surface, because there are no surface sources. If we call $\underline{n}(\underline{r})$ the normal to the surface at the point $\underline{r}$ on the surface, then we have on the whole surface:

$$(3)\quad \psi_{vac}(\underline{r}) = \psi_{cryst.}(\underline{r})$$

$$\text{and } \underline{n}(\underline{r}) \cdot \frac{d\psi_{vac}}{d\underline{r}} = \underline{n}(\underline{r}) \cdot \frac{d\psi_{cryst}}{d\underline{r}}$$

It is important to see that in (2) we cannot restrict ourselves to plane waves with real $\underline{K}_i$'s or Bloch waves with real $\underline{k}_j$'s, as we always can in an infinite vacuum, or in an infinite crystal, respectively. Rather we have to take complex $\underline{K}_i$ and $\underline{k}_j$ into account, too, representing waves evanescent from the surfaces.

That the solution $\psi(\underline{r})$ has the form (2), can also be studied at Born's integral equation for $\psi(\underline{r})$.

$$(4) \quad \psi(\underline{r}) = e^{i\underline{K}\underline{r}} + \int d\underline{r}'\ G_o(\underline{r}-\underline{r}')\ V(\underline{r}')\ \psi(\underline{r}')$$

$$\text{with } G_o(\underline{r},\underline{r}') = -\frac{2m}{\hbar^2}\frac{e^{iK|\underline{r}-\underline{r}'|}}{4\pi|\underline{r}-\underline{r}'|} \text{ and } K = |\underline{K}|$$

Due to (1) $V(\underline{r})$ can be replaced by $V_\infty(\underline{r})$ if the integration is restricted to the crystal volume Ω_{cryst}. Therefore in the vacuum the wave function consists of the incident wave and a sum of spherical waves with the energy E, out-going from the crystal volume. For $\underline{r}$ within Ω_{cryst}, equation (4) with the incident plane wave $\underline{K}$ seems to contradict equation (2) which contains only Blochwaves. However we have to realize that each Blochwave with the energy $E = \frac{\hbar^2 K^2}{2m}$ and therefore also the sum $\psi_{cryst} = \sum_j P_j\ \phi_{\underline{k}j}$ is a solution of the homogeneous integral equation:

$$(5) \quad \psi_{cryst}(\underline{r}) = \int_{-\infty}^{\infty} d\underline{r}'\ G_o(\underline{r}-\underline{r}')\ V_\infty(\underline{r}')\ \psi_{cryst}(\underline{r}')$$

By comparing this with (4) we get

$$(6) \quad 0 = e^{i\underline{K}\underline{R}} - \int_{vacuum} d\underline{r}'\ G_o(\underline{r}-\underline{r}')\ V_\infty(\underline{r}')\ \psi_{cryst}(\underline{r}')$$

Therefore we can see that the plane wave $\underline{K}$ is extincted in the crystal by fictive spherical waves outgoing from the vacuum. This "extinction theorem" can also be put into another form by using the Schroedinger equations for $\psi_{cryst}(\underline{r})$ and $G_o(\underline{r}-\underline{r}')$.

$$(7)\quad \left(-\frac{\hbar^2}{2m}\partial_{\underline{r}}^2 + V_\infty(\underline{r}) - E\right)\psi_{cryst}(\underline{r}) = 0$$

$$\left(-\frac{\hbar^2}{2m}\partial_{\underline{r}}^2 - E\right) G_o(\underline{r}-\underline{r}') = -\delta(\underline{r}-\underline{r}')$$

From this we obtain after some simple calculations

$$(8)\quad G_o(\underline{r}-\underline{r}')\, V_\infty(\underline{r}')\, \psi_{cryst}(\underline{r}') = \delta(\underline{r}-\underline{r}')\, \psi_{cryst}(\underline{r}')$$

$$+\frac{\hbar^2}{2m}\partial_{\underline{r}'}\Big\{ G_o(\underline{r}-\underline{r}')\left(\partial_{\underline{r}'}\psi_c(\underline{r}')\right)$$

$$-\left(\partial_{\underline{r}'} G_o(\underline{r}-\underline{r}')\right)\psi_c(\underline{r}')\Big\}$$

Finally we get by performing the volume integral in (4) into a surface integral over the crystal surface S :

$$(9)\quad e^{i\underline{K}\underline{r}} + \frac{\hbar^2}{2m}\int_S d\underline{S}\Big\{ G_o(\underline{r}-\underline{r}')\left(\partial_{\underline{r}'}\psi(\underline{r}')\right)$$

$$- \left(\partial_{\underline{r}'} G_o(\underline{r}-\underline{r}')\right)\psi(\underline{r}')\Big\} =$$

$$= \begin{cases} \psi(\underline{r}) & \text{vacuum} \\ \text{in the} & \\ 0 & \text{crystal} \end{cases}$$

Accordingly in the vacuum the scattered wave is a sum of spherical waves with energy E outgoing from the surfaces, which in the crystal extinct the incident wave.

Analogously to (1) we choose for the nonlocal optical potential $U(\underline{r},\underline{r}')$ a cut-off of the form:

(10) $U(\underline{r},\underline{r}') = s_\Omega(\underline{r})\ s_\Omega(\underline{r}')\ U_\infty(\underline{r},\underline{r}')$

where U_∞ is the optical potential of an infinite crystal. Unfortunately, the decomposition (2) of Ψ in plane waves and Blochwaves is no longer exact for a nonlocal potential. However, the range $|\underline{r}-\underline{r}'|$, over which $U_\infty(\underline{r},\underline{r}')$ is unequal zero, is normally much smaller than an extinction length (besides in LEED). Therefore the ansatz (2) is nevertheless a good approximation, especially because U is local anyway in a first approximation.

3.2. Scattering by a Crystal Slab I [21]

For a crystal slab, filling the space $0 \leq z \leq d$, the potential (1) is given by

(11) $V(\underline{r}) = s(z)\cdot s(d-z)\cdot V_\infty(\underline{r})$ with $s(z) = \begin{cases} 1 & \text{for } z > 0 \\ 0 & \text{for } z < 0 \end{cases}$

Therefore $V(\underline{r})$ is periodic with respect to any surface translation vector $\underline{\mathfrak{R}}^n$ in the x-y-plane, both in the crystal and in the vacuum.

(12) $V(\underline{r}) = V(r+\underline{\mathfrak{R}}^n)$

where $\underline{\mathfrak{R}}^n = \{\mathfrak{R}^n_x, \mathfrak{R}^n_y, 0\} = n_1\ \underline{a}_1 + n_2 \underline{a}_2$

The vectors $\underline{a}_1$, $\underline{a}_2$, forming the unit mesh on the surface, are shown for the (100) surface of a f.c.c. lattice in Fig. 6 (see section 2.5.). Of course, equation (12) holds only, because both surfaces z = 0 and z = d are

parallel.

Due to (12) the eigensolution $\Psi(\underline{r})$ can be chosen as a Blochwave with respect to the x-y-coordinates, where the plane Blochvector $\underline{\tilde{k}}$ is determined by the x-y-component of the incident wave $\underline{K} = (\underline{\tilde{k}}, K_z)$. Writing $\underline{r}$ as $\underline{r} = (\underline{\rho}, z)$ we have

$$(13) \qquad \Psi_{\underline{\tilde{k}}}(\underline{\rho}, z) = e^{i\underline{\tilde{k}}\underline{\rho}}\, u_{\underline{\tilde{k}}}(\underline{\rho}, z) \text{ with } u_{\underline{\tilde{k}}}(\underline{\rho}+\underline{R}^n; z) = u_{\underline{\tilde{k}}}(\underline{\rho}, z)$$

With the reciprocal lattice vectors $\underline{g}$ of the surface net

$$(14) \qquad \underline{g} = \underline{g}^m = \{g_x^m, g_y^m, 0\} = m_1\underline{b}_1 + m_2\underline{b}_2 \text{ with } \underline{b}_i\underline{a}_j = 2\pi\delta_{ij}$$

the Blochfunction $u_{\underline{\tilde{k}}}$ and the potential $V(\underline{r})$ can therefore be expanded in terms of plane "surface" waves $e^{i\underline{g}\underline{\rho}}$, where the coefficients $\Gamma_{\underline{g}}$ and $V_{\underline{g}}$ depend still on z.

$$(15) \qquad \Psi_{\underline{\tilde{k}}}(\underline{\rho}, z) = \sum_{\underline{g}} \Gamma_{\underline{g}}(z)\, e^{i(\underline{\tilde{k}}+\underline{g})\underline{\rho}}$$

$$(16) \qquad V(\underline{\rho}, z) = \sum_{\underline{g}} V_{\underline{g}}(z)\, e^{i\underline{g}\underline{\rho}}$$

$$(17) \qquad \text{with } V_{\underline{g}}(z) = \frac{1}{S_o} \int_{S_o} d\underline{\rho}\, e^{-i(\underline{g}-\underline{g}')\underline{\rho}}\, V(\underline{\rho}, z)$$

Here $S_o = \underline{a}_1 \cdot \underline{a}_2$ is the surface of the unit mesh. By introducing (15) and (16) into the Schroedinger equation we get a set of coupled equations determining the z-dependence of $\Gamma_{\underline{g}}(z)$ $\left(v_{\underline{g}} = \frac{2m}{\hbar^2} V_{\underline{g}} \right)$:

$$(18)\quad \left\{ \partial_z^2 + (\underline{K}^2 - (\underline{k}+\underline{g})^2 \right\} \Gamma_{\underline{g}}(z) = \sum_{\underline{g}'} v_{\underline{g}-\underline{g}'}(z)\, \Gamma_{\underline{g}'}(z)$$

Thus the remaining energy for the motion of $\Gamma_{\underline{g}}(z)$ in z-direction is $\frac{\hbar^2}{2m}\left(\underline{K}^2 - (\underline{k}+\underline{g})^2\right)$. For each $\underline{g}$ the total energy $\frac{\hbar K^2}{2m}$ is therefore splitted up in the x-y-energy $\frac{h^2(\underline{k}+\underline{g})^2}{2m}$ and the energy in z-direction. Because $(\underline{k}+\underline{g})^2$ gets arbitrarily large for sufficiently large $\underline{g}$, the remaining energy for the z-direction can be negative. These waves decay exponentially in the vacuum, as can be seen below.

The equations (18) also can be written in integral form by using the linear Green's function $G_o(z-z')$. $G_o(z-z')$ fulfills the equation.

$$(19)\quad \left(\partial_z^2 + K_o^2 \right) G_o(z) = \delta(z)$$

With the correct retardation it is given by:

$$(20)\quad G_o(z) = \begin{cases} \dfrac{e^{iK_o|z|}}{2iK_o} \; ; \; K_o > 0 & K_o^2 > 0 \\ \qquad\qquad \text{for} & \\ \dfrac{e^{-\varkappa_o z}}{-2\varkappa_o} \; ; \; \varkappa_o > 0 & K_o^2 = -\varkappa_o^2 < 0 \end{cases}$$

Considering, that we have an incident wave $e^{iK_z z}$ for $\underline{g} = 0$ only, we get the integral equations:

$$(21)\qquad \Gamma_{\underline{g}}(z) = \delta_{\underline{g},0}\, e^{iK_z z} + \int dz'\, \frac{e^{iK_{\underline{g}}|z-z'|}}{2iK_{\underline{g}}} \cdot \sum_{\underline{g}'} v_{\underline{g}-\underline{g}'}(z')\, \Gamma_{\underline{g}'}(z')$$

$$\text{with } K_{\underline{g}} = \sqrt{K^2-(\underline{k}+\underline{g})^2} > 0, \text{ if } K_{\underline{g}}^2 > 0$$

$$\text{or } K_{\underline{g}} = i\varkappa_{\underline{g}},\ \varkappa_{\underline{g}} > 0, \text{ if } K_{\underline{g}}^2 < 0$$

Now we can directly see the form of $\Gamma_{\underline{g}}(z)$ in the vacuum. For $z < 0$ we have $|z-z'| < 0$ due to $0 \leq z' \leq d$ according to (11). Therefore we get for $z < 0$

$$(22)\qquad \Gamma_{\underline{g}}(z) = \delta_{\underline{g},0} e^{iK_z z} + R_{\underline{g}}\, e^{-iK_{\underline{g}} z}$$

$$(23)\quad \text{with } R_{\underline{g}} = \frac{1}{2iK_{\underline{g}}} \int_0^d e^{+iK_{\underline{g}} z'} \sum_{\underline{g}'} v_{\underline{g}-\underline{g}'}(z')\ \Gamma_{\underline{g}'}(z')\, dz'$$

and analogously for $z > d$:

$$(24)\qquad \Gamma_{\underline{g}}(z) = \delta_{\underline{g},0}\, e^{iK_z z} + \tilde{T}_{\underline{g}}\ e^{iK_{\underline{g}} z}$$

$$(25)\quad \text{with } \tilde{T}_{\underline{g}} = \frac{1}{2iK_{\underline{g}}} \int_0^d e^{-iK_{\underline{g}} z'} \sum_{\underline{g}'} v_{\underline{g}-\underline{g}'}(z')\ \Gamma_{\underline{g}'}(z')\, dz'$$

$R_{\underline{g}}$ and $\tilde{T}_{\underline{g}}$ are called reflection and transmission coefficients. Only for $K_{\underline{g}}^2 > 0$, i.e. $\underline{K}^2 > (\underline{k}+\underline{g})^2$, we get an reflected plane wave $\underline{K}_{\underline{g}}^- = (\underline{k}+\underline{g}, -K_{\underline{g}})$ and a transmitted plane wave $\underline{K}_{\underline{g}}^+ = (\underline{k}+\underline{g}, +K_{\underline{g}})$ respectively. The waves with $\underline{K}^2 < (\underline{k}+\underline{g})^2$ or $K_{\underline{g}} = i\varkappa_{\underline{g}}$ decrease exponentially into the vacuum. Whereas we only can have a finite number of reflected or transmitted waves with $\underline{K}^2 > (\underline{k}+\underline{g})^2$, we always

have an infinite number of decaying waves corresponding to the infinite number of $\underline{g}$ vectors with $(\underline{k}+\underline{g})^2 > \underline{K}^2$.

In the kinematical theory one replaces $\Gamma_{\underline{g}}(z')$ in the integral (21) by the incident wave (first Born approximation). This gives for $R_{\underline{g}}$ and $\tilde{T}_{\underline{g}}$

$$(26) \qquad R_{\underline{g}} = \sum_{g} \frac{\left(1 - e^{i(K_z+K_{\underline{g}}+g)d}\right)}{2K_{\underline{g}}(K_z+K_{\underline{g}}+g)} v_{\underline{g},g}$$

$$(27) \qquad \tilde{T}_{\underline{g}} = \sum_{g} \frac{\left(1 - e^{i(K_z-K_{\underline{g}}+g)d}\right)}{2K_{\underline{g}}(K_z-K_{\underline{g}}+g)} v_{\underline{g},g}$$

We have used the Fourierexpansion ($g = n\frac{2\pi}{a_3}$, $n=0,\pm1,\cdots$)

$$v_{\underline{g}}(z) = \sum_{g} e^{igz} v_{\underline{g},g}(z)$$

From (26) and (27) we can see that the kinematical theory fails in two cases. First for $K_{\underline{g}} = 0$, where a socalled "surface wave" $\underline{K}_{\underline{g}} = (\underline{k}+\underline{g},0)$ moves parallel to the surface[22]. Second, for the case of a Bragg reflection $K_z \pm K_{\underline{g}} + g = 0$. For this the intensity of the wave $\underline{K}_{\underline{g}} = \underline{K} + (\underline{g},g)$ is proportional to d^2 and diverges for $d\to\infty$. In the Laue case $(K_z - K_{\underline{g}} + g = 0)$ this is a transmitted wave, whereas in the Bragg case $(K_z + K + g = 0)$ it is a reflected wave. For high energies $\underline{K}^2 \gg v_{\underline{g},g}$ equations (26)(27) show that we get appreciable intensity only if one or more of these Bragg conditions are fulfilled However for LEED ($\underline{K}_o^2 \gtrapprox v_{\underline{g},g}$) this is no more necessary and all waves get more or less intensity.

3.3. Scattering by a Crystal Slab II

Now we construct the wave field in the vacuum and in the crystal by following equation (2). In the vacuum we have scattered plane waves $\underline{K}_i$ having the same energy as the incident wave $\underline{K}$. Further, due to the surface periodicity of the total potential (12) the x-y-component $\underline{\kappa}_i$ of $\underline{K}_i$ only can be different from the x-y-component $\underline{\kappa}$ of the incident wave $\underline{K}$ by a reciprocal lattice vector $\underline{g}$ of the surface net (see also (15)). Moreover we only have outgoing waves, meaning that for real $\underline{K}_i$ the z-component K_{iz} has to be positive for $z > d$ and negative for $z < 0$. For complex $K_{iz} = i\varkappa_{iz}$ the waves have to decrease from the surface leading to $\varkappa_{iz} > 0$ for $z > d$ and $\varkappa_{iz} < 0$ for $z < 0$. Thus for each $\underline{g}$ we get two waves

$$\underline{K}_{\underline{g}}^{\pm} = (\underline{\kappa}+\underline{g}, \pm K_{z\underline{g}})$$

$$\text{with } K_{z\underline{g}} = \sqrt{\underline{K}^2-(\underline{\kappa}+\underline{g})^2} > 0 \qquad \text{for } \underline{K}^2 > (\underline{\kappa}+\underline{g})^2$$

$$\text{and } K_{z\underline{g}} = i\varkappa_{z\underline{g}}\,,\ \varkappa_{z\underline{g}} > 0 \qquad \text{for } \underline{K}^2 < (\underline{\kappa}+\underline{g})^2$$

$\underline{K}_{\underline{g}}^{+}$ is allowed for $z > d$, $\underline{K}_{\underline{g}}^{-}$ for $z < 0$. A graphical construction for the waves $\underline{K}_{\underline{g}}^{\pm}$ is shown in Fig. 18. All $\underline{K}_{\underline{g}}^{\pm}$ vectors lie on the sphere of radius K. Four allowed real wave vectors $\underline{K}_{\underline{g}}^{\pm}$, $\underline{K}_{2\underline{g}}^{\pm}$ are shown. We have assumed that $\underline{g}$ lies in the plane of $\underline{K}$ and the surface normal. The vectors $\underline{K}_{3\underline{g}}$, $\underline{K}_{4\underline{g}}$... and $\underline{K}_{-\underline{g}}$... have purely imaginary z-components.-Therefore the wave function in the vacuum is, in agreement with the equations (22, 24) of the last section:

(28) $\psi(\underline{r}) = e^{i\underline{K}\underline{r}} + \sum_{\underline{g}} R_{\underline{g}}\, e^{i\underline{K}^-_{\underline{g}}\,\underline{r}}$ for $z < 0$

(29) $\psi(\underline{r}) = \sum_{\underline{g}} T_{\underline{g}}\, e^{i\underline{K}^+_{\underline{g}}\,\underline{r}}$ for $z > d$

In the crystal only those Bloch waves $\underline{k}_i$ with $E_\nu(\underline{k}_i) = \frac{\hbar^2 K^2}{2m}$ are allowed. Moreover the x-y-component of $\underline{k}_i$ has to be equal to $\underline{\tilde{k}}$ up to a reciprocal lattice vector $\underline{g}$ of the surface net. Because $E_\nu(\underline{k})$ and the Bloch waves $\phi_{\underline{k},\nu}$ are periodic in the reciprocal lattice, we can set $\underline{k}_i = (\underline{\tilde{k}}, k_{iz})$. Therefore the z-components k_{iz} have to be determined from $E_\nu(\underline{\tilde{k}}, k_z) = \frac{\hbar^2 K^2}{2m}$. Fig 19 shows schematically the band structure $E_\nu(k_z)$ as a function of $k_z = k_z' + ik_z''$ For each energy $E = \frac{\hbar^2 K^2}{2m}$, the intersection of $E_\nu(k_z)$ with the plane E = const. give the allowed k_z-values. From the symmetries (2.59) it follows, that simultaneously with k_z also $-k_z$ and k_z^* is a solution. There is always an infinitely large number of intersections with the "reserved"parabolas giving infinitely many k_z with arbitrarily large k_z'', of which only two are shown in Fig. 19. Further we get a finite number of real k_z (two in Fig. 19). With these $\underline{k}_j$-vectors the wavefunction for $0 \leq z \leq d$ is

(30) $\psi(\underline{r}) = \sum_j P_j\, \phi_{\underline{k}_j}(\underline{r}) = \sum_{j,\underline{g},g} P_j C_{\underline{g},g}(\underline{k}_j) \cdot$

$\cdot\, e^{i(\underline{\tilde{k}}+\underline{g})\underline{\kappa}}\, e^{i(k_{zj}+g)z}$

Here we have expanded the Bloch waves into plane waves $e^{i(\underline{k}+\underline{h})\underline{r}}$, and the reciprocal lattice vector $\underline{h}$ is written as $\underline{h} = (\underline{\ell},g)$ with $g = n\frac{2\pi}{a_3}$.

Now according to (3) $\psi(\underline{r})$ and $\frac{\partial\psi}{\partial z}$ have to be contineous at z = 0 and z = d. Therefore we get from (28) und (30) for z = 0 by comparing the coefficients of the plane waves $e^{i(\underline{k}+\underline{\ell})\underline{r}}$

$$(31) \qquad \delta_{\underline{\ell},0} + R_{\underline{\ell}} = \sum_{jg} C_{\underline{\ell},g}(\underline{k}_j)\ P_j$$

and

$$(32) \qquad (\delta_{\underline{\ell},0} - R_{\underline{\ell}}) = \sum_{j,g} \frac{k_{zj}+g}{K_z} C_{\underline{\ell},g}(\underline{k}_j)\ P_j$$

Similarly we have for z = d

$$(33) \qquad T_{\underline{\ell}} = \sum_{j,g} C_{\underline{\ell},g}(\underline{k}_j)\ e^{i(k_{zj}+g-K_z)d}\ P_j$$

$$(34) \qquad T_{\underline{\ell}} = \sum_{j,g} \frac{k_{zj}+g}{K_z} C_{\underline{\ell},g}(\underline{k}_j)\ e^{i(k_{zj}+g-K_z)d}\ P_j$$

By adding (32) and (31) and by subtracting (34) from (33) we get a set of equations for the coefficients P_j alone, namely

$$(35) \qquad z = 0: \quad \delta_{\underline{\ell},0} = \sum_{j,g} \frac{k_{zj}+g+K_z}{2K_z} C_{\underline{\ell},g}(\underline{k}_j)\ P_j$$

$$(36) \qquad z = d: \quad 0 = \sum_{j,g} \frac{k_{zj}+g-K_z}{2K_z} C_{\underline{\ell},g}(\underline{k}_j) e^{i(k_{zj}+g-K_z)d}\ P_j$$

This is an infinite number of equations for the infinite number of unknown P_j's. However are the P_j's unique? To discuss this we consider the N-beam case assuming that in the plane wave expansion of the Blochwaves only N beams $\underline{h} = (\underline{\ell}, g)$ are excited. In this case the determinant (2.22.) is an algebraic equation of the order 2N in k_z, giving 2N solutions k_{zj}, j=1,...,2N. Further, if all reciprocal lattice vectors $\underline{h}$ have different x-y-components $\underline{\ell}$, then (35) and (36) are exactly 2N equations, too. However if some of the $\underline{h}$-vectors only differ in the z-direction by a reciprocal lattice vector $g\underline{b}_3$, then we have less than 2N equations. For instance, let us assume that we have an infinite number of $\underline{h}$-vectors, say $\underline{h}^n = (0, n\frac{2\pi}{a_3})$ with n=0,±1,±2,..., which all have the same x-y-component $\underline{\ell}$=0. Then $E_\nu(k_z)$ has a typical one dimensional band structure as shown in Fig. 4. Of course, the determinant (2.22) gives an infinite number of k_z-values for each energy, but only two of them are non equivalent and lie in the first Brillouin zone $-\frac{\pi}{a_3} < k_z' < \frac{\pi}{a_3}$. Therefore we only have two linear independent Bloch functions and two P_j's, which can be determined from the two equations (35,36) for $\underline{\ell} = 0$. Similarly if we have two different $\underline{\ell}$-vectors, say $\underline{\ell}_1$ and $\underline{\ell}_2$, then we get the band structure as shown in Fig. 8 and Fig. 19 which is essentially a superposition of two one dimensional band structures. Then for each energy we always get 4 non equivalent $\underline{k}$-values and the $P_1 \ldots P_4$ can be determined from (35, 36) for $\underline{\ell} = \underline{\ell}_1$ and $\underline{\ell} = \underline{\ell}_2$. Therefore in general for n different $\underline{\ell}$-vectors we get 2n k_z-values with

$\frac{-\pi}{a_3} \leq k_z' < \frac{\pi}{a_3}$ and the coefficients $P_1 \ldots P_{2n}$ can be determined by the 2n equations (35) and (36).

If we have a <u>half crystal</u> filling the half space $z > 0$, then the above treatment has to be modified. Practically we also can treat a crystal slab as a half crystal, if d is very much larger than an absorption length. In this case, practically no intensity reaches the surface $z = d$ and all $T_{\underline{g}}$ vanish. For $z < 0$ the wavefield has the form (28) with the reflected waves $\underline{K}_{\underline{g}}^{-}$. However, in the crystal we only can have outgoing waves, because in the absence of the surface $z = d$ no waves are incident from $z = +\infty$. Therefore only those k_z are allowed, for which

$$(37) \quad \frac{\partial E}{\partial k_z} \gtrless 0 \quad , \text{ if } k_z \text{ is real}$$

or

$$(38) \quad k_z'' \geq 0 \quad , \text{ if } k_z = k_z' + ik_z'' \text{ is complex.}$$

(37) means that the z-component of the group velocity is positive, whereas (38) forbids waves which increase exponentially for $z \to +\infty$. Since together with k_z also $-k_z$ and k_z^* are solutions of the dispersion relation, the conditions (37) and (38) are fulfilled for exactly half the k_z-values allowed for the crystal slab. For if equation (37) holds for a given k_z, it does not hold for $-k_z$. Similarly equation (38) can only be fulfilled for either k_z or k_z^*. Therefore we now have one half of the coefficients P_j of the crystal slab, which can be uniquely determined by the equations (35) alone. Then from (31) we can get the reflection coefficients $R_{\underline{g}}$.

3.4. Current Conservation [23]

A useful relation between the coefficients $R_{\underline{g}}$, $T_{\underline{f}}$ and $P_{\underline{j}}$ can be obtained from the continuity equation. By multiplying the time dependent Schroedinger equation for $\Psi(\underline{r},t)$ by $\Psi^*(\underline{r},t)$ and subtracting the analogous equation for $\Psi^*(\underline{r},t)$, one has

$$(39)\quad \partial_t \left|\Psi(\underline{r},t)\right|^2 + \partial_{\underline{r}} \cdot \underline{j}(\underline{r},t) = \frac{2}{\hbar}\left(\mathrm{Im}\ V(\underline{r})\right)\cdot\left|\Psi(\underline{r},t)\right|^2$$

where "Im" means imaginary part. The current $\underline{j}$ is given by expression (2.29). For stationary problems $\underline{j}$ and $|\Psi|^2$ are independent of t and ∂_t vanishes. Therefore we have for a real potential $V(\underline{r})$ by decomposing $\underline{r}$ into x-y-component $\underline{\rho}$ and z-component:

$$(40)\quad \partial_{\underline{r}} \cdot \underline{j}(\underline{r}) = 0 = \partial_{\underline{\rho}} \cdot \underline{j}_{\underline{\rho}}(\underline{r}) + \partial_z \cdot j_z(\underline{r})$$

Here $\underline{j}_{\underline{\rho}}$ is the x-y-component of $\underline{j}$. Due to the x-y-periodicity of $V(\underline{r})$ (12), the current of the "plane" Bloch wave $\underline{k}$ (13) is periodic in the x-y-plane.

$$(41)\quad \underline{j}(\underline{r}+\underline{R}) = \underline{j}(\underline{r})$$

By integrating (40) over a unit mesh $S_o = (\underline{a}_1 \cdot \underline{a}_2)$ of the surface, the term $\partial_{\underline{\rho}} \cdot \underline{j}_{\underline{\rho}}$ can be integrated by parts and vanishes due to the periodicity (41). Therefore the average over S_o of the current in z-direction is constant and independent of z. By calculating this average for $z < 0$ and $z > d$, we obtain by using the ansatz (28,29)

$$(42)\qquad \overline{j_z}^{S_o} = \frac{\hbar}{m}\left(K_z - \sum_{\underline{g}}{}' K_{z\underline{g}} |R_{\underline{g}}|^2 \right) = \frac{\hbar}{m} \sum_{\underline{g}}{}' K_{z\underline{g}} |T_{\underline{g}}|^2 \geq 0$$

The $\sum'$ means a summation over the finite number of $\underline{g}$'s with real $\underline{K}_{\underline{g}}$ only. All evanescent waves with $K_{z\underline{g}} = i\varkappa_{z\underline{g}}$ do not give any contribution to the current. Equation (42) expresses the conservation of the current in z-direction. The incident intensity is distributed between the reflected and transmitted beams such that the current is conserved.

For the half crystal we can derive an equation as (42), too. Here, in the crystal, outgoing waves (37,38) are allowed only. Further evanescent Bloch waves give no contribution. This can be seen by evaluating j_z, which is independent of z, for $z \to +\infty$. Moreover we can average over the unit cell V_c instead of S_o and use equation (2.32) because j_z is constant anyway. Then one gets

$$(43)\qquad \overline{j}_z = \frac{\hbar}{m}\left(K_z - \sum_{\underline{g}} K_{z\underline{g}} |R_{\underline{g}}|^2 \right) = \sum_{j}{}' \frac{1}{\hbar} \frac{\partial E}{\partial k_{zj}} |P_j|^2 \geq 0$$

In the case of absorption, $V(\underline{r})$ is complex and the current in z-direction is no longer conserved. Instead we get by integrating (40) over z from 0 to d and averaging over S_o as before

$$(44)\qquad \frac{\hbar}{m} K_z = \sum_{\underline{g}}{}' \frac{\hbar}{m} K_{z\underline{g}} \left(|R_{\underline{g}}|^2 + |T_{\underline{g}}|^2 \right) -$$

$$- \frac{1}{S_o} \int_{S_o} d\underline{r} \int_0^d dz \, \frac{2}{\hbar} \left(\mathrm{Im}\, V(\underline{r}) \right) \cdot |\psi(\underline{r})|^2$$

The last term represents the intensity absorbed by the crystal (Im $V(\underline{r}) > 0$). The current of the scattered waves $\underline{K}$ is always less than the incident one.

For the case of the nonlocal potential $U(\underline{r},\underline{r}')$ the time independent continuity equation is:

$$(45) \qquad \partial_{\underline{r}} \cdot \underline{j}(\underline{r}) = -\frac{i}{\hbar} \int_{-\infty}^{\infty} d\underline{r}' \left(\psi^*(\underline{r})\, U(\underline{r},\underline{r}')\, \psi(\underline{r}') - \text{c.c.} \right)$$

Here the right-hand side does not vanish even for $U=U^\dagger$. Further instead of equation (44) we get by using the periodicity of U and the cut-off (10):

$$(46) \qquad \frac{\hbar K_z}{m} = \sum_{\underline{g}}{}' \frac{\hbar}{m} K_{z\underline{g}} \left(|R_{\underline{g}}|^2 + |T_{\underline{g}}|^2 \right) \qquad +$$

$$+ \frac{1}{S_o} \int_{S_o} d\underline{\nu} \int_{-\infty}^{\infty} dz d\underline{r}' \frac{i}{\hbar} \psi^*(\underline{r}) \left(U(\underline{r},\underline{r}') - U^\dagger(\underline{r},\underline{r}') \right) \psi(\underline{r}')$$

The absorption term vanishes for $U = U^\dagger$. Whereas for $U = U^\dagger$ the current is not conserved locally (45), it is conserved globally (46) as in the case of a local and real potential.

3.5. Symmetrical Laue-Case

Now we apply the results of the foregoing sections to the case where only one Bragg reflection $\underline{h}$ is excited. Then the Bloch waves are well described by the two beam approximation of section 2.6. Two different situations can occur. For a plane wave $\underline{K}$ incident from $z = -\infty$, the Bragg reflected wave $\underline{K}+\underline{h}$ either is scattered into the forward direction and

penetrates the crystal (Laue case) or it is scattered backwards (Bragg case). Both cases are illustrated in Fig. 20. Here we will restrict ourselves to the "symmetrical" Laue-case, for which the reflecting planes are perpendicular to the surface and for which $\underline{h}$ only has an x-y-component $\underline{h} = (\underline{\ell},0)$. In the next section, the symmetrical Bragg-case will be treated, for which the reflecting planes are parallel to the surface. Because a fairly large number of articles exists about these cases, our presentation will be relatively short. For more details, for instance integrated intensities etc., as well as for the unsymmetrical Laue- and Bragg-cases we refer to the literature [5-12]

In the symmetrical Laue case we have the following plane waves in the vacuum: in the region $z > d$ the transmitted wave $\underline{K} = \underline{K}_o^+ = (\underline{\tilde{k}}, K_z)$ and the Bragg reflected wave $\underline{K}_{\underline{\ell}}^+ = (\underline{\tilde{k}}+\underline{\ell}, K_{z\underline{\ell}})$ and in the region $z < 0$ the incident wave $\underline{K}$, the surface reflected wave $\underline{K}_o^- = (\underline{\tilde{k}}, -K_z)$, and the wave $\underline{K}_{\underline{\ell}}^- = (\underline{\tilde{k}}+\underline{\ell}, -K_{z\underline{\ell}})$ being the surface reflected wave of $\underline{K}_{\underline{\ell}}^+$. These wave vectors are shown in Fig. 21. The vectors $\underline{K} = \vec{AO}$ and $\underline{K}_o^- = \vec{DO}$ lie on the sphere of radius K around O and have the same x-y-component $\underline{\tilde{k}}$, whereas $\underline{K}_{\underline{\ell}}^+ = \vec{BH}$ and $\underline{K}_{\underline{\ell}}^- = \vec{CH}$ have the x-y-component $\underline{\tilde{k}}+\underline{\ell}$ and lie on the sphere around H. In the crystal we get four Blochwaves $\underline{k}_j = (\underline{\tilde{k}}, k_{jz})$ where k_{jz} are determined by the dispersion relation

$$(47)\quad (K_o^2 - \underline{\tilde{k}}^2 - k_z^2)\,(K_o^2 - (\underline{\tilde{k}}+\underline{\ell})^2 - k_z^2) = |v_{\underline{h}}|^2$$

The dispersion surface as well as $\underline{k}_1, \ldots, \underline{k}_4$ are shown

in Fig. 21. Note that the radius $K_o = \sqrt{K^2 - v_o}$ is larger than K for electrons. However the difference $\frac{K_o - K}{K} \approx -\frac{1}{2}\frac{v_o}{K^2}$, is extremely small for high energy electrons and is very much enhanced in Fig. 21. For instance, for E = 100 keV and $-V_o$ = 10eV one gets $5 \cdot 10^{-5}$. Therefore the vectors $\underline{K}$, $\underline{k}_1$ and $\underline{k}_2$ in Fig. 21 practically coincide.

In order to determine the Bloch wave coefficients $P_1, \ldots, P_4$, we have to solve the equations (35) and (36), which are in our case

$$(48) \quad z=0: \quad 1 = \sum_{j=1}^{4} \frac{k_{jz}+K_z}{2K_z} \, C_o^j \, P_j$$

$$0 = \sum_{j=1}^{4} \frac{k_{zj}+K_z}{2K_z} \, C_{\underline{g}}^j \, P_j$$

$$(49) \quad z=d: \quad 0 = \sum_{j=1}^{4} \frac{k_{jz}-K_z}{2K_z} \, C_o^j \, e^{i(k_{jz}-K_z)d} \, P_j$$

$$0 = \sum_{j=1}^{4} \frac{k_{jz}-K_z}{2K_z} \, C_{\underline{g}}^j \, e^{i(k_{jz}-K_z)d} \, P_j$$

Near the Bragg condition the factor $(k_{jz}+K_z)/2K_z$ has the order of magnitude

$$(50) \quad \frac{k_{jz}+K_z}{2K_z} = \begin{cases} 1+O(10^{-4}) & j=1 \text{ and } 2 \\ \text{for} & \\ O\,(10^{-4}) & j=3 \text{ and } 4 \end{cases}$$

Therefore the coefficients P_3 and P_4 practically do not enter into the equations (48). Moreover one sees from the equations (49) containing the factors $\frac{k_{jz}-K_z}{2K_z}$ that P_3 and P_4 themselves are of the order of 10^{-4}. Therefore the error in (48) by neglecting P_3 and P_4 is of the order of 10^{-8} only. The reflection coefficients $R_{\underline{g}}$ are according to (31,32) given by

$$(51) \qquad R_{\underline{g}} = \sum_{j,g} \frac{-k_{jz}+K_z}{2K_z} \; C^{\,j}_{\underline{g},g} \; P_j$$

It can be seen, that R_o and $R_{\underline{g}}$ are of the order of 10^{-4}, too. Therefore in the vacuum we practically have only the incident wave $\underline{K}$ and the transmitted wave $\underline{K}^+_{\underline{g}}$, whereas in the crystal only the two Bloch waves $\underline{k}_1$ and $\underline{k}_2$ are important. For P_1 and P_2 we get the"simplified" boundary conditions:

$$(52 \qquad 1 = C^1_o \; P_1 + C^2_o \; P_2 \quad \text{and} \quad 0 = C^1_{\underline{h}} \; P_1 + C^2_{\underline{h}} \; P_2$$

the solutions of which are very simple. The $C_{\underline{h}}{}^j$'s are given by (2,80). By comparing with (2.83) we get:

$$(53) \qquad P_j = C_o{}^j \quad , \quad j = 1,2$$

From (33) we get then for the transmission-coefficients T_o and $T_{\underline{g}}$:

$$(54) \qquad T_o = \sum_{j=1}^{2} (C_o{}^j)^2 \; e^{i(k_{jz}-K_z)d}$$

$$T_{\underline{g}} = \sum_{j=1}^{2} C_o{}^j \; C^{\,j}_{\underline{g}} \; e^{i(k_{jz}-K_z)d}$$

For the difference $k_{z1} - k_{z2}$ we obtain from (47)

$k_{z1} - k_{z2} = \Delta k \sqrt{1+W^2}$

where Δk and W are given by (2.77) and (2.79). Further using (2.80) we get after some calculation

$$(55) \qquad |T_o|^2 = \frac{W^2}{1+W^2} + \frac{1}{1+W^2} \cos^2\left(\frac{\Delta kd\sqrt{1+W^2}}{2}\right)$$

$$|T_{\underline{h}}|^2 = \frac{1}{1+W^2} \sin^2\left(\frac{\Delta kd\sqrt{1+W^2}}{2}\right)$$

From this one verifies that

$$(56) \qquad |T_o|^2 + |T_{\underline{h}}|^2 = 1$$

which is in agreement with the current conservation (42) due to $R_{\underline{h}} \cong 0$ and $K_{z\underline{h}} \cong K_z$.

Exactly in the Bragg condition (W = 0) we get

$$(57) \qquad |T_o|^2 = \cos^2 \frac{\Delta kd}{2}$$

$$|T_{\underline{h}}|^2 = \sin^2 \frac{\Delta kd}{2}$$

which represents the socalled "pendulum solution". By varying the thickness the intensity oscillates between the transmitted wave $\underline{K}$ and the reflected wave $\underline{K}+\underline{h}$. The length for a complete oscillation is the extinction length $d_{ext} = \frac{2\pi}{\Delta k}$ (2.77), whose name refers to the extinction of the primary wave $\underline{K}$ for $d = \frac{1}{2} d_{ext}$.

From (53) and (2.80) we obtain for the wave field in the crystal

$$(58)\quad \psi(\underline{r}) = e^{i\underline{k}_B\underline{r}}\, e^{i\delta\underline{k}\underline{r}} \left\{ \cos\left(\frac{\Delta k}{2}\sqrt{1+W^2}\, z\right) + \right.$$

$$\left. + i\,\frac{1}{\sqrt{1+W^2}}\left(e^{i\underline{h}\underline{r}} + W\right)\sin\left(\frac{\Delta k}{2}\sqrt{1+W^2}\, z\right)\right\}$$

with $\underline{k} = \underline{k}_B + \delta\underline{k}$, $\delta\underline{k}^{1,2} = \left\{\delta\underline{k},\ \pm\frac{\Delta k}{2}\sqrt{1+W^2}\right\}$

and where Δk and W are given by (2.77) and 2.79).

Also at the wave field we can see the "pendulum solution". Namely for W = 0 we get $\left(\underline{k}_B = (\underline{k}_1+\underline{k}_2)/2\right)$

$$(59)\quad \psi(\underline{r}) = e^{i\underline{k}_B\underline{r}}\ \cos\left(\frac{\Delta k z}{2}\right) + i\, e^{i(\underline{k}_B+\underline{h})\underline{r}}\ \sin\left(\frac{\Delta k z}{2}\right)$$

The plane waves $\underline{k}_B$ and $\underline{k}_B+\underline{h}$ have a depth dependent amplitude. The whole wave field is schematically shown in Fig. 22a. For $|W| \gg 1$ we get the kinematical result, namely

$$(60)\quad \psi(\underline{r}) = e^{i\underline{k}\underline{r}} + \frac{i}{|W|}\ e^{i(\underline{k}_B+\delta\underline{k}+\underline{h})\underline{r}}\ \sin\frac{\Delta k\,|W|\,z}{2}$$

In this case the primary wave has the amplitude 1, whereas the reflected wave being only weakly excited has a faster oscillating modulation factor. (Fig. 22b). In an absorbing crystal, we have to consider that the two Bloch waves $\underline{k}_1$ and $\underline{k}_2$ are absorbed very differently as has been discussed in section 2.6. The Bloch wave of type II (Fig.14) lying for $v_{\underline{h}} < 0$ on the inner branch of the dispersion surface has an anomalously low absorption, whereas the Bloch wave on the outer branch has a much stronger

absorption (Fig. 15). For very thick crystals only the wave field II remains. Because the pendulum solution is due to the interference of the Bloch wave I and II, it is diminished for thicker crystals and disappears totally for very large ones [5-12].

Finally we want to discuss some aspects of the general Laue-case with many beams. Here we can use successfully the orthogonality relations for the Bloch functions on the dispersion surface (section 2.8). By assuming, that all reciprocal lattice vectors $\underline{h}=(\underline{\kappa},g)$ have a different planar component $\underline{\kappa}$ and give rise to transmitted beams only, we obtain from (31), since all $R_{\underline{h}} \cong 0$:

$$(61) \quad \delta_{\underline{h},o} = \sum_{j} P_j \; C_{\underline{h}}(\underline{k}_j)$$

These equations for the coefficients P_j can directly been solved by using the orthogonality relation (2.114). First we have $\underline{k}_j=(\underline{K},k_{zj})=\underline{K}+\{0,\delta k_j\}$, i.e. the direction $\underline{n}$ in (2.114) coincides with the z-axis. Since we consider transmitted beams only with $\cos\Theta_{\underline{h}}=\frac{(\underline{K}+\underline{h})_z}{K+h} > 0$, and if $V(\underline{r})$ is real, we obtain from (2.114) further

$$(62) \quad \sum_{\underline{h}} C^*_{\underline{h}}(\underline{k}_{j'}) \; C_{\underline{h}}(\underline{k}_j) \; \cos\Theta_{\underline{h}} = \delta_{j',j} \qquad (*)$$

Then by multiplying (61) with $C^*_{\underline{h}}(\underline{k}_{j'}) \cos\Theta_{\underline{h}}$ and summing over $\underline{h}$ we get the result

$$(63) \quad P_j = C^*_o(\underline{k}_j) \cos\Theta_o$$

Under the same conditions the transmission coefficients $T_{\underline{h}}$ of (33) are given by

---

(*) Note, that for j'=j the normalisation is quite different from the one used normally $\left(\sum_{\underline{h}} |C_{\underline{h}}|^2 = 1;\ \text{equ. } 2.26\right)$.

$$(64) \qquad T_{\underline{h}} = \sum_{j} C_o^*(\underline{k}_j)\, C_{\underline{h}}(\underline{k}_j)\, \cos\Theta_o\, e^{i\delta k_j d}$$

It is interesting to see, that in this case the flux incident on the crystal is totally transmitted, since $V(\underline{r})$ is real and there are no reflected beams. Indeed we get from the current conservation (42)

$$(65) \qquad \bar{j}_z^{So} = \frac{\hbar}{m} K_z = \frac{\hbar}{m} K \sum_{\underline{h}} \cos\Theta_{\underline{h}}\, |T_{\underline{h}}|^2$$

which can directly been verified by using (2.114) and (64).

If the potential is complex ($V=V^{\dagger}$), then we can use equation (2.115) to get a similar relation for $T_{\underline{h}}$. Of course the current is then no longer conserved.

3.6. Symmetrical Bragg Case

In the symmetrical Bragg case the reflecting planes lie parallel to the surface and we have $\underline{h} = (0,-h)$ as shown in Fig 23. For high energy electrons the Bragg case only can be realized by nearly glancing incidence which is due to the small Bragg angles. However this does not apply to LEED or to neutrons. Here we will consider only the reflection at a half crystal, whereas for the scattering at a slab we refer to the literature [5-12]

In the vacuum we have first the incident plane wave $\underline{K} = (\underline{\kappa}, K_z)$ being equal to $\vec{AO}$ in Fig. 23. Moreover the vector $\vec{DH}$ is equal to $\vec{AO}$ and represents no new wave. All other allowed waves have to lie on one of the two spheres with radius K and have the same x-y-component $\underline{\kappa}$. Because $\vec{BH} = \vec{CO}$, only one additional wave remains, namely the specularly reflected wave $\underline{K}_o^- = (\underline{\kappa}, -K_z) = \vec{BH}$.

For the crystal we get four wave vectors $\underline{k}_1, \ldots, \underline{k}_4$ all having the same x-y-component $\underline{\kappa}$ and being marked by the points $1,\ldots,4$ in Fig 23. However $\underline{k}_3$ and $\underline{k}_4$, being essentially equivalent to $\underline{k}_2$ and $\underline{k}_1$, respectively, do not lie in the first Brillouin zone and have to be omitted. Further only $\underline{k}_1$ has a positive group

velocity (37) in z-direction, but not $\underline{k}_2$. Therefore we get only one allowed Bloch wave for the half crystal. For a slab both $\underline{k}_1$ and $\underline{k}_2$ are allowed leading to oscillations in the reflected intensity as in the Laue case.[24]

Let us have a closer look at the dispersion surface in the vicinity of the Bragg spot $\underline{k}_B$. According to (2.76) we have with the x- and z-coordinates as in Fig. 23

$$(66) \qquad \delta k_x^2 - \delta k_z^2 \, tg^2\theta_B = \frac{|v_{\underline{h}}|^2}{4K_o^2 \cos^2\theta_B}$$

For real δk_x and δk_z this represents a hyperbola as has already been discussed in section 2.6. However for $|\delta k_x| < \frac{|v_{\underline{h}}|}{2K \cos\theta_B}$, i.e. between the branches of the hyperbola, δk_z is complex. Setting $\delta k_z = i\delta k_z''$, the dispersion surface in the $\{\delta k_x , \delta k_z''\}$ plane is an ellipse. The maximum value of $\delta k_z''$ is $\delta k_{max}'' = \frac{|v_{\underline{h}}|}{h}$, representing the exponential attanuation of the wave field in the crystal.

By enlarging the x-y-component $\underline{\alpha}$ of the incident wave in Fig. 23 the Bloch vector $\underline{k}_1$ moves along the dispersion surface as indicated by arrows in Fig. 24. For the case of no absorption it follows from the current conservation (43) that $|R_o|^2 = 1$ as long as $\underline{k}_1$ is complex, because we only have one reflected wave and one Bloch wave which carries no current.

The boundary conditions at the surface z = 0 are (31, 32)

$$(67) \qquad 1 + R_o = (C_o + C_{\underline{h}})\ P_1$$

$$1 - R_o = \left(\frac{k_z}{K_z}\ C_o + \frac{k_z - h}{K_z}\ C_{\underline{h}}\right) P_1$$

For high energies we have $K_z \cong k_z \cong \frac{h}{2}$. Therefore we get immediately

$$(68) \qquad R_o = \frac{C_{\underline{h}}}{C_o} \qquad \text{and } P_1 = \frac{1}{C_o}$$

Near the Bragg reflections one has

$$(69) \qquad \frac{C_{\underline{h}}}{C_o} = \frac{V_h}{K_o^2 - (\underline{k}+\underline{h})^2} \cong \frac{V_{\underline{h}}}{-2K_o \cos\theta_B\ \delta k_x + h\delta k_z}$$

By using (66) we get therefore

$$(70) \qquad |R_o|^2 = \left| \frac{1}{-y \pm \sqrt{y^2-1}} \right|^2$$

$$\text{with} \quad y = 2\,\frac{\delta k_x}{\Delta k} = \frac{2K_o \cos\theta_B\ \delta k_x}{|V_h|}$$

Here the + sign is valid on the outer branch of the hyperbola and on the ellipse in Fig. 24 where the - sign refers to the inner branch. For $|y| \leq 1$, i.e. for δk_x between the two branches of the hyperbola, the reflection coefficient $|R_o|^2 = 1$. As a function

of y the reflection coefficient $|R_o|^2$ is shown in Fig. 25a. It decreases rapidly for $y > 1$.

In the case of absorption the result is elementary but rather lengthy. Here we give only the results for weak absorption and for

$\delta k_x = \pm \frac{\Delta k}{2}$ and $\delta k_x = 0$. By writing $v_o = v_o' + iv_o''$, and $v_{\underline{h}} = v_{\underline{h}}' + iv_{\underline{h}}''$ one obtains for $|v_o''| \ll |v_o'|$ and $|v_{\underline{h}}''| \ll |v_{\underline{h}}'|$:

$$(71) \qquad |R_o|^2 = \begin{cases} 1 - 2\sqrt{\left|\frac{v_o'' - v_{\underline{h}}''}{v_{\underline{h}}'}\right|} & \delta k_x = \frac{\Delta k}{2} \\ 1 - 2\left|\frac{v_o''}{v_{\underline{h}}'}\right| & \text{for} \quad \delta k_x = 0 \\ 1 - 2\sqrt{\left|\frac{v_o'' + v_{\underline{h}}''}{v_{\underline{h}}'}\right|} & \delta k_x = -\frac{\Delta k}{2} \end{cases}$$

First we see, that at the edges of the two branches the absorption is especially effective and $|R_o|^2$ decreases with the square root of the perturbation. However the correction is different on both branches, which is due to the different Bloch waves on both branches. On the inner branch the Bloch wave of type II avoids the atoms and is absorbed weaker than Bloch wave I (Fig. 14). In Fig. 25b we have plotted $|R_o|^2$ for $v_o'' = v_{\underline{h}}''$ and for $\left|v_o''/v_{\underline{h}}'\right| = 0{,}1$ (full lines). Physically $v_o'' = v_{\underline{h}}''$ means that the atoms are treated as points as far as absorption is concerned. Therefore the sin-wave of Fig. 14 cannot be absorbed and $|R_o|^2 = 1$ on the edge of the

inner branch. For the case of a uniform absorption ($v_{\underline{h}}'' = 0$) the reflection is symmetrical with respect to $\delta' k_x = 0$ because then the absorption is the same for both Bloch waves.(dashed lines in Fig. 25b). All three curves in Fig. 24 can be obtained experimentally. E.g., for neutrons the absorption is negligible and one gets for thick crystals the reflection curve of Fig. 25a. In the X-ray case the photoelectric absorption is concentrated at the inner shells resulting in a strong anomalous transmission effect and in asymmetrical curves as in Fig. 25b. For LEED the plasma losses give a uniform absorption and the reflection curve should be more or less symmetrical. However here the simple two-beam approximation does not apply and the situation is much more complicated.

4. Single Scattering Matrices and Neutron Scattering

In diffraction experiments with low energy electrons the energy is typically of the order of 50 eV and therefore comparable with the mean potential V_o or the potential of a single atom. Such low energies give rise to many complications. One of these is due to the fact that even the interaction with an isolated atom can no longer be calculated by Born's approximation but has to be treated exactly. With respect to this, the situation is even worse for thermal neutron scattering where the, extremely short range, interaction with the nucleus is of the order of several tens of MeV, compared with the neutron energy of $\cong$ 0,025 ev. Here the interaction potential normally is replaced by Fermi's pseudo potential [25]. However this procedure is restricted to the first Born approximation. A dynamical theory has to reconsider this problem as was done first in [26]. In the first section we will show, that the difficulty due to the strong single particle interaction can be overcome by the introduction of single scattering matrices.

4.1. Multiple Scattering with Single Scattering Matrices. [27]

We start with the Lippmann-Schwinger equation which is the operator version of the integral equation (3.4.)

$$(1) \quad \Psi = \varphi + G_o V \Psi \quad \text{with} \quad G_o = \frac{1}{E+i\varepsilon-H_o}$$

Here φ stands for the incident wave $\varphi(\underline{r}) = e^{i\underline{K}\underline{r}}$

and $G_o(\underline{r},\underline{r}')$ is the free Green's function (3.4).

Equation (1) also can be written in the form

$$(2) \quad \Psi = \varphi + G_o\, T\, \varphi$$

where the transition or scattering matrix T is given by

$$(3) \quad T = V \frac{1}{1-G_oV} = \frac{1}{1-VG_o} V = V + VG_oV + \ldots.$$

$$= V + VG_oT = V + TG_oV$$

Considering the scattering by many centres, the potential V is a sum of the single-centre contributions $v_n(\underline{r})$.

$$(4) \quad V(\underline{r}) = \sum_n v_n(\underline{r}) = \sum_n v(\underline{r}-\underline{R}^n) \quad , \text{ if all centres are equal.}$$

Now the scattering by the potential v_n alone can be described by the single scattering matrix t_n.

$$(5) \quad t_n = v_n \frac{1}{1-G_ov_n} = v_n + v_n\, G_o\, t_n$$

For we get $T = t_n$, if only the centre n is present ($V = v_n$). In analogy to the incident wave in (2) we introduce an "effective incident wave" φ_n for the atom n by writing

$$(6) \quad \Psi = \varphi_n + G_o\, t_n\, \varphi_n$$

By multiplying (6) with v_n and using (5) one gets

$$(7) \qquad v_n \psi = t_n \varphi_n$$

Introducing this into the Lippmann-Schwinger equation (1) the wave function ψ can be expressed in terms of the effective fields φ_m.

$$(8) \qquad \psi = \varphi + G_o \sum_m t_m \varphi_m$$

Moreover, by comparing this with the defining equation (6) the φ_n's have to be solutions of the coupled equations

$$(9) \qquad \varphi_n = \varphi + \sum_{m(\neq n)} G_o \, t_m \varphi_m$$

Therefore the effective incident field φ_n for the centre n consists of the incident plane wave φ plus the scattered waves $G_o \, t_m \varphi_m = G_o \, v_m \psi$ from the other centres $m \neq n$, as is illustrated in Fig. 26. These equations have the advantage of clearly separating the scattering properties of the single centres, given by t_m, from the multiple scattering properties of the whole system. However we have paid for this by getting a system of coupled equations (9) instead of the single equation(1).

For convenience we may also write (8) and (9) in the $\underline{r}$-representation. Considering that for equal centres $v_n(\underline{r}) = v\,(\underline{r}-\underline{R}_n)$ and consequently $t_n(\underline{r},\underline{r}') = t(\underline{r}-\underline{R}^n,\underline{r}'-\underline{R}^n)$ we get

$$(8a) \qquad \psi(\underline{r}) = e^{i\underline{K}\underline{r}} + \int d\underline{r}'\, d\underline{r}''\, G_o(\underline{r}-\underline{r}') \sum_n t(\underline{r}'-\underline{R}^n,\underline{r}''-\underline{R}^n)\varphi_n(\underline{r}'')$$

and

$$(9a)\quad \varphi_n(\underline{r}) = e^{i\underline{K}\underline{r}} + \int d\underline{r}'d\underline{r}''\; G_o(\underline{r}-\underline{r}') \cdot \cdot \sum_{m(\neq n)}{}' t(\underline{r}'-\underline{R}^m, \underline{r}''-\underline{R}^m)\; \varphi_m(\underline{r}'')$$

From (8) or (8a) one can get a modified Born approximation by replacing the effectiv field φ_m by the incident field φ.

$$(10)\quad \Psi \cong \varphi + G_o \sum_m t_m\, \varphi$$

This approximation, known as pseudo-kinematical theory in LEED, goes over into the usual Born approximation (kinematical theory) if t_m is replaced by v_m. However (10) has the advantage that the single-scattering process is treated exactly, whereas the multiple scattering by different centres is still neglected.

In an <u>infinite crystal</u> the eigenfunctions $\phi(\underline{r})$ for an energy E obeys the homogeneous equation

$$(11)\quad \phi = G_o\, V\, \phi$$

Here one can as well replace G_o by the advanced Green's function or by the principle value Green's function, i.e.

$$(12)\quad \frac{1}{E-i\varepsilon-H_o} \quad \text{or} \quad P\left(\frac{1}{E-H_o}\right)$$

By choosing the eigenfunctions ϕ as Bloch waves, we have

$$(13) \qquad \phi_{\underline{k}}(\underline{r}+\underline{R}^m) = e^{i\underline{k}\underline{R}^m}\,\phi_{\underline{k}}(\underline{r})$$

Using (13) and the periodicity of $V(\underline{r}) = \sum_n v(\underline{r}-\underline{R}^n)$, equation (11) can be written in the interesting form

$$(14a) \qquad \phi_{\underline{k}}(\underline{r}) = \int_{V_c} d\underline{r}'\; G(\underline{r},\underline{r}')\; V(\underline{r}')\; \phi_{\underline{k}}(\underline{r}')$$

$$(14b) \qquad = \int_{-\infty}^{+\infty} d\underline{r}'\; G(\underline{r},\underline{r}')\; v(\underline{r}')\; \phi_{\underline{k}}(\underline{r}')$$

Here either the integration is restricted to one lattice cell only (14a) or the integral only contains the single potential $v(\underline{r})$ (14b). Further the Green's function G, called complete Greenian by Ziman [28], is

$$(15) \qquad G(\underline{r},\underline{r}') = \sum_n G_o(\underline{r}-\underline{r}'+\underline{R}^n)\; e^{-i\underline{k}\underline{R}^n}$$

It depends explicitly on $\underline{k}$ and not only on E as G_o does. With respect to $\underline{r}$, it has the same translation property (13) as $\phi_{\underline{k}}$.

By introducing the t_n-matrices by (5) and the effective fields φ_n as in (6) we may also write equation (11) in the form

$$(16) \qquad \phi = G_o \sum_n t_n\, \varphi_n \quad \text{and} \quad \varphi_n = G_o \sum_{m(\neq n)} t_m\, \varphi_m$$

which is quite analogous to the multiple scattering equations (8) and (9). Further one can see from (6) or (16) that the quasi-periodicity (13) also leads to a periodicity condition for the corresponding

effective field φ_n , namely

$$(17) \quad \varphi_{n+m}(\underline{r}+\underline{R}^m) = e^{i\underline{k}\underline{R}^m} \varphi_n(\underline{r})$$

Therefore all effective waves φ_n can be reduced to a single one, for instance φ_o . By doing this we get from equation (13) in the $\underline{r}$-representation

$$(18) \quad \phi(\underline{r}) = \int d\underline{r}' d\underline{r}'' \; G(\underline{r},\underline{r}') \; t(\underline{r}',\underline{r}'') \; \varphi_o(r'')$$

$$(19) \quad \varphi_o(\underline{r}) = \int d\underline{r}' d\underline{r}' \; G'(\underline{r},\underline{r}') \; t(\underline{r}',\underline{r}'') \; \varphi_o(\underline{r}'')$$

with

$$(20) \quad G'(\underline{r},\underline{r}') = \sum_{n\neq 0} G_o(\underline{r}-\underline{r}'+\underline{R}^n) \; e^{-i\underline{k}\underline{R}^n}$$

$$= G(\underline{r},\underline{r}') - G_o(\underline{r},\underline{r}')$$

These equations can also be obtained directly from (14b) by substituting $v(\underline{r}') \; \phi(\underline{r}')$ by $t \; \varphi_o$.

4.2. Scattering by Muffin-Tin Potentials

Now we apply the multiple scattering equations of the last section to a system of spherically symmetric , but non-overlapping potentials. Then the potential $v(\underline{r})$ of a single centre is

$$(21) \quad v(\underline{r}) = \begin{cases} v(|\underline{r}|) & < \\ & \text{for } r \quad r_s \\ 0 & > \end{cases}$$

In order to get no overlap between the potentials of the different atoms, r_s has to be smaller than $d_{nn}/2$, where d_{nn} is the nearest neighbour distance. Such potentials, known as "muffin-tin potentials", have been used extensively for band structure calculations [29]

By substituting $\underline{r}-\underline{R}^n \to \underline{r}$ and $\underline{r}'-\underline{R}^m \to \underline{r}'$ etc., into (9a), we get

$$(22)\quad \varphi_n(\underline{R}^n+\underline{r}) = e^{i\underline{K}\underline{R}^n+i\underline{K}\underline{r}} + \int d\underline{r}'\,d\underline{r}'' \sum_{m(\neq n)} G_o(\underline{r}-\underline{r}'+\underline{R}^n-\underline{R}^m) \cdot \cdot t(\underline{r}',\underline{r}'')\,\varphi_m(\underline{R}^m+\underline{r}'')$$

The free Green's function G_o, given by (3.4) satisfies the Schroedinger equation

$$(23)\quad \left(-\frac{\hbar^2}{2m}\partial_{\underline{r}}^2 - \frac{\hbar^2K^2}{2m}\right) G_o(\underline{r}-\underline{r}'+\underline{R}^n-\underline{R}^m) = -\delta(\underline{r}-\underline{r}'+\underline{R}^n-\underline{R}^m)$$

The same equation holds, if $\partial_{\underline{r}}$ is replaced by $\partial_{\underline{r}'}$. For $r \leq r_s < \frac{d_{nn}}{2}$ and $r' \leq r_s$ the source term in (23) vanishes and G_o satisfies the potential-free Schroedinger equation in these regions. The same applies to the incident wave $e^{i\underline{K}\underline{r}}$, of course. Then it follows from (22) that $\varphi_n(\underline{R}^n+\underline{r})$ satisfies the potential free Schroedinger equation for $r \leq r_s$, too. Therefore, by expanding $\varphi_n(\underline{R}^n+\underline{r})$ (or G_o and $e^{i\underline{K}\underline{r}}$) into spherical har-

monics $Y_{\ell m}\left(\frac{r}{r}\right)$, the radial function $R_\ell(r)$ satisfies the equation:

$$(24) \quad \left\{-\frac{1}{r}\partial_r^2\, r + \frac{\ell(\ell+1)}{r^2} - K^2\right\} R_\ell(r) = 0$$

for $r \leq r_s$.

For given K there are two linearly independent solutions namely the spherical Bessel functions $j_\ell(Kr)$ and $n_\ell(Kr)$. They are elementary functions and behave as

$$(25) \quad j_\ell(x) = \sqrt{\frac{\pi}{2x}}\, J_{\ell+1/2}(x) \to \frac{1}{x}\sin(x-\ell\pi/2) \text{ for } |x|\gg 1$$

$$\to \frac{\sqrt{\pi}}{2^{\ell+1}\Gamma(\ell+\frac{3}{2})}\, x^\ell \text{ for } |x|\ll 1$$

$$(26) \quad n_\ell(x) = \sqrt{\frac{\pi}{2x}}\, J_{-\ell-1/2}(x) \sim \frac{1}{x^{\ell+1}} \quad \text{for } |x| \ll 1$$

Here $J_{\ell+1/2}(x)$ is an ordinary Bessel function. The $n_\ell(x)$ functions are singular in the origin and therefore give no contribution. Thus the following expansion for φ_n is valid for $r \leq r_s$:

$$(27) \quad \varphi_n(\underline{R}^n+\underline{r}) = \sum_L i^\ell \varphi_L^n\, j_\ell(Kr)\, Y_L\left(\frac{\underline{r}}{r}\right)$$

Here the index $L = (\ell, m)$ stands for the angular momentum index ℓ and for the magnetic index m. The φ_L^n's are unknown coefficients, and the spherical har-

monics are orthonormalized.

$$(28)\quad \int d\Omega\, Y_{L'}^{*}\left(\frac{\underline{r}}{r}\right) Y_{L}\left(\frac{\underline{r}}{r}\right) = \delta_{L,L'} = \delta_{\ell,\ell'}\,\delta_{m,m'}$$

Similarly we get a double expansion for $G_o = G_o(\underline{r},\underline{r}')$ for $r \leq r_s$ and $r' \leq r_s$.

$$(29)\quad G_o(\underline{r}-\underline{r}'+\underline{R}^n-\underline{R}^m) = \frac{2m}{\hbar^2} \sum_{L,L'} i^{\ell-\ell'}\, G^{n-m}_{L,L'} \cdot$$

$$\cdot\; j_\ell(Kr)\; j_{\ell'}(Kr')\; Y_L\left(\frac{\underline{r}}{r}\right) Y_{L'}^{*}\left(\frac{\underline{r}}{r}\right)$$

The corresponding expansion for $e^{i\underline{K}\underline{r}}$ is [30]

$$(30)\quad e^{i\underline{K}\underline{r}} = \sum_{L} i^{\ell}\, 4\pi\, Y_L^{*}\left(\frac{\underline{K}}{K}\right)\; j_\ell(Kr)\; Y_L\left(\frac{\underline{r}}{r}\right)$$

Further, due to the rotation invariance of $v(r)$, the scattering matrix $t(\underline{r},\underline{r}')$ depends only on r,r' and the angle Θ between $\underline{r}$ and $\underline{r}'$. Therefore an expansion of the form

$$(31)\quad t(\underline{r},\underline{r}') = \sum_{\ell} \frac{2\ell+1}{4\pi}\, t_\ell(r,r')\, P_\ell\,(\cos\Theta)$$

$$= \sum_{L} t_\ell(r,r')\; Y_L\left(\frac{\underline{r}}{r}\right) Y_L^{*}\left(\frac{\underline{r}'}{r}\right)$$

holds, where for the last line we have used the addition theorem for spherical harmonics [30]. Now, we introduce the expansions (27,29,30,31) in equation (22) and obtain by using the orthogonality of the Y_L's:

$$(32)\quad \varphi_L^n = e^{i\underline{K}\underline{R}^n} \cdot 4\pi Y_L^*\left(\frac{\underline{K}}{K}\right) + \sum_{\substack{m(\neq n)\\ L'}} G_{L,L'}^{n-m}\, \tau_\ell\, \varphi_{L'}^m$$

Here τ_ℓ is given by

$$(33)\quad \tau_\ell = \int_0^\infty r'^2 dr' r''^2 dr''\; j_\ell(Kr')\; t_\ell(r',r'')\; j_\ell(Kr'')$$

$$= -\frac{1}{K} e^{i\delta_\ell} \sin\delta_\ell$$

as can be shown by partial wave analysis. δ_ℓ is the phase shift of the ℓ^{th} partial wave. Thus we have reduced the solution of the integral equation (22) to the solution of the algebraic equations (32). This was only possible because the single potentials do not overlap what we have used explicitly in the expansions (27,29). The division into single centre properties and properties of the whole system is still apparent in (32). All the information we need about the single potential is contained in τ_ℓ or in the phase shifts δ_ℓ, whereas the coefficients $G_{L,L'}^{n-m}$ are determined by the structure of the system alone. Further, we should point out that by knowing the coefficients φ_L^n and the effective fields $\varphi_n(\underline{r})$ we simply can get the wave function Ψ from (8a).

The solution of the algebraic equations (32) for a crystal slab or half crystal is still a formidable problem because of the infinite number of atoms and angular momenta involved. Of some help is here the x-y-periodicity, which reduces all effective fields

of the same atomic layer in the x-y-plane to a single field for each layer. Namely, in analogy to (17) we have for a "plane" translation $\underline{\mathcal{R}}^m$.

$$(34) \quad \varphi_{n+m}(\underline{r}+\underline{\mathcal{R}}^m) = e^{i\underline{k}\underline{\mathcal{R}}^m} \varphi_n(\underline{r})$$

Therefore the number of unknown φ_L^n 's in (32) is the product of the number of atomic layers times the number of angular momenta considered. An especially simple but also instructive problem is the case of a monolayer of atoms scattering isotropically (L = 0). For this we only have one constant, say φ_o^o . The result, given in [22,31], shows interesting resonances, which are due to quasi-localized surface states, as well as certain threshold effects connected with "surface waves".

For a real crystal one may either try to solve the equations connecting the different monolayers. This method, proposed by Beeby [32], has been successfully used for LEED in [33] . Or one may try to solve the equations for an infinite crystal, as will be shown below. Then one has to match the allowed Bloch waves and allowed plane waves at the crystal surfaces. This method has been used in LEED, too [34].

To obtain the Bloch wave $\phi_k(\underline{r})$ (18) for an infinite crystal we have to solve the equation (19) for the effective field φ_o. Again for muffin-tin potentials $\varphi_o(\underline{r})$ and the Green's function $G'(\underline{r},\underline{r}')$ satisfy for $r,r' \leq r_s$ the potential-and source-free Schroedinger equation. Therefore we get expansions of the form

$$(35)\quad \varphi_0(\underline{r}) = \sum_L i^\ell \varphi_L\, j_\ell(Kr)\; Y_L\left(\frac{\underline{r}}{r}\right) \text{ for } r \leq r_s$$

$$(36)\quad G'(\underline{r},\underline{r}') = \sum_{L,L'} i^{\ell-\ell'} G_{LL'}\, j_\ell(Kr) j_{\ell'}(Kr') \; Y_L\left(\frac{\underline{r}}{r}\right)\; Y_{L'}^{*}\left(\frac{\underline{r}'}{r}\right) \quad \text{for } r,r' \leq r_s$$

Introducing these relations into (19) and using the expansion for $t(\underline{r},\underline{r}')$ (31), we get the homogeneous equations

$$(37)\quad \varphi_L = \sum_{L'} G_{LL'}\, \tau_{\ell'}\, \varphi_{L'}$$

They have only solutions, if the dispersion condition

$$(38)\quad \det \left| G_{LL'}\, \tau_{\ell'} - \delta_{L,L'} \right| = 0$$

is satisfied connecting the allowed $\underline{k}$- and E-values. This is the t-matrix version [35] of the Korringa-Kohn-Rostoker-method (KKR-method) for band structure calculation [36]. In practical cases the evaluation of the "structure constants" $G_{LL'}$ represents most of the work. They only depend on the structure of the crystal and on the energy and Bloch vector, but not on the potential. There exists a large number of different expressions for $G_{LL'}$, which can be evaluated from (20). However none of them is especially simple and hence we refer to the original articles [36]. For cubic lattices and for symmetry directions of $\underline{k}$ the coefficients have been calculated numerically.

For the case of s-scattering only, the determinant simply gives $G_{oo}\ \tau_o = 1$. This case is essentially equivalent to the treatment in the following section.

4.3. Diffraction of Neutrons

In this section we want to apply the multiple scattering equations to the diffraction of neutrons by an ideal crystal. However let us first discuss the scattering by a single nucleus. Because the wave length ($\sim$1Å) is very much larger than the radius r_o of the nucleus ($\sim 10^{-13}$cm), we only have s-scattering. For the evaluation of the scattering amplitude, we can set the energy E = 0. The case of higher energies is discussed later on. Then we get from the Schroedinger equation for E = 0:

$$(39)\quad \left(\partial_r^2 - v(r)\right) r\psi(r) = 0$$

If $v(r) = 0$ for $r \geq r_o$, then $\psi(r)$ behaves as

$$(40)\quad \psi(r) = 1 - \frac{a_o}{r} \quad \text{or} \quad r\psi(r) = r - a_o \quad \text{for } r \geq r_o$$

The real constant a_o is the scattering length for E=0 which is connected with the cross section by $\sigma = 4\pi a_o^2$. Graphically the scattering length can be obtained by the intersection of straight line $r-a_o$ with the r axis (Fig. 27). For an attractive potential ($v(r) < 0$) the curvature of $r\psi$ is according to (39) negative, if $r\psi$ is positive and vice versa. Further $r\psi$ vanishes at the origin. For a relatively weak, but negative potential we may therefore get the curve

of Fig. 27a, leading to a negative scattering length. If the potential strength increases, then a_o goes to $-\infty$ and the cross section diverges. This is due to the fact that there exists a bound state with zero energy in this case. Namely for a bound state with energy $E = -\frac{\hbar^2 \varkappa^2}{2m}$, the wave function for $r \geq r_o$ is $r\psi(r) \sim e^{-\varkappa r}$, which gives a constant for $\varkappa = 0$. But this is equivalent to the condition $a_o \to \pm\infty$. By further increasing the strength of the potential, we get a curve as shown in Fig. 27b, resulting in a positive scattering length. Further $r\psi(r)$ has now an extrema for $r \leq r_o$ which is connected with the bound state of the potential. By further increasing the potential, a_o will become negative again, etc. Whenever a_o goes to $-\infty$, a new bound state with energy $E = 0$ is produced, and $r\psi(r)$ will have as many extrema as there are bound states. On the other hand for an repulsive potential the situation is quite different (Fig. 27c). Here a_o is always positive and smaller r_o.

As an illustrative example, we discuss the scattering by a spherical potential well of depth $-V_o$ and radius r_o. Here one gets

$$(41) \qquad a_o = r_o \left\{ 1 - \frac{\mathrm{tg} K_o r_o}{K_o r_o} \right\} \quad \text{with} \quad K_o = \sqrt{\frac{2m}{\hbar^2} V_o}$$

Fig. 28 shows a_o as a function of $K_o r_o$ for an attractive potential (full lines) and for a repulsive potential (dashed lines). Reasonable values for V_o and r_o are [37] :

$V_o \approx 45$ MeV, $r_o \approx 1.45\ A^{1/3}\ 10^{-13}$cm, where A is the atomic weight of the nucleus. For $A \approx 100$ we get $K_o r_o \approx 10$. Further from Fig. 28, we see that for such large values of $K_o r_o$ the scattering length a_o will be more or less equal to r_o. Negative a_o values only occur in very small intervalls $\Delta(K_o r_o) \sim \frac{1}{K_o r_o}$. Therefore the chance to get a negative scattering length would be $p \approx \frac{1}{\pi K_o r_o} \approx 3\%$. The chances to get especially large $|a_o|$ values are even smaller.

In the case of absorption, the potential v(r) is complex and the scattering length for E = 0 becomes complex, too: $a_o = a_o' + i a_o''$. However neutrons are very weakly absorbed and normally $\left|\frac{a_o''}{a_o'}\right| \approx 10^{-5}$. Even for such a strong absorber as boron the ratio $\left|\frac{a_o''}{a_o'}\right|$ is only 0.04.

So far we tacitly assumed that the nucleus has no spin (S = 0). In this case the interaction does not affect the spin of the neutron which therefore must not be taken into account explicitly. However for $S \neq 0$ two relative orientations of the spin $\underline{\sigma}$ of the nucleus and spin $\underline{S}$ of the nucleus are possible, namely $\underline{\sigma}$ parallel or antiparallel to $\underline{S}$ giving a total spin of $S + {}^1/_2$ or $S - {}^1/_2$ respectively. The interaction potential can be simply expressed by two projection operators P_+ and P_- which project a spin function $\chi(\underline{\sigma}, \underline{S})$ on the subspaces $S + {}^1/_2$ and $S - {}^1/_2$

$$(42) \quad P_+ = P_+^2 = \frac{S+1+2\underline{\sigma}\cdot\underline{S}}{2S+1} \;, \quad P_- = P_-^2 = \frac{S-2\underline{\sigma}\cdot\underline{S}}{2S+1}$$

$$P_+ + P_- = 1$$

Thus the potential, depending explicitly on $\underline{\sigma}$ and $\underline{S}$, can be written as

$$(43) \quad V(\underline{r};\underline{\sigma},\underline{S}) = V_+(r)\, P_+ + V_-(r)\, P_-$$

For each potential $V_+(r)$ and $V_-(r)$ we get a different scattering length a_o^+ and a_o^-, so that we can write

$$(44) \quad a_o = a_o^+ P_+ + a_o^- P_-$$

If we have no polarization, then the averages $\langle \underline{\sigma} \rangle = 0$ and $\langle \underline{S} \rangle = 0$, and we get for the socalled coherent scattering length

$$(45) \quad a_o^{coh} = \langle a_o \rangle = \frac{S+1}{2S+1}\, a_o^+ + \frac{S}{2S+1}\, a_o^-$$

The average cross section is

$$(46) \quad \langle \sigma \rangle = 4\pi \left\{ \frac{S+1}{2S+1}\, (a_o^+)^2 + \frac{S}{2S+1}\, (a_o^-)^2 \right\}$$

$$= 4\pi\, (a_o^{coh})^2 + 4\pi\, \frac{S(S+1)}{(2S+1)^2}\, (a_o^+ - a_o^-)^2$$

The first term is the "coherent cross section", the second one, depending only on the difference $a_o^+ - a_o^-$, the "incoherent cross section".

Multiple scattering: For the scattering of neutrons the multiple scattering equations can be simplified essentially. Because the range r_o of the potential is very much smaller than both the wave length and the lattice constant, in equation (8a) $G_o(\underline{r}-\underline{r}')$ and $\varphi_n(\underline{r}'')$ can be replaced by $G_o(\underline{r}-\underline{R}^n)$ and $\varphi_n(\underline{R}^n)$. Then the single-scattering matrix $t(\underline{r}',\underline{r}'')$ only enters through the integral $\int d\underline{r}'d\underline{r}''\ t(\underline{r}',\underline{r}'')$. This approximation is equivalent to replacing the t-matrix by

$$(47)\qquad t(\underline{r},\underline{r}') = \frac{\hbar^2}{2m}\ 4\pi a\ \delta(\underline{r})\ \delta(\underline{r}')$$

Here a is the scattering length for the energy E. With (47) we get from (8a)

$$(48)\qquad \psi(\underline{r}) = e^{i\underline{K}\underline{r}} - \sum_n a\ \frac{e^{iK|\underline{r}-\underline{R}_n|}}{|\underline{r}-\underline{R}_n|}\ \varphi_n(\underline{R}_n)$$

Therefore we only need the effective field φ_n at the position $\underline{R}_n$ of the nucleus No. n. Then equation (9a) gives

$$(49)\qquad \varphi_n(\underline{R}_n) = e^{i\underline{K}\underline{R}_n} - \sum_{m(\neq n)} a\ \frac{e^{iK|\underline{R}_n-\underline{R}_m|}}{|\underline{R}_n-\underline{R}_m|}\ \varphi_n(\underline{R}_m)$$

These algebraic equations are quite analogous to the equations (32) for muffin-tin potentials. However due to the s-scattering we only have one unknown constant per nucleus, namely $\varphi_n(\underline{R}_n)$.

The scattering length a for an energy E is in a simple way connected with the scattering length a_o for E = 0. From (5) we have

$$(50) \qquad t = v + v\,\frac{1}{E+i\varepsilon-H_o}\,t$$

$$= v\,\frac{1}{i\varepsilon-H_o}\,t + v + v\left(\frac{1}{E+i\varepsilon-H_o} - \frac{1}{i\varepsilon-H_o}\right)t$$

By taking the term $v\,\frac{1}{i\varepsilon-H_o}\,t$ to the left hand side and dividing by $1-v\,\frac{1}{i\varepsilon-H_o}$, one gets

$$(51) \qquad t = t_o + t_o\left(\frac{1}{E+i\varepsilon-H_o} - \frac{1}{i\varepsilon-H_o}\right)t$$

with $$t_o = \frac{1}{1-v\,\frac{1}{i\varepsilon-H_o}}\,v$$

Here t_o, being real, is the single-scattering matrix for zero energy. In the $\underline{r}$-representation equation (51) is

$$(52) \qquad t(\underline{r},\underline{r}') = t_o(\underline{r},\underline{r}') + \int d\underline{r}''d\underline{r}'''\; t_o(\underline{r},\underline{r}'')\cdot$$

$$\cdot\left(\frac{-2m}{\hbar^2 4\pi}\right)\frac{e^{iK|\underline{r}''-\underline{r}'''|}-1}{|\underline{r}''-\underline{r}'''|}\;t(\underline{r}''',\underline{r}')$$

Now if both t and t_o have the form (47) with scattering lengths a and a_o, we get from (52)

$$(53) \qquad a = a_o - iKa_oa = \frac{a_o}{1+iKa_o}$$

Because $|Ka_o| \ll 1$ normally, $a \cong a_o$. In principle, however, a_o can be arbitrarily large. Then a is limited by $\frac{1}{K}$.

By setting $K = i\varkappa$, the scattering length diverges for $\varkappa = \frac{1}{a_o}$, if $a_o > 0$. This indicates that for $a_o > 0$ the potential $v(r)$ has a bound state with the energy $E = -\frac{\hbar^2}{2m}\frac{1}{a_o^2}$, which, for instance, vanishes for $a_o \to \infty$.

Equation (47) represents the t-matrix for a potential of "zero range", i.e. in the limit $Kr_o \to 0$. For a repulsive potential the scattering length a_o vanishes in this limit because always $0 \leq a_o \leq r_o$. However for an attractive potential a finite value of a_o can always be obtained by adjusting the potential depth, e.g. V_o in equation (41). Further we have at most one bound state. All others have energies $E \sim -\frac{\hbar^2}{2m}\frac{1}{r_o^2}$ moving to $-\infty$ for $r_o \to 0$.

To determine the eigenfunctions for potentials of zero range in an infinite crystal, we introduce the ansatz (47) for t in (18) and (19). Then the Bloch wave $\phi_{\underline{k}}$ is given by

$$(54) \quad \phi_{\underline{k}}(\underline{r}) = G(\underline{r},0)\frac{\hbar^2}{2m}4\pi a\,\varphi_o(0)$$

$$= -\left(\sum_n \frac{e^{iK|\underline{r}+\underline{R}_n|}}{|\underline{r}+\underline{R}_n|}\, e^{-i\underline{k}\underline{R}_n}\right) a\,\varphi_o(0)$$

Here $\varphi_o(0)$ only is a normalization constant. Equation (19) gives the dispersion condition connecting the allowed $\underline{k}$ values with the energy $\frac{\hbar^2 K^2}{2m}$.

$$(55) \qquad 1 = G'(0,0)\,\frac{\hbar^2}{2m}\,4\pi a = -\,a\sum_{n\neq 0}\frac{e^{iK|\underline{R}_n|}}{|\underline{R}_n|}\,e^{-i\underline{k}\underline{R}_n}$$

The equations (54) and (55) can also be written in a different form with sums over the reciprocal lattice. For instance by Fourier transformation we get from (54)

$$(56a) \qquad \phi_{\underline{k}}(\underline{r}) = 4\pi a\,\varphi_o(0)\int\frac{d\underline{K}'}{(2\pi)^3}\,\frac{e^{i\underline{K}'\underline{r}}}{K^2-K'^2+i\varepsilon}\cdot$$

$$\cdot\sum_n e^{i(\underline{K}'-\underline{k})\underline{R}_n}$$

$$(56b) \qquad = \frac{4\pi a}{V_c}\,\varphi_o(0)\sum_{\underline{h}}\frac{e^{i(\underline{k}+\underline{h})\underline{r}}}{K^2-(\underline{k}+\underline{h})^2}$$

The sum in (56a) gives a δ-function, if $\underline{K}'$ is equal to $\underline{k}$ up to a reciprocal lattice vector $\underline{h}$. Similarly one gets from (55) by adding and subtracting the term n = 0:

$$(57) \qquad \frac{1}{a} = 4\pi\int\frac{d\underline{K}'}{(2\pi)^3}\,\frac{1}{K^2+i\varepsilon-K'^2}\left(\frac{(2\pi)^3}{V_c}\sum_{\underline{h}}\delta(\underline{K}'-\underline{k}-\underline{h})\;-1\right)$$

The two terms in the bracket cannot be integrated separately, because both diverge. For the first term, being a discrete sum, the $i\varepsilon$ in the denominator is unnecessary, whereas the imaginary part of the second term is iK. With the expression (53) for a, the imaginary term iK cancels on both sides and the remaining quantities are real. Substituting $\underline{K}' = \underline{h}+\underline{k}'$ the second integral can be written as a sum over $\underline{h}$

too with integrals $d\underline{k}'$ over the first Brillouin zone. Thus we get

$$(58) \qquad 1 = \frac{4\pi a_o}{V_c} \sum_{\underline{h}} \left\{ \frac{1}{K^2-(\underline{k}+\underline{h})^2} - \frac{V_c}{(2\pi)^3} \int_{I.B.Z.} d\underline{k}' \, \frac{1}{K^2-(\underline{k}'+\underline{h})^2} \right\}$$

The sum over $\underline{h}$ converges because the integral cancels the first term for large $\underline{h}$. However the sum of the first term or second term alone diverges. This is directly connected with the difference between the effective field and the wave function. According to (6) we have

$$(59) \qquad \phi(\underline{r}) = \varphi_o(\underline{r}) - a \frac{e^{iKr}}{r} \varphi_o(0)$$

Therefore $\phi(\underline{r})$ diverges as $\frac{1}{r}$ for $\underline{r} \to 0$ and similarly for $\underline{r} \to \underline{R}_n$. However the effective incident field φ_o does not diverge for $r \to 0$. The divergence of $\phi(\underline{r})$ can be seen in equ. (56b) too, where the sum over $\underline{h}$ diverges for $\underline{r} = \underline{R}_n$. Therefore the convergence of (58) is due to the subtraction of the term $\frac{a}{r}$ in (59) or the term n = 0 in (57,58). Practically, however, the difference between $\phi(\underline{r})$ and $\varphi_o(\underline{r})$ is important only in the immediate vicinity of the nucleus, but not everywhere else in the first unit cell.

In the one-beam case, i.e. if the Bragg condition is not fulfilled, we get from (58)

$$(60) \qquad 1 = \frac{4\pi a_o}{V_c} \frac{1}{K^2 - \underline{k}^2} \quad \text{or} \quad K^2 - \frac{4\pi a_o}{V_c} - \underline{k}^2 = 0$$

The other terms in (58) have the order of magnitude $\frac{4\pi a_o}{V_c} \frac{1}{K^2} \approx O(10^{-5})$ and can be neglected. However this would not be possible for extremely large $a_o \approx O(1/K)$. For $a_o > 0$ the refractive index $n = \frac{k}{K}$ is $n \cong 1 - \frac{2\pi a_o}{V_c K^2} < 1$ leading to total reflection for nearly glancing incidence. On the other hand, for $a_o < 0$ and consequently $K^2 < k^2$ or $n > 1$ the neutron can be bound by the crystal similarly to a band electron. However the binding energy is only of the order of 10^{-7} eV. Nevertheless such bound states may have some physical significance in temporarily capturing neutrons [38]

If the Bragg condition is fulfilled for a number of beams, say $\underline{k}$, $\underline{k}+\underline{h}_1$,..., $\underline{k}+\underline{h}_n$, then we get from (58) by neglecting the integral as before:

$$(61) \qquad 1 = \frac{4\pi a_o}{V_c} \sum_{\underline{h}=0}^{\underline{h}_n} \frac{1}{K^2 - (\underline{k}+\underline{h})^2}$$

This can also be written in a more familiar form. Namely from (56b) one gets for $\underline{h} = 0, \ldots, \underline{h}_n$:

$$(62) \qquad \left(K^2 - (\underline{k}+\underline{h})^2 \right) C_{\underline{h}} = \frac{4\pi a_o}{V_c} \varphi_o(0) = \frac{4\pi a_o}{V_c} \sum_{\underline{h}'=0}^{\underline{h}_n} C_{\underline{h}'}$$

where the last identity follows by using (61).

This equation is identical with the basic equation for electron diffraction, if all $v_{\underline{h}}$ are replaced by $\frac{4\pi a_o}{V_c}$. Therefore one may derive (62) as well without any t-matrix formalism simply by using Fermi's pseudo potential

$$(63) \qquad v_F(\underline{r}) = \frac{\hbar^2}{2m} 4\pi a_o \delta(\underline{r})$$

By neglecting the integral in (58), the effective field $\varphi_o(\underline{r})$ and $\phi(\underline{r})$ become equal. Physically this is due to the fact that with a small number of beams the difference (59) between $\varphi_o(\underline{r})$ and $\phi(\underline{r})$, being only important at the position of the nucleus, cannot be resolved. Therefore, by restricting to a few strongly excited beams, the Fermi potential (63) can be used and the whole formalism of electron diffraction remains applicable, e.g. two beam case, boundary conditions, etc. However in addition to the assumption of zero-range potentials ($r_o \ll \lambda, d_{nn}$) used to derive the representation (47) for the t-matrix or for the dispersion condition(58), we have used the condition $|a_o| \ll \lambda, d_{nn}$ in order to derive (62) or Fermi's pseudo potential(63). Therefore deviations from (62) are expected for extremely large a_o's, for instance near resonances.

5. Dynamical Diffraction of X-rays

The theory for X-ray diffraction is quite analogous to the theory for electron diffraction, except that we have to consider a vector field instead of a scalar field. Therefore we have to start with Maxwell's equations replacing the Schroedinger equation.

5.1. Fundamental equations for X-ray-diffraction

For simplicity we will treat the electrons of the crystal classically. A more thorough quantum mechanical treatment is given in part II. The frequencies of the motion of atomic electrons are of the order $\omega_o \approx v/a_B$ where v is the electron velocity and a_B is Bohr's radius. Because the X-ray wave length is comparable to a_B, these frequencies are small compared to the X-ray frequency $\omega = 2\pi \frac{c}{\lambda}$, since $v \ll c$.*) Therefore the electrons may be treated as free. Their motion due to an electric field $\underline{E} \sim e^{-i\omega t}$ is described by

$$(1) \qquad m\ddot{\underline{r}} = e\,\underline{E}(\underline{r},t)$$

If we denote the space dependent density of electrons by $\varrho(\underline{r})$, then the density of the charge current is

*) In the scattering by heavier elements, this condition may only be fulfilled for the outer electron shells, but not for the inner ones. See part II for this case, too.

$$(2) \quad \underline{j}(\underline{r}) = e\,\varrho(\underline{r})\,\dot{\underline{r}} = i\,\frac{e^2}{m\omega}\,\varrho(\underline{r})\,\underline{E}(\underline{r},t)$$

Now we introduce this current into Maxwell's equations, which are for harmonic time dependence $\sim e^{-i\omega t}$

$$(3) \quad \partial_{\underline{r}} \times \underline{E} = i\,\frac{\omega}{c}\,\underline{H}$$

$$(4) \quad \partial_{\underline{r}} \times \underline{H} = -i\,\frac{\omega}{c}\,\underline{E} + \frac{4\pi}{c}\,\underline{j} = -i\,\frac{\omega}{c}\,\varepsilon\,\underline{E} = -i\,\frac{\omega}{c}\,\underline{D}$$

Here the dielectric constant ε is given by

$$(5) \quad \varepsilon(\underline{r},\omega) = 1 - \frac{4\pi e^2}{m\omega^2}\,\varrho(\underline{r})$$

It follows directly from (3) and (4) that

$$(6) \quad \partial_{\underline{r}} \cdot \underline{D} = 0 = \partial_{\underline{r}} \cdot \underline{H}$$

Further, one gets by eliminating $\underline{H}$ from (3) and (4)

$$(7) \quad \partial_{\underline{r}} \times \partial_{\underline{r}} \times \underline{E} = \left(\frac{\omega}{c}\right)^2 \underline{D}$$

Actually the deviation of ε from 1 is very small for X-rays. With the classical electron radius

$r_e = \frac{e^2}{mc^2} = 2{,}82 \;\; 10^{-13}$ cm one has

$$(8) \quad \chi(\underline{r}) = \varepsilon(\underline{r}) - 1 = -\,\frac{4\pi r_e}{K^2}\,\varrho(\underline{r}) \text{ with } \frac{\omega}{c} = K = \frac{2\pi}{\lambda}$$

For $\lambda \cong 1$ Å we have $|\chi| \leq 10^{-4}$ for most elements. Therefore $\underline{E}$ as a function of $\underline{D}$ is given by

$$(9) \qquad \underline{E} = \frac{1}{\epsilon}\underline{D} \cong \underline{D} - \chi\cdot\underline{D}$$

Substituting this into (7) and using (6) we get an equation for $\underline{D}$ alone.

$$(10) \qquad \left(\partial_{\underline{r}}^2 + K^2\right)\underline{D}(\underline{r}) = -\,\partial_{\underline{r}} \times \partial_{\underline{r}} \times \left(\chi(\underline{r})\ \underline{D}\ (\underline{r})\right)$$

Sometimes, e.g. in order to derive the kinematical theory, it es useful to write this equation as an integral equation by using the Green's function (3.4)

Then for an incident wave $\hat{\underline{D}}\ e^{i\underline{K}\underline{r}}$ one has

$$(11) \qquad \underline{D}(\underline{r}) = \hat{\underline{D}}\ e^{i\underline{K}\underline{r}} + \partial_{\underline{r}} \times \partial_{\underline{r}} \times \int d\underline{r}'\ \frac{e^{iK|\underline{r}-\underline{r}'|}}{4\pi|\underline{r}-\underline{r}'|}\cdot$$

$$\cdot\ \chi(\underline{r}')\ \underline{D}(\underline{r}')$$

In an <u>infinite crystal</u> the electron density $\varrho(\underline{r})$ has the periodicity of the lattice. Therefore, the eigenfunctions can be chosen as Bloch waves and can be expanded into plane waves analogously to (2.20)

$$(12) \qquad \underline{D}_{\underline{k}}(\underline{r}) = \sum_{\underline{h}} \underline{D}_{\underline{h}}\ e^{i(\underline{k}+\underline{h})\underline{r}} \quad \text{with } \underline{D}_{\underline{h}}\cdot(\underline{k}+\underline{h}) = 0$$

Since $\partial_{\underline{r}}\cdot\underline{D} = 0$ the vectors $\underline{D}_{\underline{h}}$ are perpendicular to $\underline{k}+\underline{h}$. Due to its periodicity $\chi(\underline{r})$ can be written as (compare (2.4, 2.6)):

$$(13) \qquad \chi(\underline{r}) = \sum_{\underline{h}} \chi_{\underline{h}}\ e^{i\underline{h}\underline{r}}$$

with

$$\chi_{\underline{h}} = -\frac{4\pi r_e}{K^2}\ \frac{1}{V_c}\ \int_{V_c} e^{-i\underline{h}\underline{r}}\ \varrho(\underline{r})\,d\underline{r} = -\frac{4\pi r_e}{V_c\,K^2}\ f_{\underline{h}}$$

where $f_{\underline{h}}$ is the atomic scattering factor for X-rays (2.7). Introducing (12) and (13) in (10) we get by comparing the coefficients of $e^{i(\underline{k}+\underline{h})\underline{r}}$:

$$(14) \quad \left(K^2 - (\underline{k}+\underline{h})^2\right) \underline{D}_{\underline{h}} = -(\underline{k}+\underline{h})^2 \sum_{\underline{h}'} \chi_{\underline{h}-\underline{h}'} \underline{D}_{\underline{h}'}[\underline{h}]$$

with

$$(15) \quad \underline{D}_{\underline{h}'}[\underline{h}] = \underline{D}_{\underline{h}'} - \frac{(\underline{k}+\underline{h})\left((\underline{k}+\underline{h}) \cdot \underline{D}_{\underline{h}'}\right)}{(\underline{k}+\underline{h})^2}$$

Due to $\underline{D}_{\underline{h}} \cdot (\underline{k}+\underline{h}) = 0$ the term on the right-hand side has to be perpendicular to $\underline{k}+\underline{h}$, which is indeed the case, since $\underline{D}_{\underline{h}'}[\underline{h}]$ is the projection of $\underline{D}_{\underline{h}'}$ on the plane perpendicular to $\underline{k}+\underline{h}$. Due to the smallness of $\chi_{\underline{h}}$, only the plane waves with $K^2 \approx (\underline{k}+\underline{h})^2$ are strongly excited. Therefore we can replace $(k+h)^2$ on the right side of (14) by K^2.

$$(16) \quad \left(K^2 - (\underline{k}+\underline{h})^2\right) \underline{D}_{\underline{h}} = \sum_{\underline{h}'} \mathcal{U}_{\underline{h}-\underline{h}'} \underline{D}_{\underline{h}'}[\underline{h}]$$

$$\text{with } \mathcal{U}_{\underline{h}-\underline{h}'} = \frac{4\pi r_e}{V_c} f_{\underline{h}-\underline{h}'}$$

These equations are very similar to the corresponding equations (2.21, 2.71) for electrons or (4.62) for neutrons. The main difference is that the $\underline{D}_{\underline{h}}$'s are vectors. $\mathcal{U}_{\underline{h}}$ is the analogue to the potential coefficient $\frac{2m}{\hbar^2} V_{\underline{h}}$ (2.14) for electrons or to $\frac{4\pi a_o}{V_c}$ (4.62) for neutrons.

For each plane wave $\underline{k}+\underline{h}$ we can introduce two polarization vectors $\underline{e}_{\underline{h}}^{s}$ ($s = 1,2$) being perpendicular to $\underline{k}+\underline{h}$.

$$(17) \quad \underline{e}_{\underline{h}}^{s} \cdot (\underline{k}+\underline{h}) = 0 \quad \text{and} \quad \underline{e}_{\underline{h}}^{s} \cdot \underline{e}_{\underline{h}}^{s'} = \delta_{s,s'}$$

for s and s' = 1,2

With

$$(18) \quad \underline{D}_{\underline{h}} = \sum_{s=1}^{2} D_{\underline{h}}^{s} \underline{e}_{\underline{h}}^{s}$$

we get from (16) for the scalar components $D_{\underline{h}}^{s}$:

$$(19) \quad \left(K^2 - (\underline{k}+\underline{h})^2 \right) D_{\underline{h}}^{s} = \sum_{\underline{h},s'} \mathcal{H}_{\underline{h}-\underline{h}'} \; \underline{e}_{\underline{h}}^{s} \cdot \underline{e}_{\underline{h}'}^{s'} \; D_{\underline{h}'}^{s'}$$

These are homogeneous equations which have a solution only if their determinant vanishes.

$$(20) \quad \det \left| \left(K^2 - (\underline{k}+\underline{h})^2\right) \delta_{\underline{h},\underline{h}'} \; \delta_{s,s'} - \mathcal{H}_{\underline{h}-\underline{h}'} \; \underline{e}_{\underline{h}}^{s} \cdot \underline{e}_{\underline{h}'}^{s'} \right| = 0$$

This gives us for a given $\underline{k}$-vector the allowed frequencies $cK = \omega_{\nu}(\underline{k})$, which form bands. The Bloch waves for different $\underline{k}$'s and ν's are orthogonal, namely

$$(21) \quad \int \frac{d\underline{r}'}{(2\pi)^3} \; \underline{D}^{*}_{\underline{k}',\nu'}(\underline{r}) \; \underline{D}_{\underline{k},\nu}(\underline{r}) = \delta(\underline{k}-\underline{k}') \; \delta_{\nu,\nu'}$$

Quite analogously to (2.26) we have then for the coefficients $\underline{D}_{\underline{h}}$, $D_{\underline{h}}^{s}$ respectively:

$$(22) \quad \sum_{\underline{h}} \underline{D}_{\underline{h}}^{*}(\underline{k},\nu') \; \underline{D}_{\underline{h}}(\underline{k},\nu) = \delta_{\nu,\nu'} = \sum_{\underline{h},s} D^{*s}_{\underline{h}}(\underline{k},\nu') D^{s}_{\underline{h}}(k,\nu)$$

Most of the other results of section 2. are valid for X-rays, too. For instance, we have the symmetries:

$$(23) \qquad \omega_\nu(\underline{k}) = \omega_\nu(\underline{k}+\underline{h}) = \omega_\nu(S\underline{k}) = \omega_\nu(-\underline{k}) = \omega_\nu^*(\underline{k}^*)$$

if $\varrho(\underline{r})$ has the following properties (in the same sequence as (23)): periodic (2.33), symmetrical with respect to S (2.35), local(2.36), real (2.37). Similarly the theorems about the real lines and the behaviour for complex $\underline{k}$ are valid without change.

There are two simple cases where the vector equation (16) reduces to two equal and decoupled equation for the components $D_{\underline{h}}^{s}$, thus leading to a scalar theory for each component. First, in the vacuum we have $\varkappa_{\underline{h}-\underline{h}'} = 0$ and the two polarisations are degenerate. Second, for very small wave lengths $K^2 \gg h^2$, i.e. for very small Bragg angles, all wave vectors $\underline{k}+\underline{h}$, $\underline{k}+\underline{h}'$ of the strongly excited waves are approximately equal. Then in (16) $\underline{D}_{\underline{h}'}[\underline{h}] \cong \underline{D}_{\underline{h}'}$ or in (19) $\underline{e}_{\underline{h}}^{s} \cdot \underline{e}_{\underline{h}'}^{s'} = \delta_{ss'}$ and we get the same equation for the polarisations s = 1 and s = 2.

Together with the dielectric field $\underline{D}(\underline{r})$ the electric field $\underline{E}(\underline{r})$ and the magnetic field $\underline{H}(\underline{r})$ can be expanded into plane waves, too.

$$(24) \qquad \underline{E}(\underline{r}) = \sum_{\underline{h}} \underline{E}_{\underline{h}} \, e^{i(\underline{k}+\underline{h})\underline{r}} \; ; \; \underline{H} = \sum_{\underline{h}} \underline{H}_{\underline{h}} \, e^{i(\underline{k}+\underline{h})\underline{r}}$$

For the direction of $\underline{H}_{\underline{h}}$ it follows from (6) and (4):

(25) $(\underline{k}+\underline{h}) \cdot \underline{H}_{\underline{h}} = 0$ and $\underline{D}_{\underline{h}} = -\frac{1}{K}(\underline{k}+\underline{h}) \times \underline{H}$

Therefore $\underline{H}_{\underline{h}}$ is perpendicular on both $\underline{k}+\underline{h}$ and $\underline{D}_{\underline{h}}$ (Fig. 29) Furhter we get from (3) and (9) for $\underline{E}_{\underline{h}}$:

(26) $\underline{H}_{\underline{h}} = \frac{1}{K}(\underline{k}+\underline{h}) \times \underline{E}_{\underline{h}}$ and $\underline{E}_{\underline{h}} = \underline{D}_{\underline{h}} - \sum_{\underline{h}'} \chi_{\underline{h}-\underline{h}'} \underline{D}_{\underline{h}'}$

Therefore $\underline{E}_{\underline{h}}$ lies in the plane of $\underline{k}+\underline{h}$ and $\underline{D}_{\underline{h}}$. It nearly coincides with $\underline{D}_{\underline{h}}$, since $|\chi| \ll 1$ (Fig. 29).

5.2. Current, Boundary conditions, etc.

The density of the energy current is given by Poynting's vector

(27) $\underline{S} = \frac{c}{4\pi} \underline{E} \times \underline{H}$ with real $\underline{E}$ and $\underline{H}$

By using complex quantities, the average of $\underline{S}$ over times $\tau \gg \frac{1}{\omega}$ is [5,39]

(28) $\overline{\underline{S}}^{t} = \frac{c}{8\pi} \mathrm{Re}(\underline{E} \times \underline{H}^{*})$

Since $|\chi| \ll 1$, we may as well replace $\underline{E}$ by $\underline{D}$. For a Blochwave $\underline{D}_{\underline{k}}(\underline{r})$, the current contains contributions oscillating in space. However the average over a unit cell is constant and given by:

(29) $\overline{\underline{S}}^{t,V_c} = \frac{c}{8\pi} \mathrm{Re} \sum_{\underline{h}} \underline{D}_{\underline{h}} \times \underline{H}_{\underline{h}}^{*} = \frac{c}{8\pi} \sum_{\underline{h}} |\underline{D}_{\underline{h}}|^2 \underline{s}_{\underline{h}}$

with $\underline{s}_{\underline{h}} = \frac{\underline{k}+\underline{h}}{|\underline{k}+\underline{h}|} \simeq \frac{\underline{k}+\underline{h}}{K}$

Now it can be shown analogously to (2.31), that

$$(30) \quad \sum_{\underline{h}} (\underline{k}+\underline{h}) \, |\underline{D}_{\underline{h}}|^2 = \frac{1}{2} \frac{\partial K^2}{\partial \underline{k}} \sum_{\underline{h}} |\underline{D}_{\underline{h}}|^2$$

Together with the normalization (22) we get therefore

$$(31) \quad \underline{S}^{t,V_c} = \frac{c}{8\pi} \frac{1}{2K} \frac{\partial K^2}{\partial \underline{k}} = \frac{1}{8\pi} \frac{\partial \omega_\nu(\underline{k})}{\partial \underline{k}}$$

As in the case of electrons the current is therefore perpendicular to the dispersion surface

$\omega_\nu(\underline{k})$ = cK = constant.

For the diffraction of X-rays by a finite crystal, the wave fields in the crystal and in the vacuum have to be matched at the crystal surface. Since $\partial_{\underline{r}} \cdot \underline{D} = 0$, the component of $\underline{D}(\underline{r})$ perpendicular to the surface is continuous . Due to $\partial_{\underline{r}} \times \underline{E} = i\frac{\omega}{c} \underline{H}$, the tangential component of $\underline{E}$ is continuous, too. Further, since $\chi(\underline{r})$ is very small, we may neglect the waves specularly reflected from the surfaces. For the same reason $\underline{E}$ and $\underline{D}$ are practivally equal. Therefore we can assume that both components $\underline{D}_{\text{normal}}$ and $\underline{D}_{\text{tang.}}$ are continuous.

Analogously to section 3.3. we can construct the wave fields in the vacuum and in the crystal. For a crystal slab we can have the plane waves $\underline{K}^{\pm}_{\underline{\ell}} = (\underline{\kappa}+\underline{\ell} \, , \pm K_{z\underline{\ell}})$ in the vacuum, so that

$$(32)\quad \underline{D}(\underline{r}) = \begin{cases} \hat{\underline{D}}\, e^{i\underline{K}\underline{r}} + \sum_{\underline{\ell}} \underline{R}_{\underline{\ell}}\, e^{i\underline{K}^{-}_{\underline{\ell}}\,\underline{r}} & \leq 0 \\ \text{for } z & \\ \sum_{\underline{\ell}} \underline{T}_{\underline{\ell}}\, e^{i\underline{K}^{+}_{\underline{\ell}}\,\underline{r}} & \geq d \end{cases}$$

$\hat{\underline{D}} \perp \underline{K}$ is the field vector of the incident wave, $\underline{R}_{\underline{\ell}}$ and $\underline{T}_{\underline{\ell}}$ are the field vectors of the reflected waves $\underline{K}^{-}_{\underline{\ell}}$ and transmitted waves $\underline{K}^{+}_{\underline{\ell}}$. Since we neglect any true reflection from the surface, either $\underline{K}^{+}_{\underline{\ell}}$ (Laue case) or $\underline{K}^{-}_{\underline{\ell}}$ (Bragg case) is a Bragg reflected wave and the other one can be omitted. In the crystal we may have a number of Bloch waves $\underline{D}_{\underline{k}j}(\underline{r})$ with $\underline{k}_j = (\underline{\tilde{K}}, k_{zj})$ and $\omega_\nu(\underline{\tilde{K}}, k_{zj}) = cK$. However, since $|\chi| \ll 1$, only outgoing waves have to be taken into account: $\frac{\partial \omega}{\partial k_z} > 0$ for real k_z or $\varkappa_z > 0$ for $k_z = k'_z + i\varkappa_z$ complex.

$$(33)\quad \underline{D}(\underline{r}) = \sum_j P_j\, \underline{D}_{\underline{k}j}(\underline{r}) \qquad \text{for } 0 \leq z \leq d$$

The boundary condition for $\underline{D}$ to be continuous for z=0 and z=d lead to similar equations as (3.31-36) from which the coefficients $\underline{R}_{\underline{\ell}}$, $\underline{T}_{\underline{\ell}}$ and P_j can be determined.

Without absorption, the z-component of the energy current is independent of z, if averaged over the time and the unit mesh S_o of the surface (section 3. 4). This gives us an additional relation between $\underline{R}_{\underline{\ell}}$, $\underline{T}_{\underline{\ell}}$ and P_j, for instance for the crystal slab

$$(34)\quad K_z |\hat{\underline{D}}|^2 = \sum_{\underline{\ell}}{}' K_{z\underline{\ell}} \left(|\underline{R}_{\underline{\ell}}|^2 + |\underline{T}_{\underline{\ell}}|^2 \right)$$

or for the half crystal

$$(35)\quad K_z|\hat{\underline{D}}|^2 = \sum_{\underline{\ell}}{}' K_{z\underline{\ell}}|\underline{R}_{\underline{\ell}}|^2 + \sum_j{}' \frac{1}{2}\frac{\partial K^2}{\partial k_{zj}}|P_j|^2$$

The sums go over real wave vectors $\underline{K}^{\pm}_{\underline{\ell}}$ and $\underline{k}_j$ only. If no Bragg reflection is excited, we only have <u>one strong beam</u>. For both polarisations the Bloch vector is determined by

$$(36)\quad (K^2 - \mathcal{U}_o - \underline{k}^2) = 0$$

The refractive index

$$(37)\quad n = \frac{k}{K} \cong 1 - \frac{2\pi r_e}{V_c K^2} f_o$$

is slightly smaller than 1, leading to total reflection for nearly glancing incidence.

If a Bragg reflection is excited, we have <u>two strong beams</u> $\underline{k}$ and $\underline{k}+\underline{h}$. In this case a natural choice for the polarisation vectors is (Fig. 30a):

$S = 1$ (σ-polarisation) : $\underline{e}^1_o = \underline{e}^1_{\underline{h}}$ perpendicular to both $\underline{k}$ and $\underline{k} + \underline{h}$

$S = 2$ (π-polarisation) : $\underline{e}^2_o$, $\underline{e}^2_{\underline{h}}$ in the plane of $\underline{k}$ and $\underline{k}+\underline{h}$

Then we have in addition to (17): $\underline{e}^1_o \cdot \underline{e}^2_{\underline{h}} = 0 = \underline{e}^1_{\underline{h}} \cdot \underline{e}^2_o$ and $\underline{e}^2_o \cdot \underline{e}^2_{\underline{h}} = \cos 2\,\Theta_B$. Therefore the equations for the different polarisations σ and π are decoupled, giving

$$(38)\qquad (K^2-\chi_o-\underline{k}^2)\ D_o^s = \chi_{-\underline{h}}\ P_s\ D_{\underline{h}}^s$$

$$(K^2-\chi_o-(\underline{k}+\underline{h})^2)\ D_{\underline{h}}^s = \chi_{\underline{h}}\ P_s\ D_o^s$$

where the polarisation factor $P_s = \underline{e}_o^s \cdot \underline{e}_{\underline{h}}^s$ is equal to

$$(39)\qquad P_s = \begin{cases} 1 & s = 1\ (\sigma) \\ \text{for} & \\ \cos 2\,\theta_B & s = 2\ (\pi) \end{cases}$$

For each polarisation the allowed $\underline{k}$-vectors lie on the dispersion surface described by

$$(40)\qquad (K^2-\chi_o-\underline{k}^2)\ (K^2-\chi_o-(\underline{k}+\underline{h})^2) = P_s^2\ |\chi_{\underline{h}}|^2$$

Far away from the Bragg condition the dispersion surfaces for both polarisations are equal and represented by the spheres of radius $\sqrt{K^2-\chi_o}$ around $\underline{k} = 0$ and $\underline{k} = \underline{h}$. Near the Bragg condition the degeneracy is removed. For instance the smallest branch separation is (2. 77):

$$(41)\qquad \Delta k_s = \frac{2\pi}{d_{ext}} = \frac{P_s \chi_{\underline{h}}}{K \cos \theta_B}$$

The dispersion surfaces are qualitatively shown in Fig. 30b. The larger spheres with radius K represent the dispersion surface in the vacuum.

The coefficients D_o^s and $D_{\underline{h}}^s$ can be taken from (2.80) by replacing $v_{\underline{h}}$ by $P_s\ \chi_{\underline{h}}$. For instance exactly in the Bragg condition we get for the σ-polarisation the

fields

$$(42) \quad \underline{D}^{\sigma}(\underline{r}) = \underline{e}_o^1 \; \frac{1}{\sqrt{2}} \, e^{i\underline{k}\underline{r}} \; (1 \pm e^{i\underline{h}\underline{r}})$$

and for the π-polarisation

$$(43) \quad \underline{D}^{\pi}(\underline{r}) = \frac{1}{\sqrt{2}} \, e^{i\underline{k}\underline{r}} \; (\underline{e}_o^2 \pm e^{i\underline{h}\underline{r}} \; \underline{e}_{\underline{h}}^2)$$

The upper sign refers to the inner branch and the lower to the outer one. The σ-fields are identical with the Bloch waves ϕ^I and ϕ^{II} of Fig. 14. However for the π-polarisation we do not get pure sin- or cos-waves, but always combinations of both, because $\underline{e}_o^2 \neq \underline{e}_{\underline{h}}^2$.

The absorption of X-rays can be described phenomenologically by a complex dielectric constant or by a complex density $\varrho(\underline{r}) = \varrho'(\underline{r}) + i\varrho''(\underline{r})$, resulting in complex coefficients $\mathcal{U}_{\underline{h}} = \mathcal{U}'_{\underline{h}} + i\,\mathcal{U}''_{\underline{h}}$. Similarly to (2.67) we get for the absorption of a Bloch wave $\underline{k}$ the expression

$$(44) \quad \mu = \sum_{\underline{h},\underline{h}'} \mu_{\underline{h}-\underline{h}'} \; \underline{D}_{\underline{h}}(\underline{k}) \; \underline{D}_{\underline{h}'}(\underline{k})$$

Especially for the two-beam case we have

$$(45) \quad \mu^s = \mu_o \pm \frac{P_s}{\sqrt{1+W_s^2}} \, \mu_{\underline{h}} \quad \text{with} \quad W_s = \frac{(\underline{k}+\frac{\underline{h}}{2})\,\underline{h}}{P_s \; \mathcal{U}_{\underline{h}}}$$

The minimal absorption is therefore $\Delta\mu^{\sigma} = \mu_o - \mu_{\underline{h}}$ for σ-, but $\Delta\mu^{\pi} = \mu_o - \cos 2\,\Theta_B \cdot \mu_{\underline{h}}$ for π-polarisa-

tion. Therefore only the σ-wave shows a strong anomalous transmission effect, but not the π-wave. This is plausible from (42,43) because both π-waves do not vanish at the atomic positions.

For multiple beam cases the different polarisation will no longer be decoupled as in the two-beam case, which complicates the problem. Multiple-beam cases are interesting for X-ray-diffraction, because even lower absorptions can be obtained than for the two-beam case, as has been demonstrated by [40] . A number of symmetrical multiple-cases has been treated in [41], including the cases of Fig. 17. For instance, for the four-beam case of Fig. 17, the minimal absorption will be obtained for very small wave lengths, for which the theory for X-rays goes over in the scalar theory for electrons. Therefore the smallest absorption is that of (2.104). The corresponding wave field vanishes quadratically at the atomic positions. Extensive treatments of the three beam case have been given in [42].

References:

1 C.G. Darwin: Phil.Mag. 27, 315; 27, 675 (1914)

2 P.P. Ewald: Ann. Physik 49, 1; 49, 117 (1916);54,519 (1917)

3 M.v.Laue: Ergeb. Exakt. Naturw. 10, 133 (1931)

4 H. Bethe: Ann. Physik 87, 55 (1928)

5 M.v.Laue: Röntgenstrahl-Interferenzen, Akad. Verlag Frankfurt, 1960

6 W.H. Zachariasen: Theory of X-Ray Diffraction in Crystals, Dover Publ., New York, 1945

7 R.W. James: The Optical Principles of the Diffraction of X-Rays, G. Bell and Sons, London, 1950

8 B.W. Battermann and H. Cole: Rev.Mod.Phys. 36,681 (1964)

9 R.W. James: Solid State Physics, Vol. 15, Acad. Press New York, 1963

10 M.v.Laue: Materiewellen und ihre Interferenzen, Akad. Verlag, Leipzig, 1944

11 R.D. Heidenreich: Fundamentals of Transmission Electron Microscopy, Interscience, New York, 1964

12 P.W. Hirsch, A. Howie, R.B. Nicholson, D.W. Pashley and M.J. Whelan: Electron Microscopy of Thin Crystals, Butterworths, London, 1965

13 G. Molière: Ann. Physik 35, 272; 35, 297 (1939)

14 H. Yoshioka: J. Phys. Soc. Jap. 12, 618 (1957)

15 e.g. W. Brauer: Einführung in die Elektrontheorie der Metalle, Vieweg, Braunschweig, 1967

J. Callaway: Energy Band Theory, Acad. Press, New York, 1964

P.T. Landsberg Ed.: Solid State Theory, Wiley-Interscience, London 1969

16 V. Heine: Proc. Phys. Soc. 81, 300 (1963), Surface Science 2, 1 (1964)

17 W. Kohn: Phys. Rev. 115, 809 (1959)

18 E.I. Blount: Solid State Physics, Vol. 13, Acad. Press, New York, 1962

19 C. Herring: Phys. Rev. 52, 365 (1937)

20 A. Howie: Phil. Mag. 14, 223 (1966)

M.J. Goringe, A. Howie, M.J. Whelan: Phil. Mag. 14, 217 (1966)

R. Serneels, R. Gevers: Phys. stat. sol. 33, 703 (1969); (b) 45, 493 (1971)

21 K. Fujiwara: J. Phys, Soc. Jap. 14, 1513 (1959)

K. Kambe: Z. Naturforschung 22a, 422 (1967)

22 E.G. McRae: J. Chem. Phys. 45, 3258 (1966)

23 P.M. Marcus, D. W. Jepsen: Phys. Rev. Let. 20 928 (1968)

24 B. W. Batterman, G. Hildebrandt: Acta Cryst. A24, 150 (1968)

25 E. Fermi: Ricerca Scientifica 7, Part 2, 13 (1936)

26 M.L. Goldberger, F. Seitz: Phys. Rev. 71, 294 (1947)

27 M.L. Goldberger, K.M. Watson: Collision Theory, Wiley, New York (1964)

28 e.g. J. Ziman: On the Band Structure Problem in: Theory of Condensed Matter, Lectures presented at an International Course, Triest 1967; Wien: IAEA, 1968

29 e.g. J.M. Ziman, Principles of the Theory of Solids, Cambridge, At the University Press, 1965

30 W. Magnus, F. Oberhettinger: Formeln und Sätze für die speziellen Funktionen der mathematischen Physik; Springer-Verlag, Berlin, 1948

31 K. Kambe: Z. Naturforschung 22a, 322 (1967)

32 J.L. Beeby: J. Phys. C 1, 82 (1968)

33 C.B. Duke, C.W. Tucker: Surface Sci. 15, 231 (1969), Phys. Rev. Letters 23, 1163 (1969)

34 D.S. Boudr eaux, V. Heine: Súrface Sci. 8, 426 (1967)

J.B. Pendry: J. Phys. C. 2, 2273 (1969)

G. Capart: Surface Science, 1971 in press

35 J.M Ziman: Proc. Phys. Soc. 86, 337 (1965)

36 W. Kohn, N. Rostocker, Phys. Rev. 94, 1111 (1954)
F.S. Ham, B. Segall: Phys. Rev. 124, 1786 (1961)

37 V. F. Turchin: Slow Neutrons

Oldoune Press, London, 1965

38 Yu. Kagan: JEPT Letters, 11, 147 (1970)

39 J.C. Slater, N.H. Frank: Electromagnetism, McGraw Hill, New York, 1947

40 G. Bormann, W. Hartwig: Z. Kristallogr. 121, 6 (1965)
W. Übach, G. Hildebrandt: Z. Kristallogr. 129, 1 (1968)

41 T. Joko, A. Fukuhara: J. Phys. Soc. Jap. 22, 597 (1967)

42 G. Hildebrandt: phys. stat. sol. 24, 245, (1967)
Y. Héno, P.P. Ewald: Acta Cryst. A 24, 5; A 24, 16 (1969)

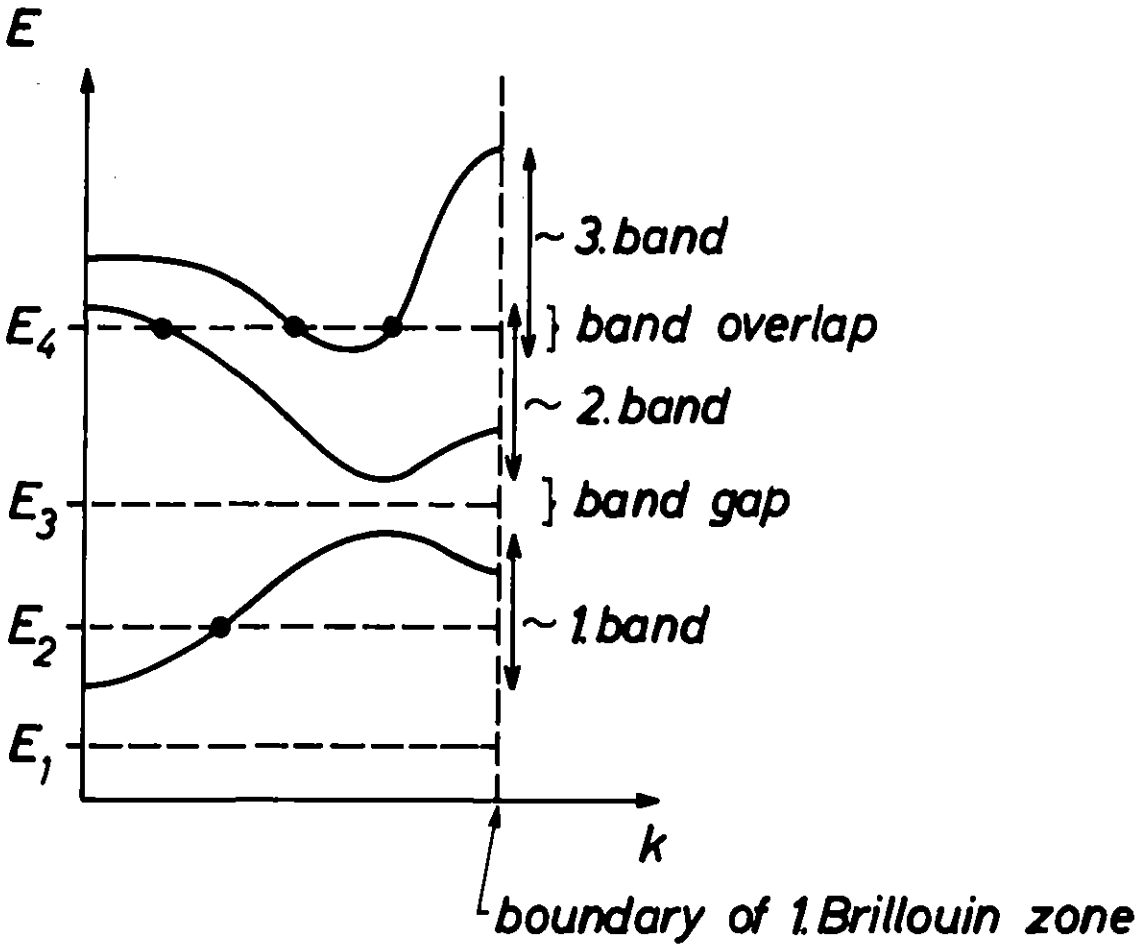

Fig.1

Qualitative scheme of bandstructure

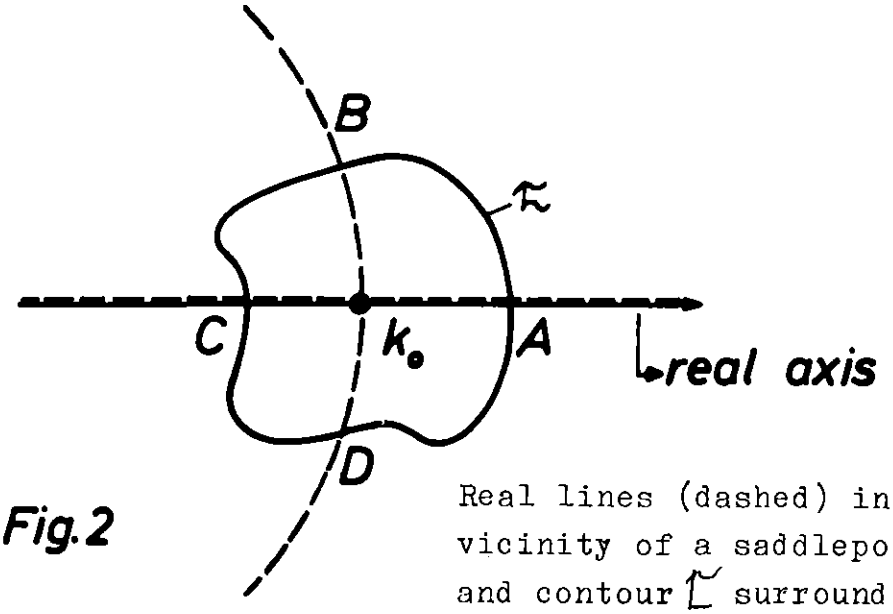

Fig.2

Real lines (dashed) in the vicinity of a saddlepoint k_o and contour Γ surrounding k_o.

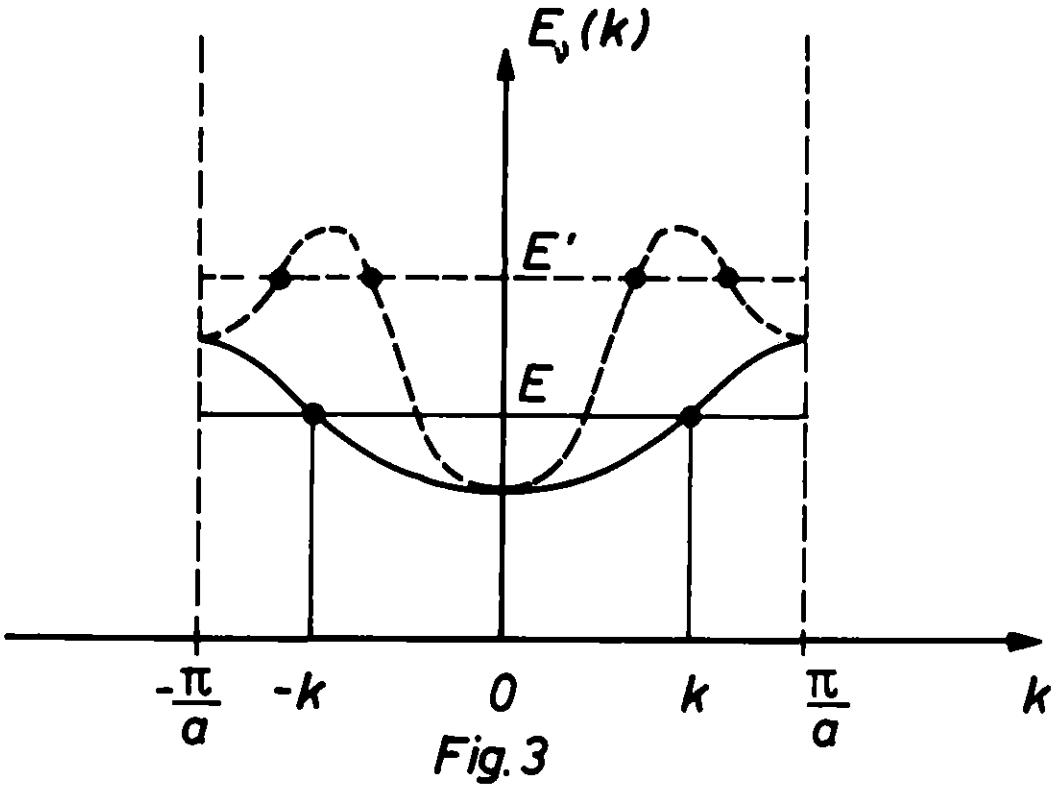

Fig. 3

Bandstructure in one dimension. For each energy E there are two linearly independent solutions k and -k (full lines). Dashed lines, giving four independent solutions, are impossible.

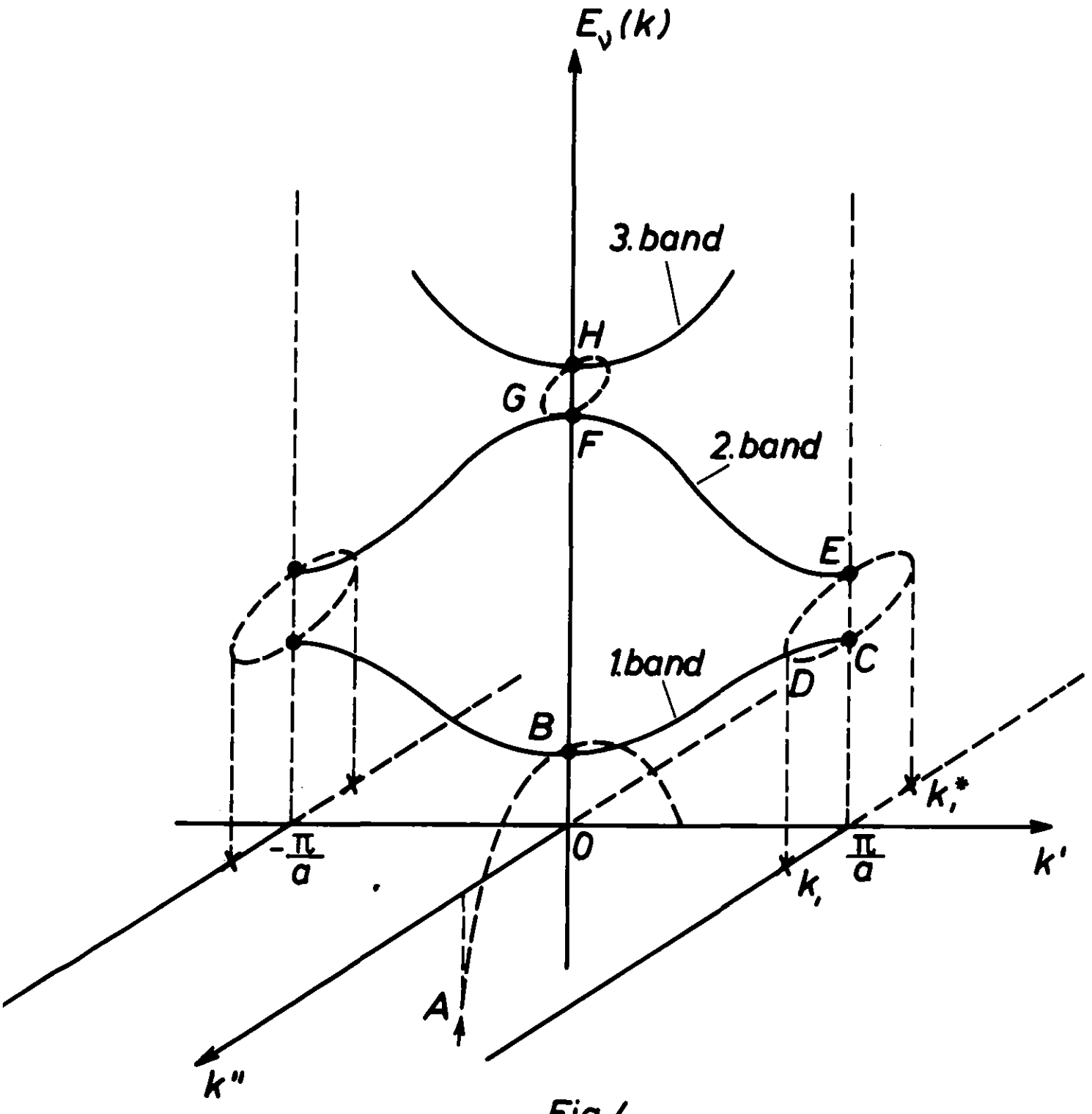

Fig.4

Complex bandstructure in one dimension (k = k'+ik'')
(● saddlepoints, X branch points, ——— k real,
- - - - k komplex)

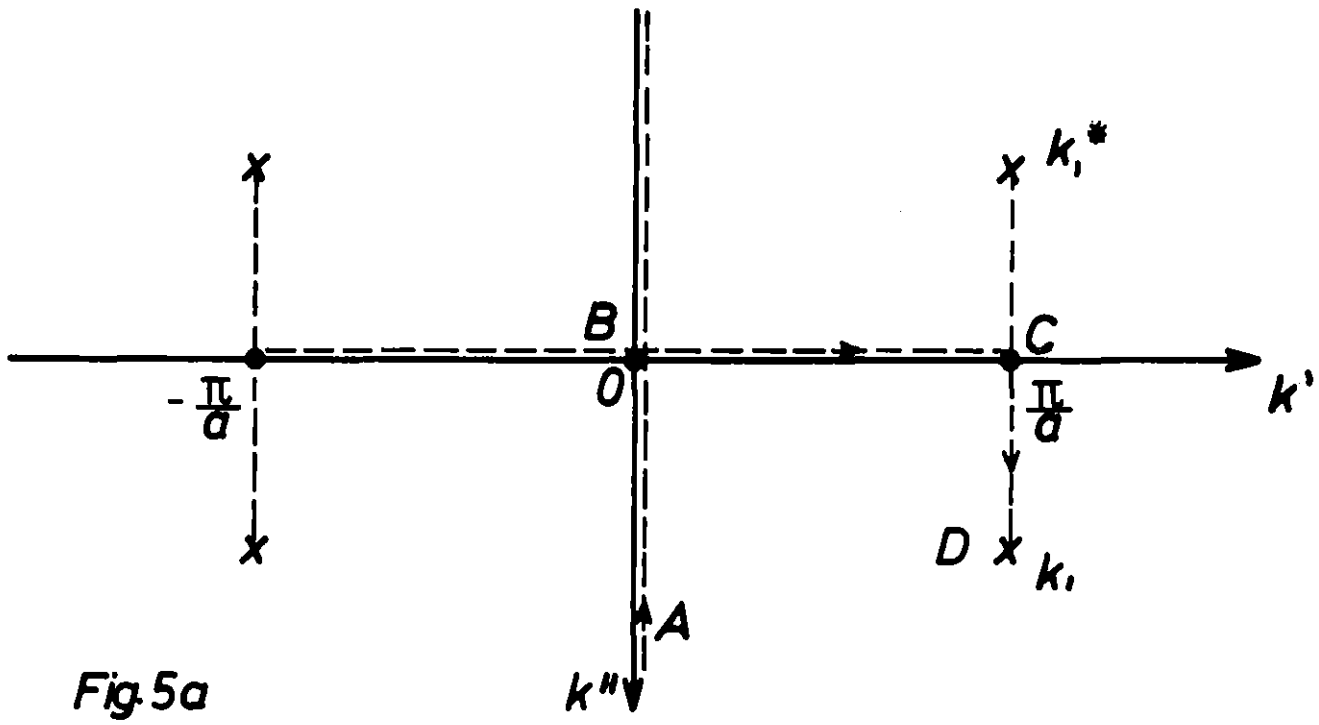

Fig. 5a

Fig. 5a Real lines in first Riemann sheet (dashed).
(● saddlepoints, X branchpoints)

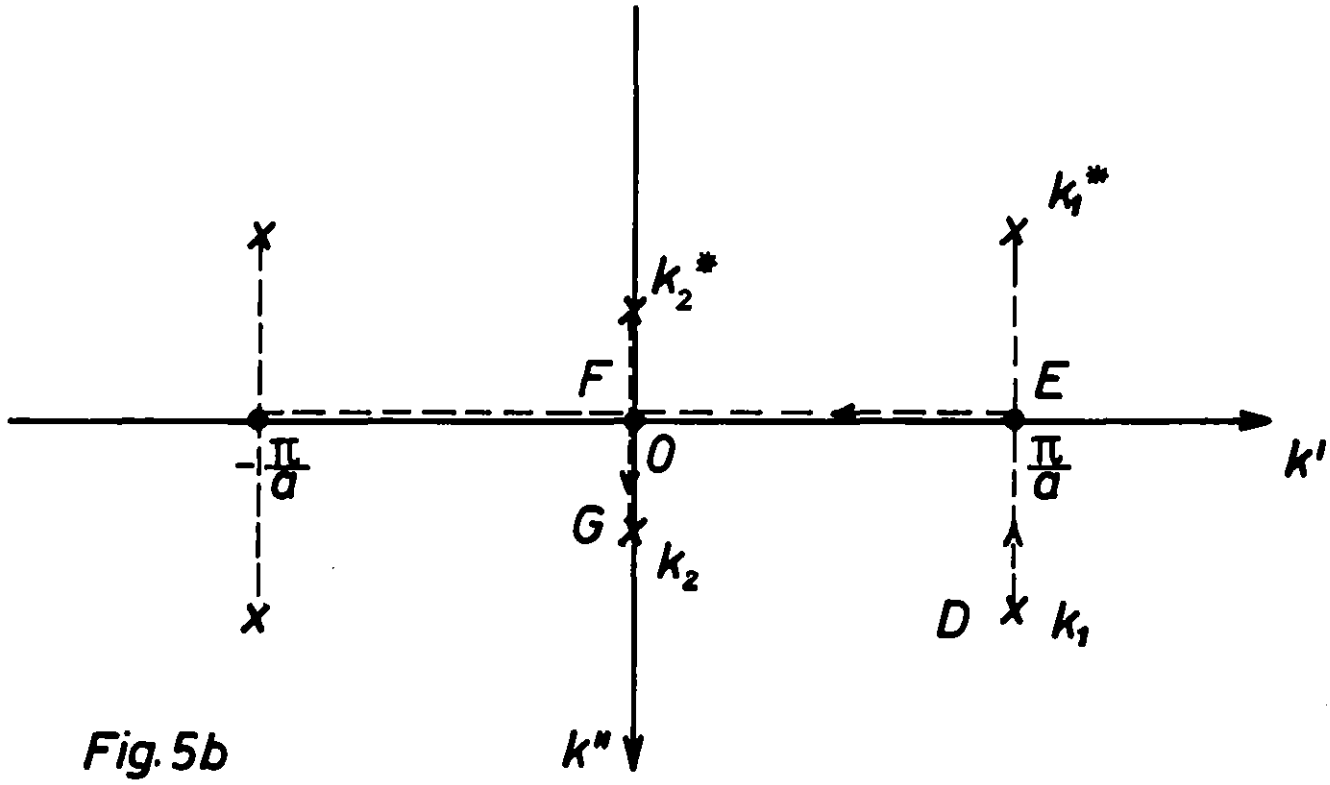

Fig. 5b

Fig. 5b Real lines in second Riemann sheet (dashed)
(● saddlepoints, X branchpoints)

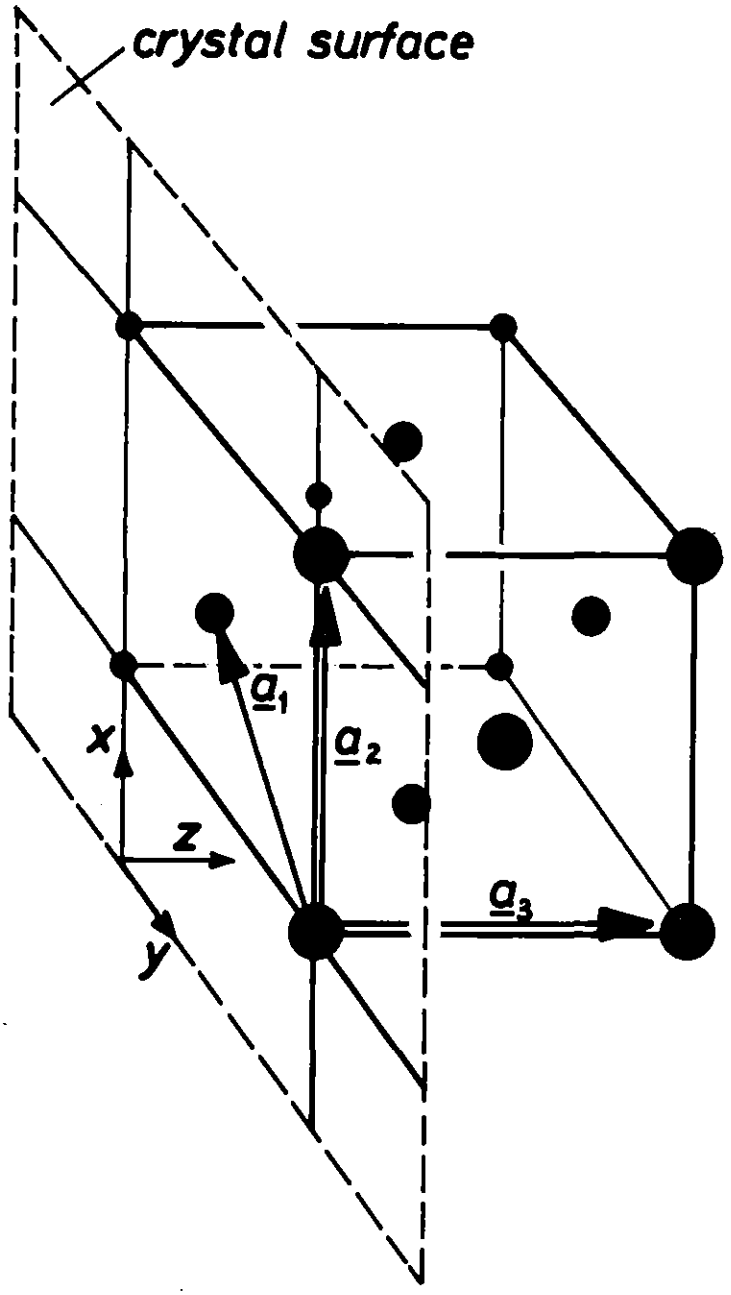

Fig. 6

Fig. 6 Choice of the basis vectors for a (100) surface of a f.c.c. crystal. ($\underline{a}_1$, $\underline{a}_2$ in crystal boundary; $\underline{a}_3$ perpendicular)

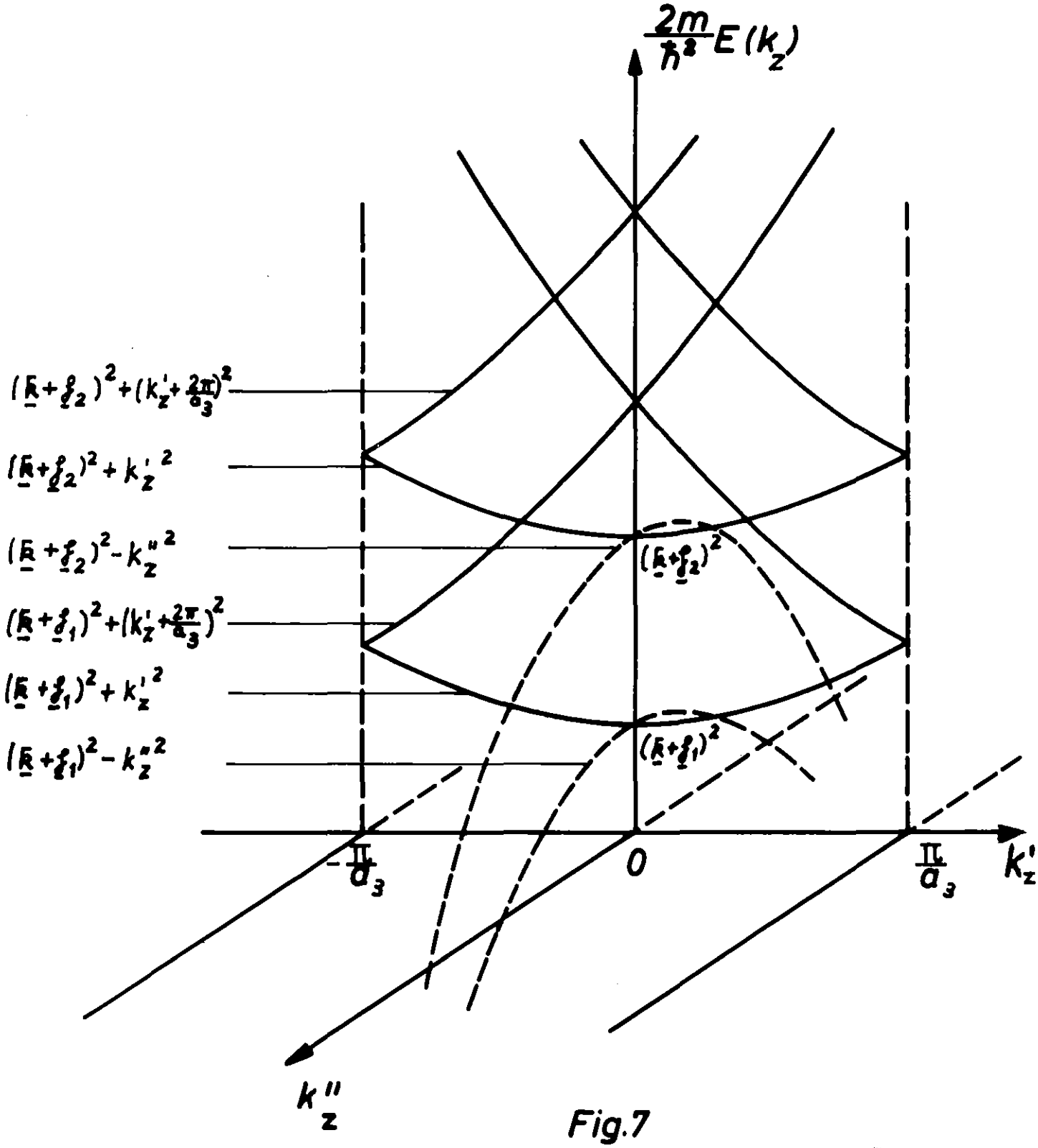

Fig.7

Fig. 7 Free electron bandstructure in three dimensions

_____ $k = k_z'$ real

- - - - k complex

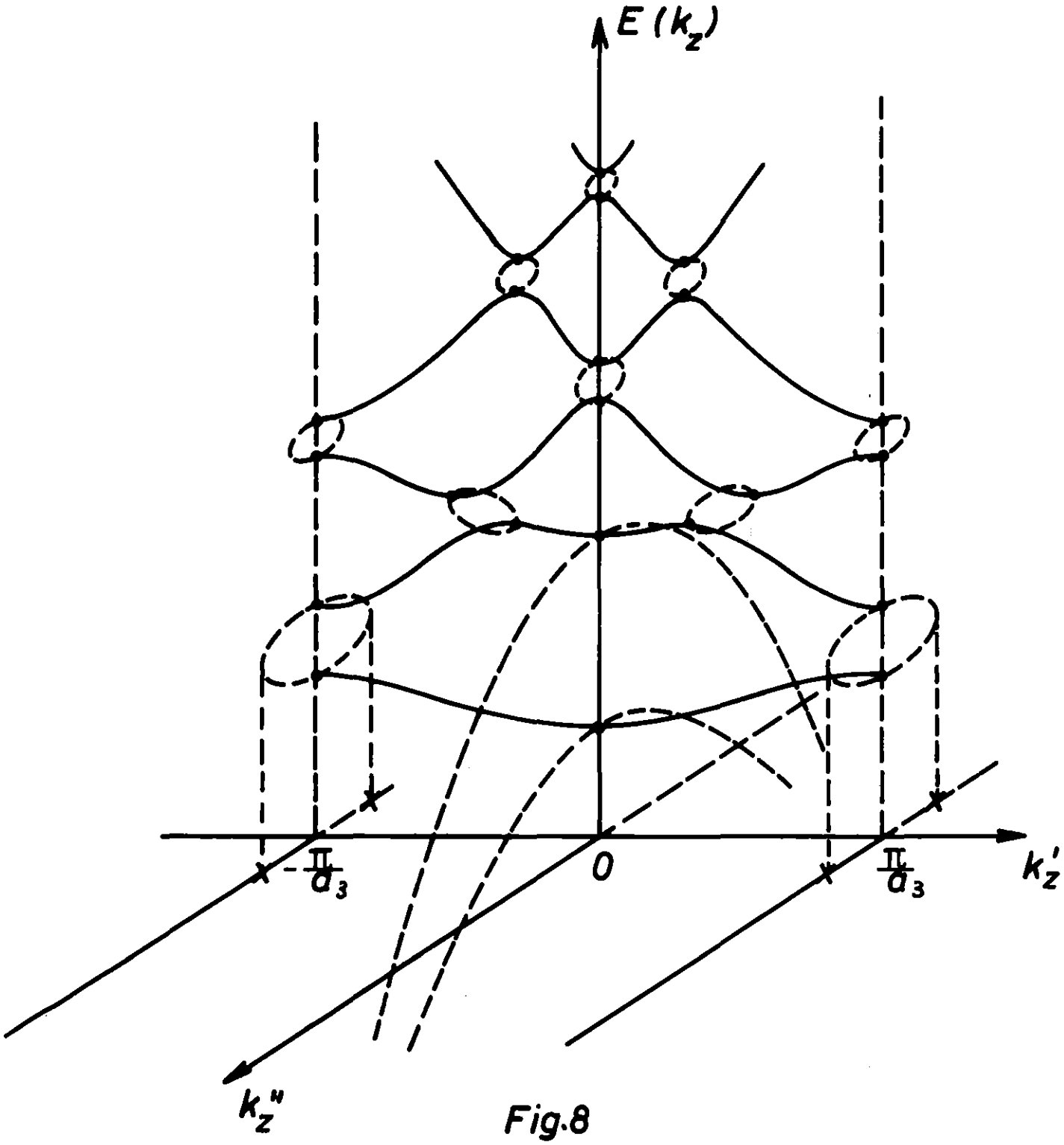

Fig.8

Fig. 8 Bandstructure in three dimensions

——— bands with real k_z

- - - bands with complex k_z

● saddlepoints

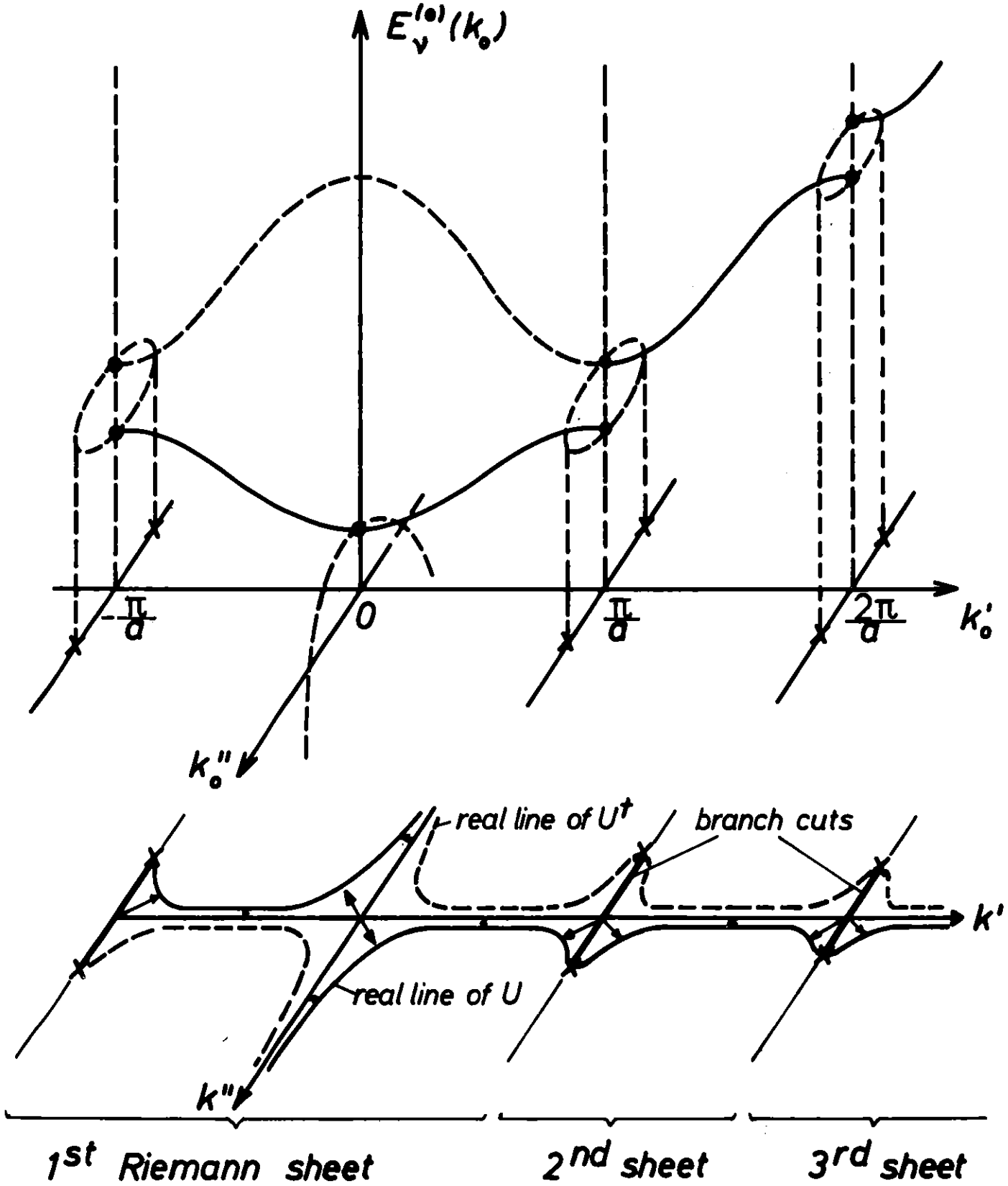

Fig. 9

Fig. 9 Real lines for nonhermitian potentials.
(● saddlepoints of U'; × branchpoints)

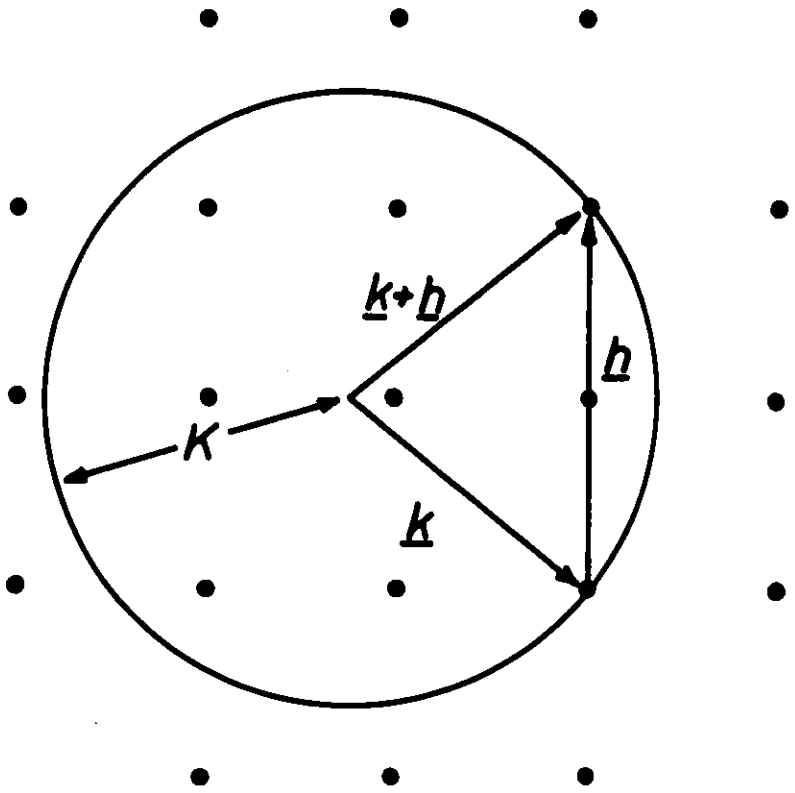

Fig.10

Fig. 10 Ewaldsphere

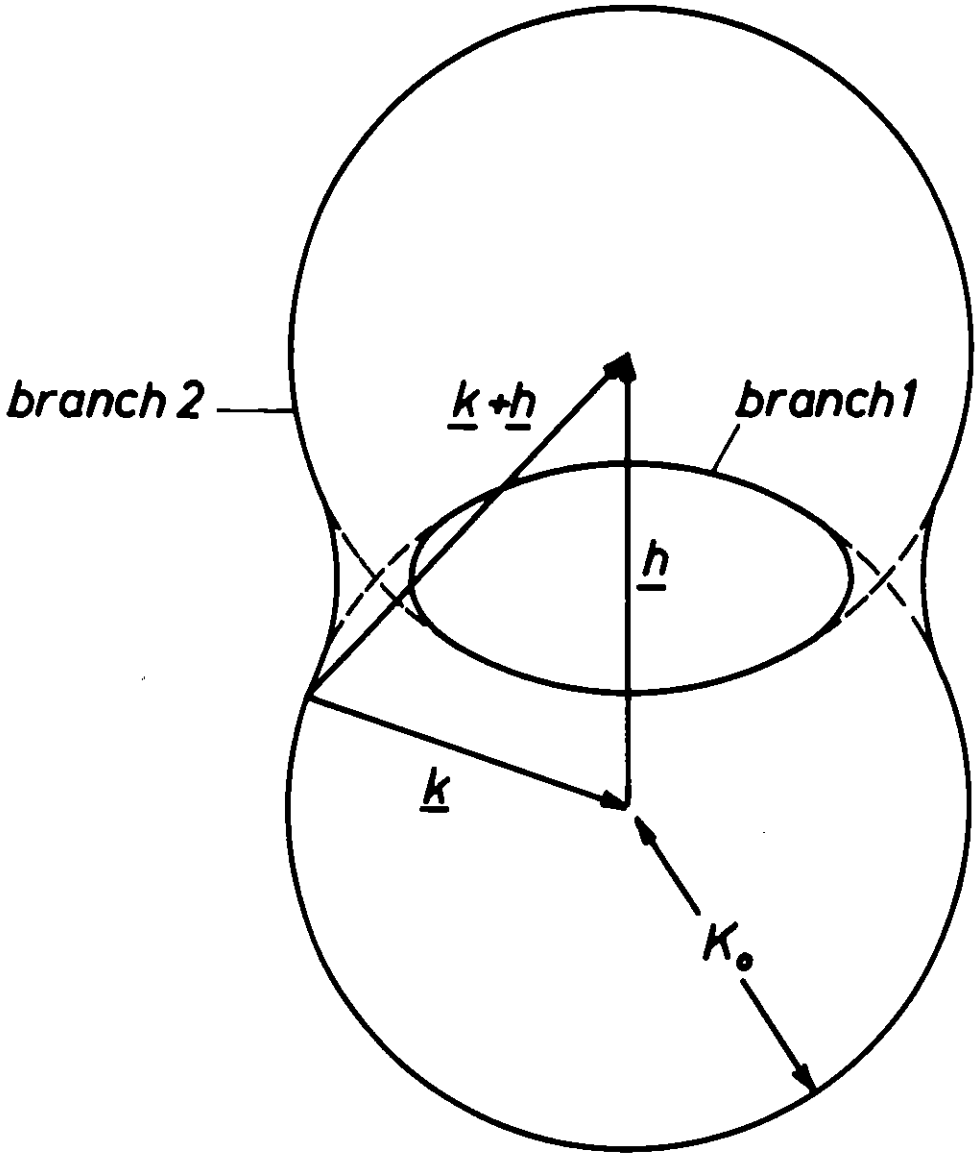

Fig·11

Fig. 11 Dispersion surface for two-beam case

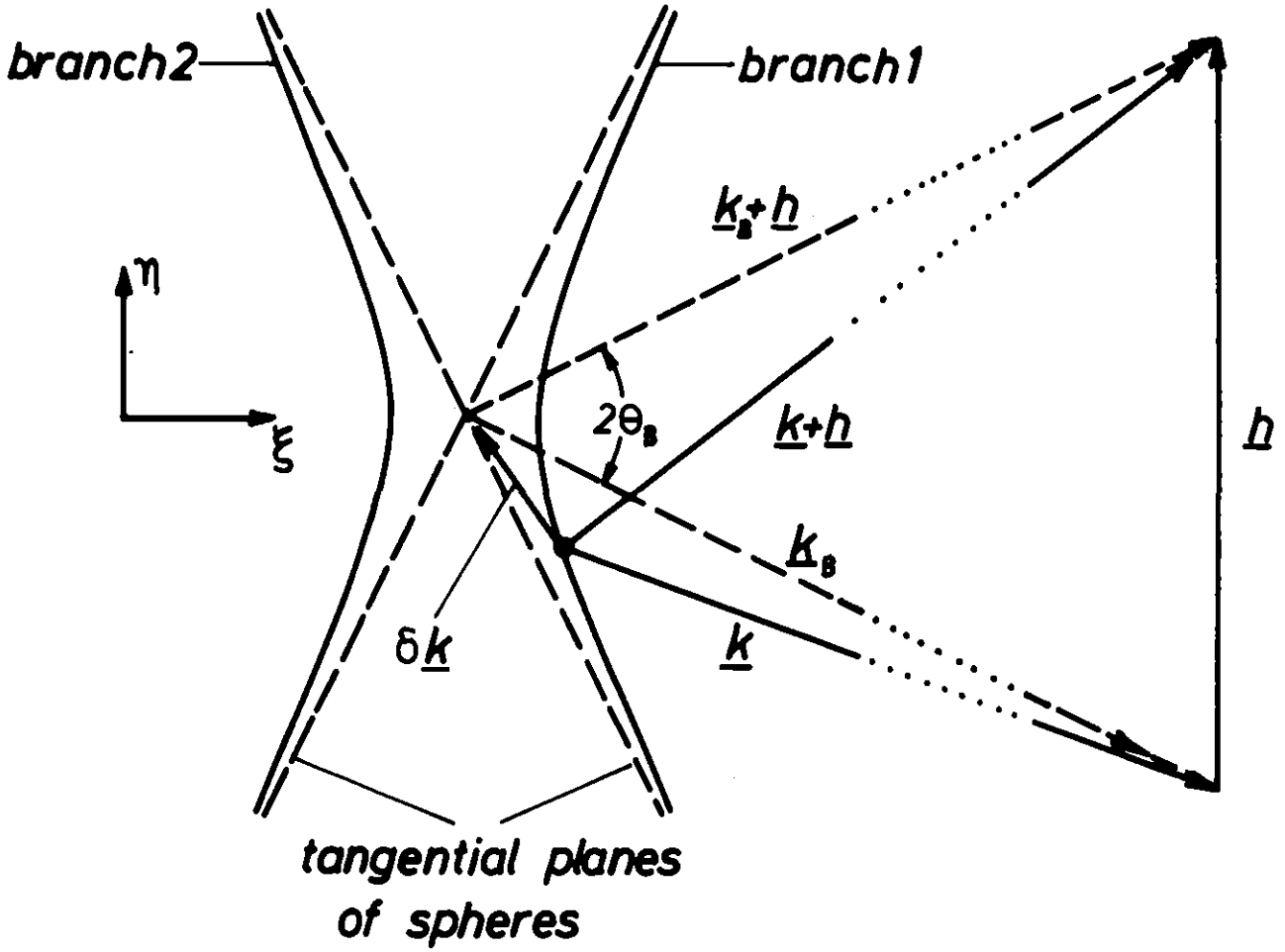

Fig.12

Fig. 12 Dispersion surface near the Bragg spot $\underline{k}_B$

ig. 13a Bandstructure for the two-beam case ($\underline{k} = (k_\eta, o, o)$)

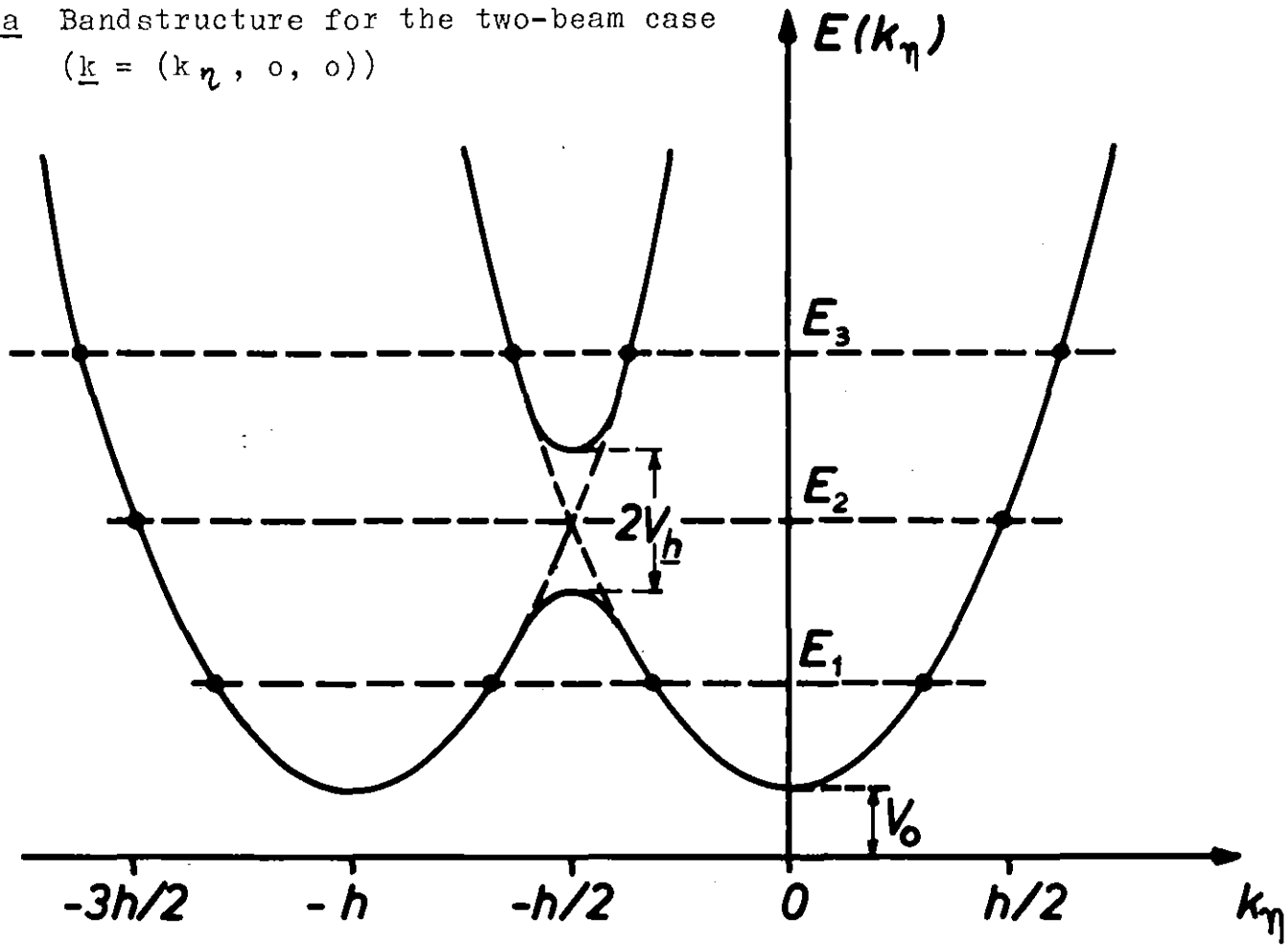

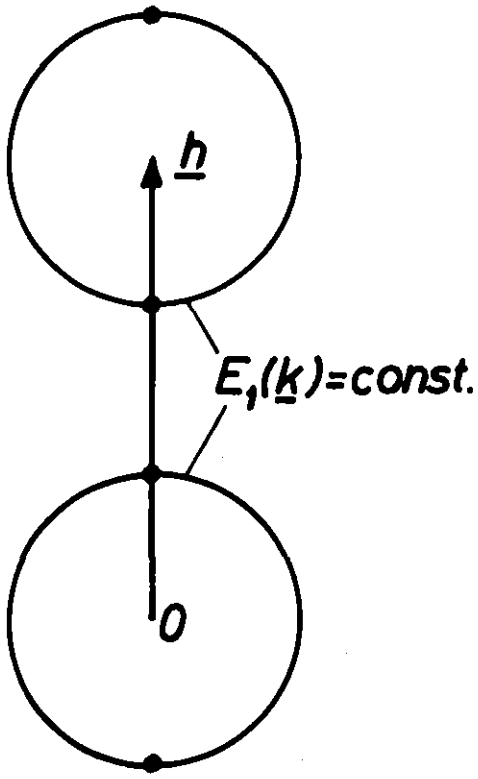

Fig.13b

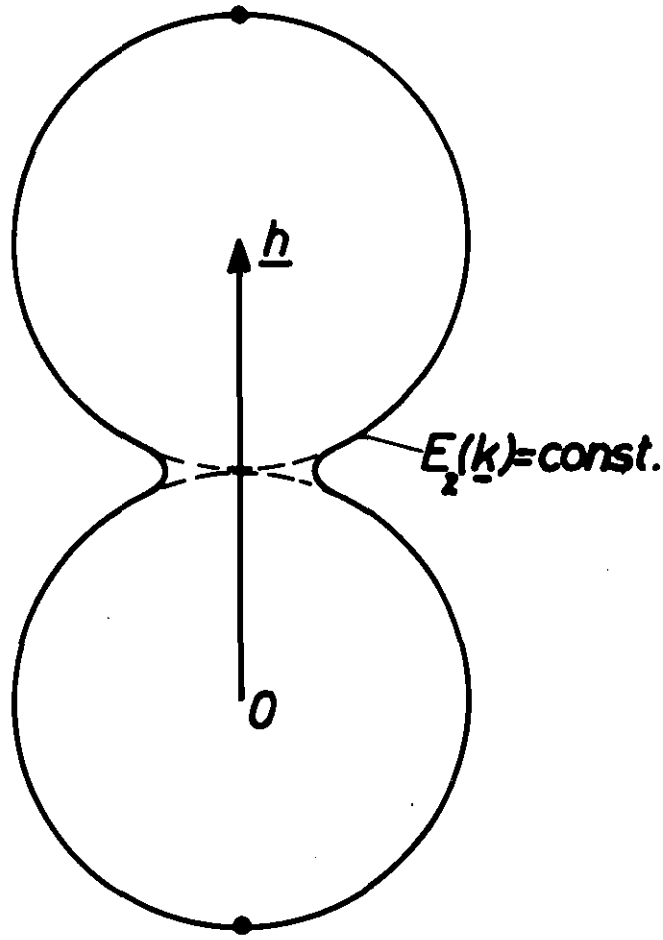

Fig.13c

Fig. 13b Dispersion surface for energy E

Fig. 13c Dispersion surface for energy E_2

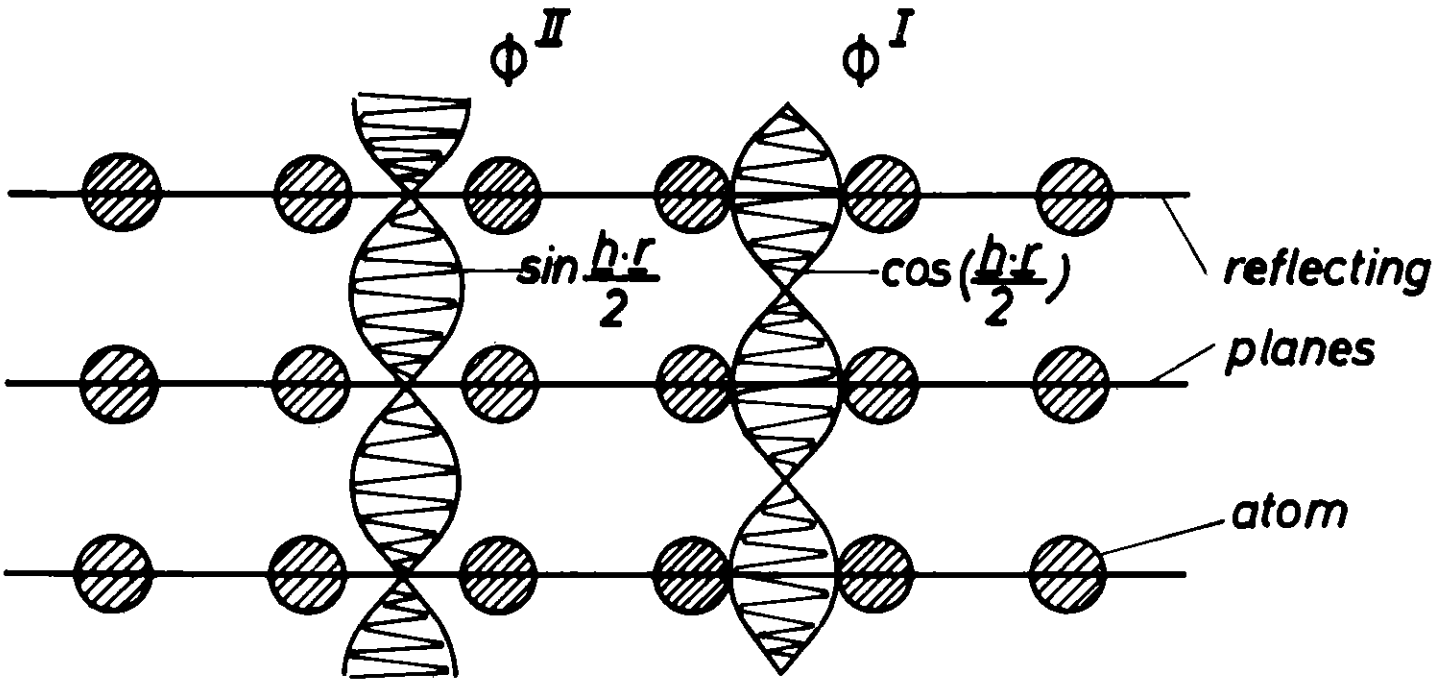

Fig.14

Fig. 14 Modulationfactors of ϕ^{I} and ϕ^{II}

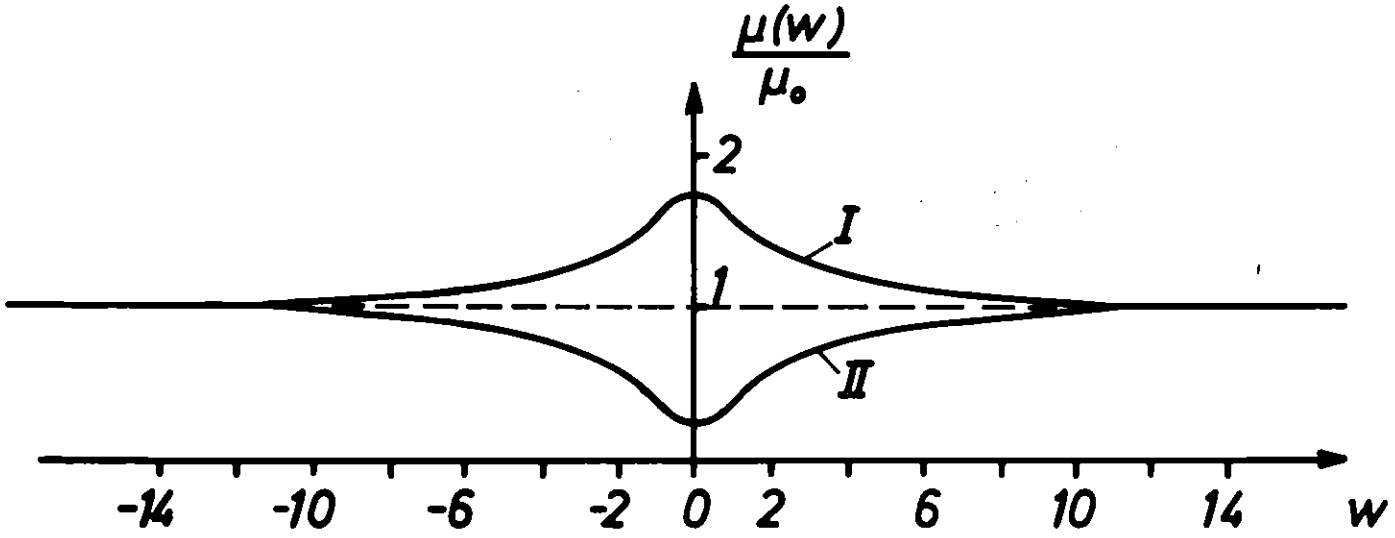

Fig. 15

Fig. 15 Absorption for Blochwave I and II (for $\mu_h = 3/4\,\mu_o$)

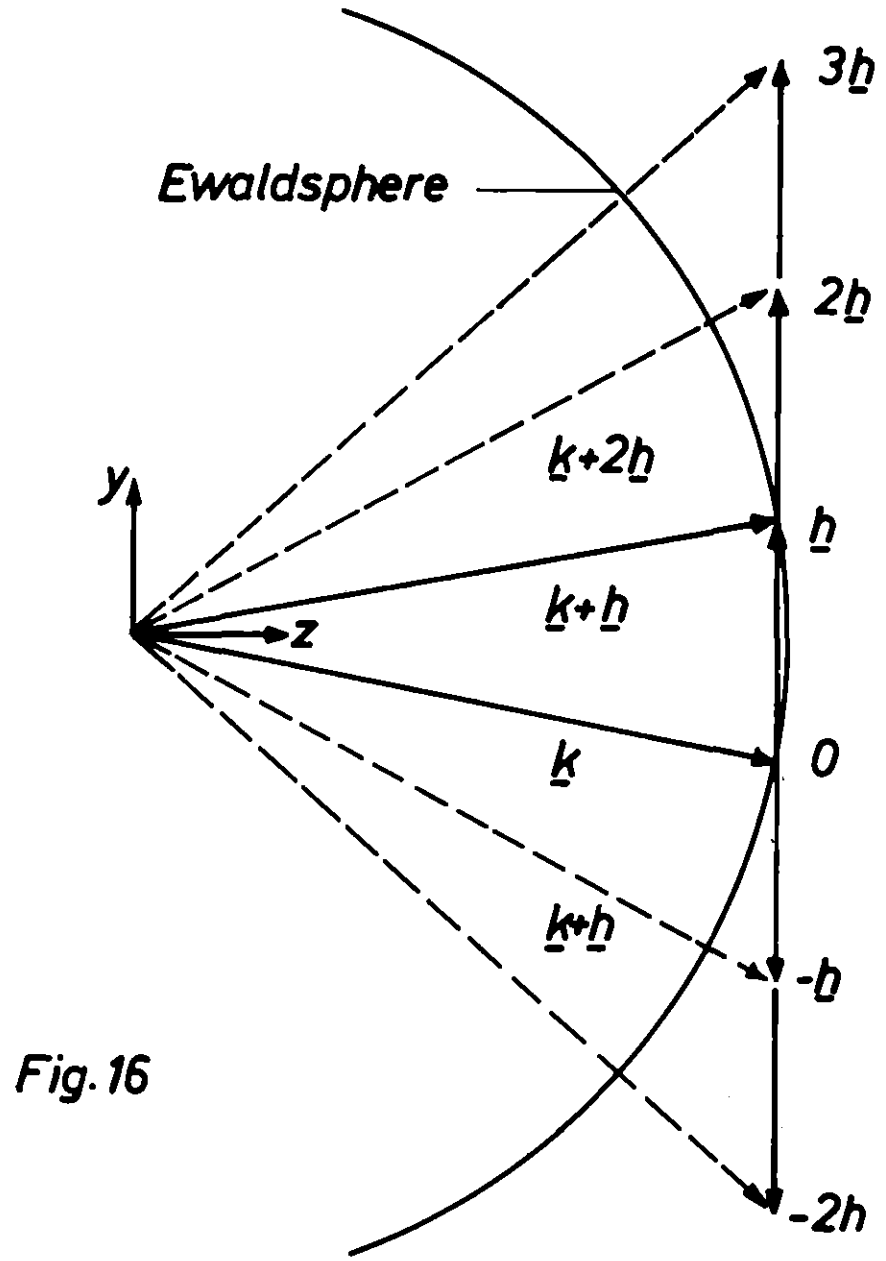

Fig. 16

Fig. 16 Systematic Reflections 2h, 3h, and -h, -2h

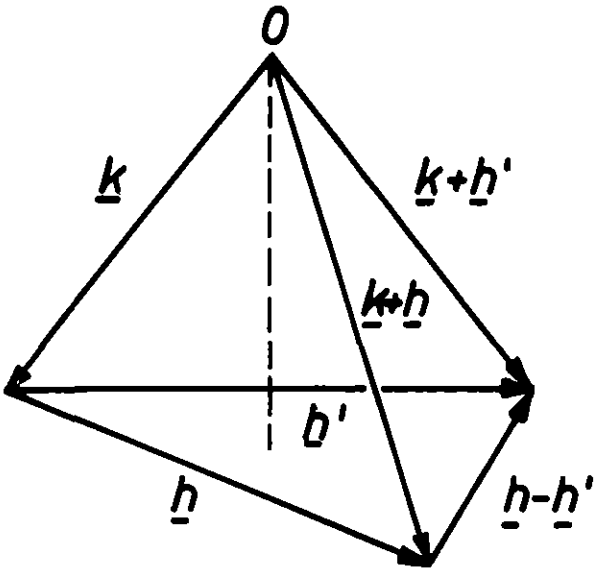

Fig.17a

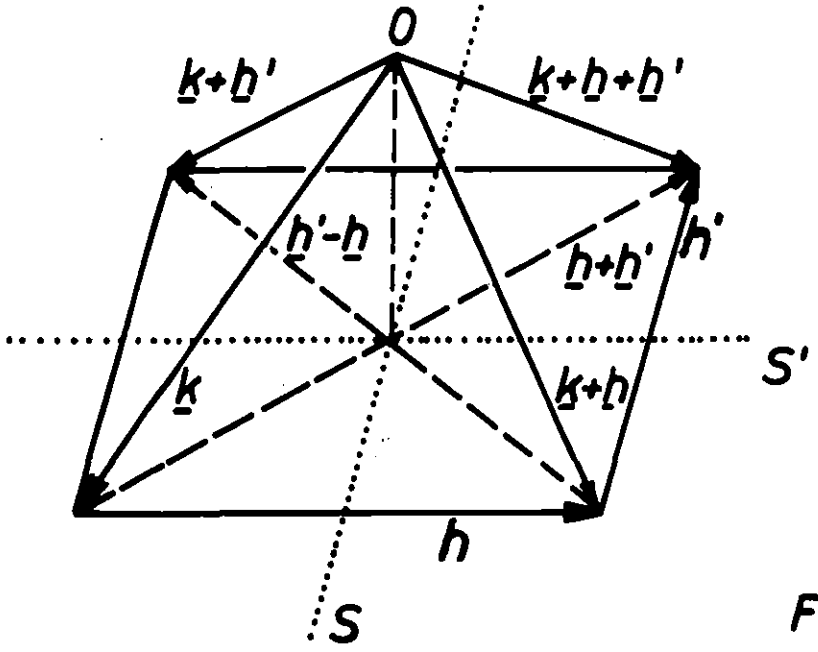

Fig.17b

Fig. 17ab Multiple-beam cases

a) three beams $\underline{k}$, $\underline{k}+\underline{h}$, $\underline{k}+\underline{h}'$ ($|\underline{h}| = |\underline{h}'|$)

b) four beams $\underline{k}$, $\underline{k}+\underline{h}$, $\underline{k}+\underline{h}'$, $\underline{k}+\underline{h}+\underline{h}'$ ($\underline{h} \perp \underline{h}'$)

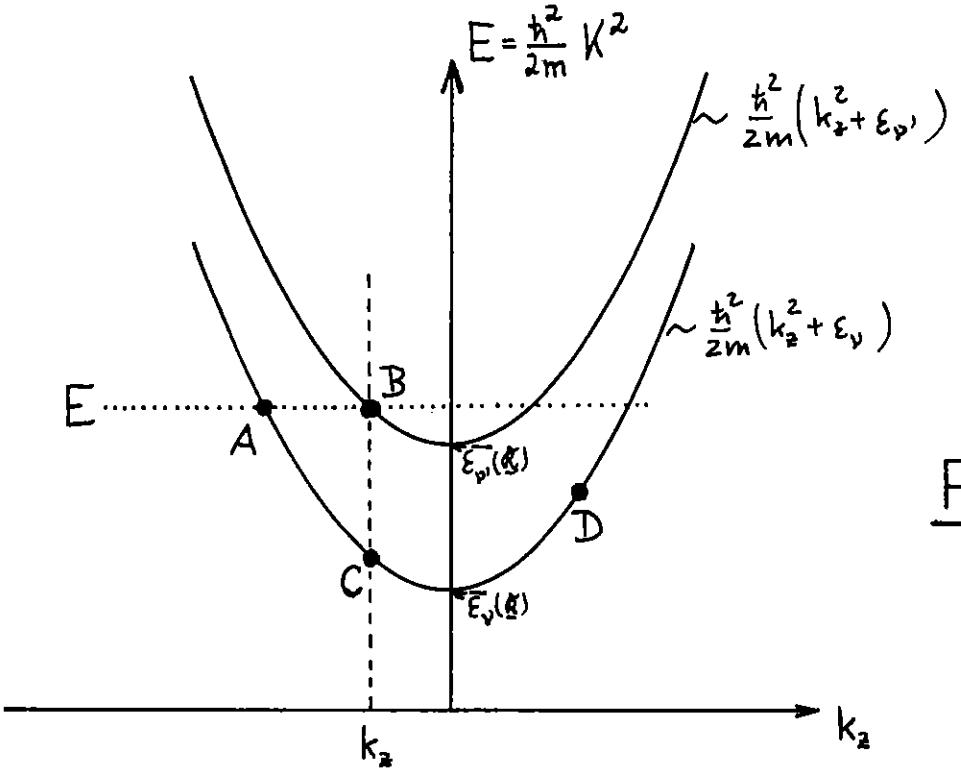

Fig. 17c

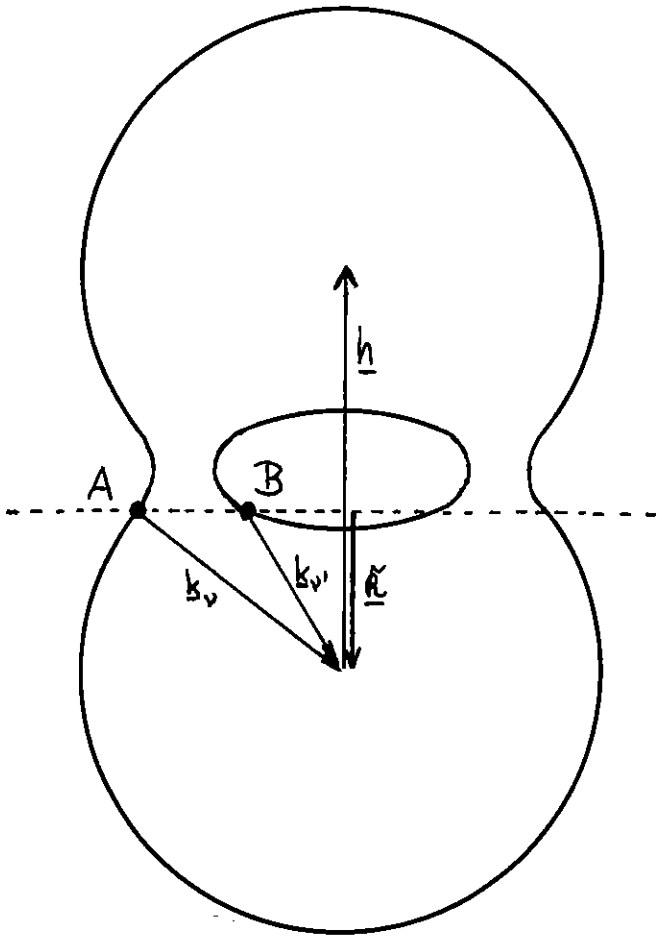

Fig. 17d

Fig. 17/cd Orthogonality of Bloch functions

c) The Bloch functions A,C and D are identical and orthogonal on B

d) The positions of A and B on the two-beam dispersion surface.

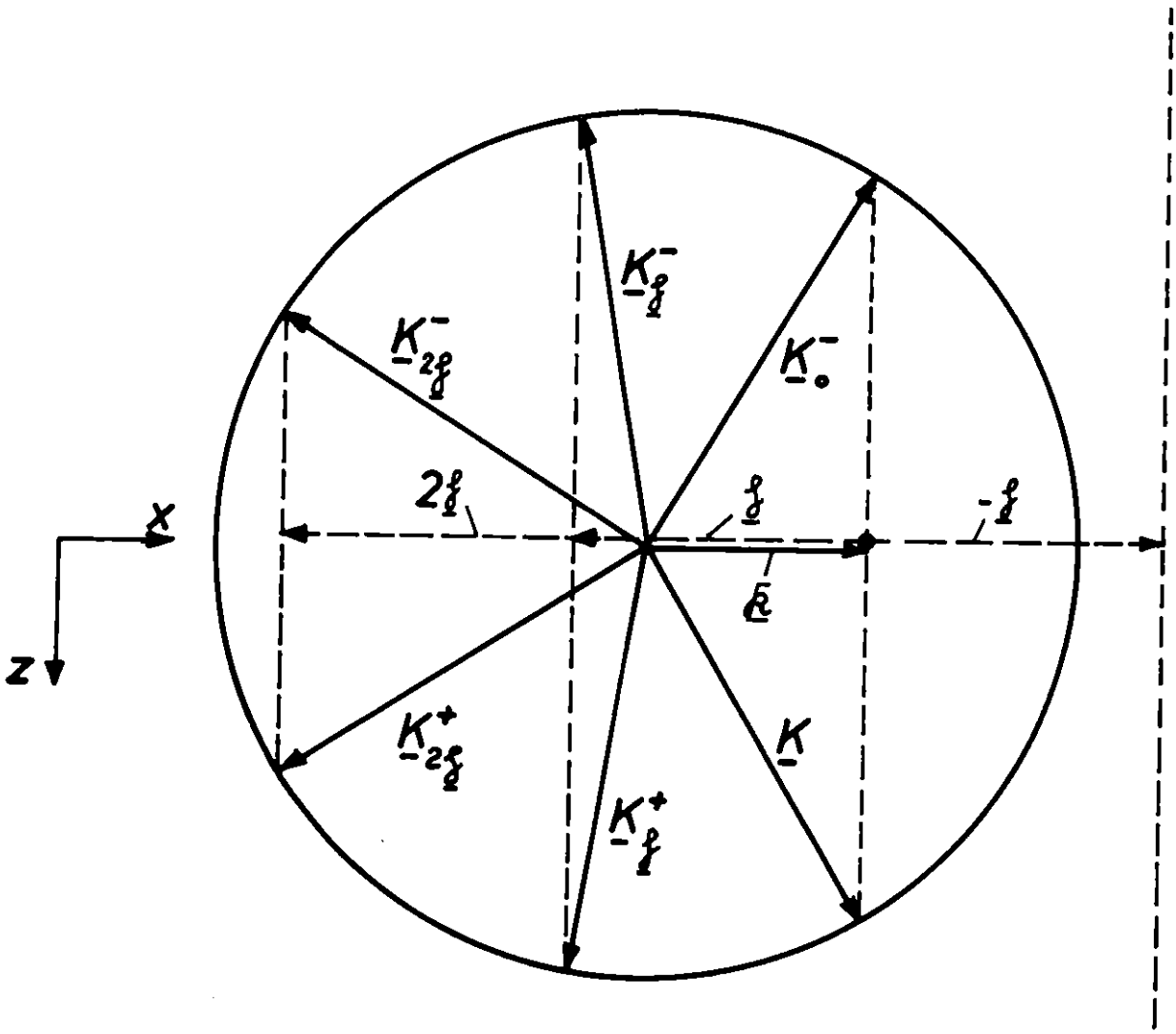

Fig. 18

Fig. 18 Plane waves $\underline{K}_{\ell}^{\pm}$ in the vacuum

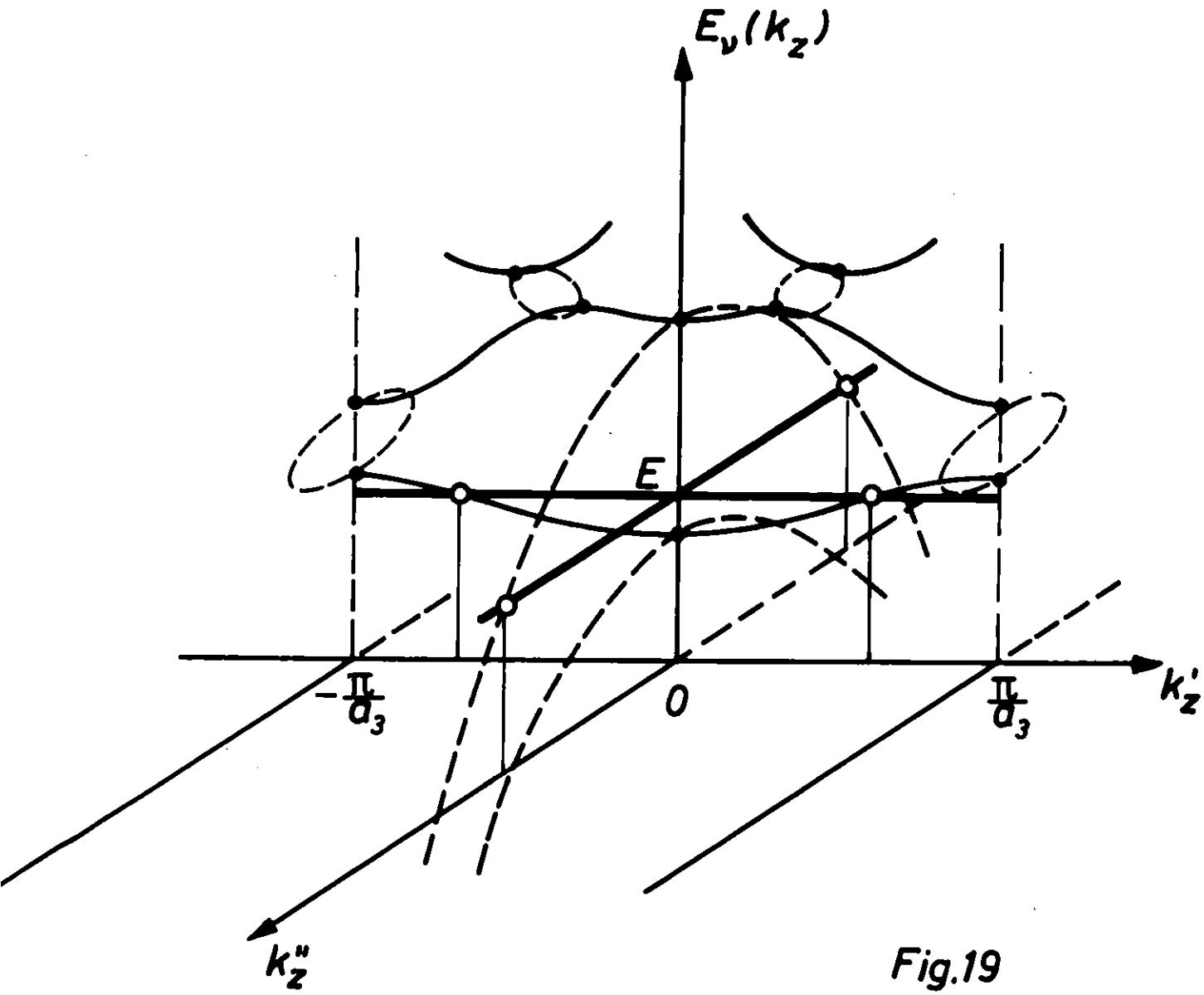

Fig.19

Fig. 19 Allowed k_z-values for a given energy E
(o allowed k_z's)

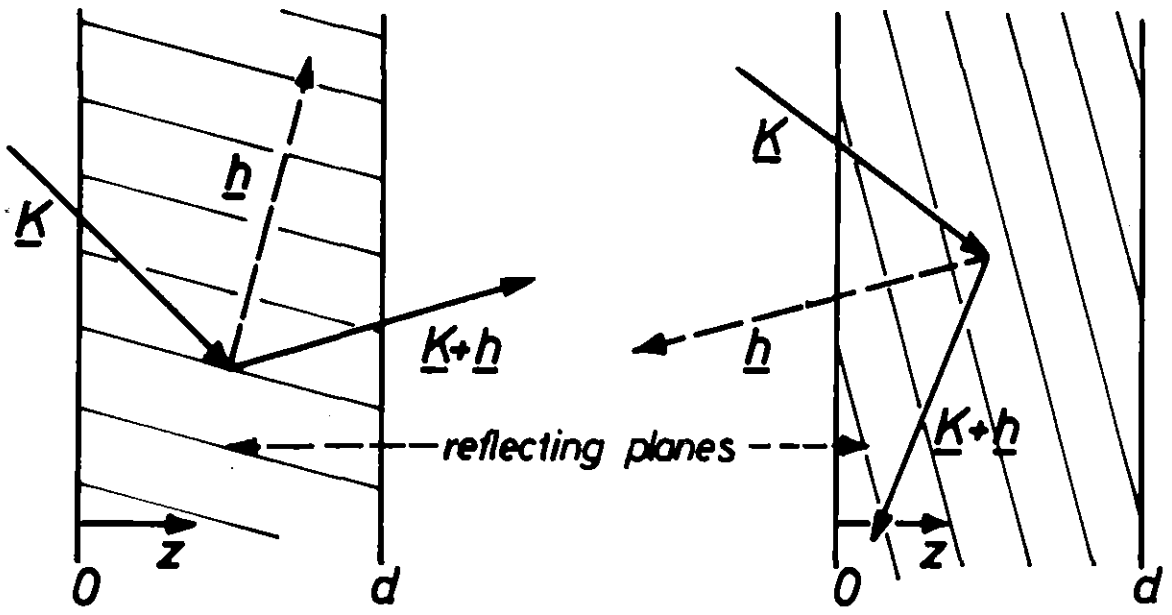

Fig.20

Fig. 20 Incident wave $\underline{K}$ and reflected wave $\underline{K} + \underline{h}$ for the Laue- and Bragg-case.

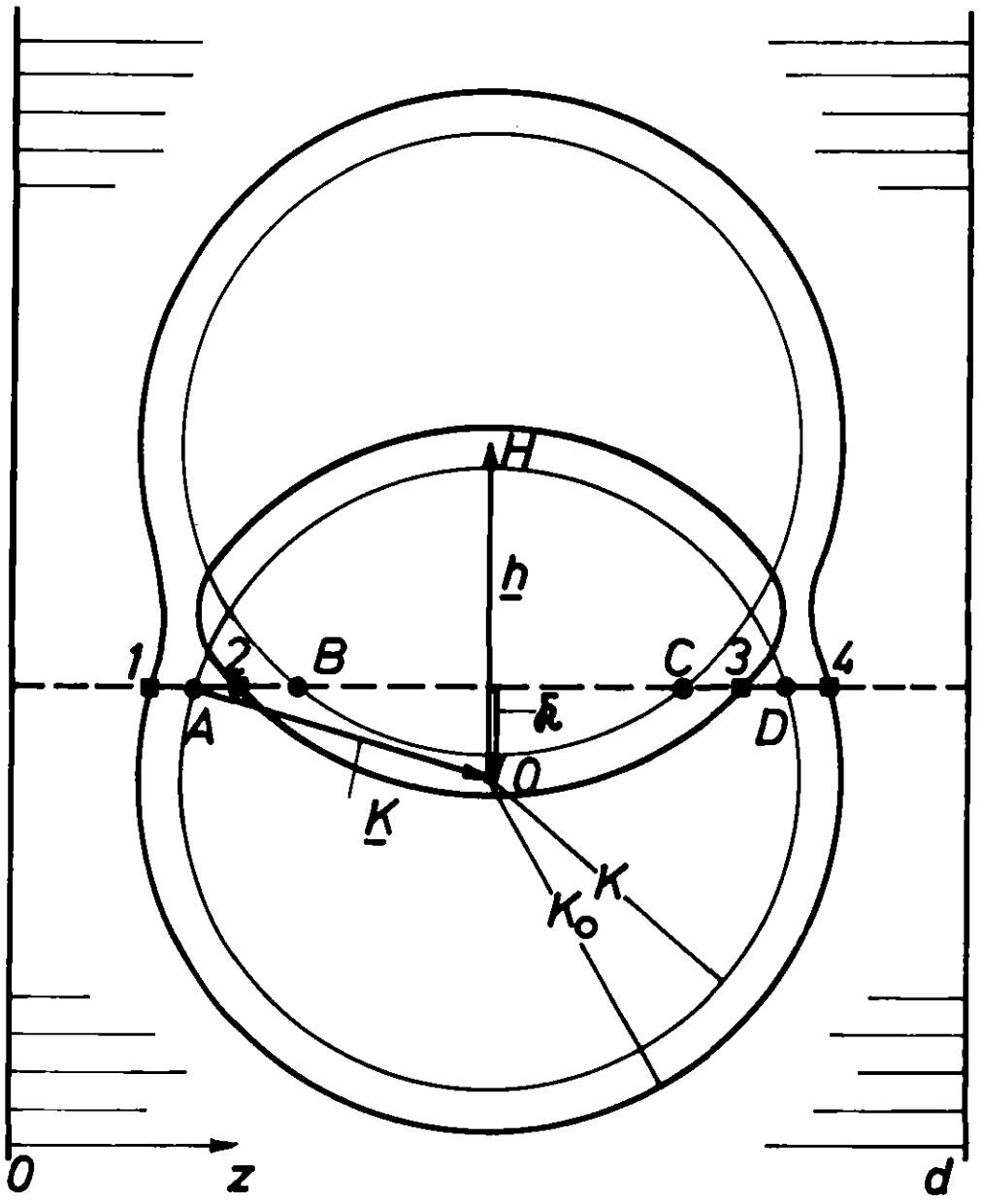

Fig.21

Fig. 21 Dispersion surface in crystal and vacuum.

——— dispersion surface in crystal

——— dispersion surface in vacuum

■ Bochvectors $\underline{k}_1$, $\underline{k}_2$, $\underline{k}_3$, $\underline{k}_4$ in the crystal

● plane waves $\underline{K}$, $\underline{K}_g^+$, $\underline{K}_g^-$, $\underline{K}_0^-$ in the vacuum

Fig. 22a

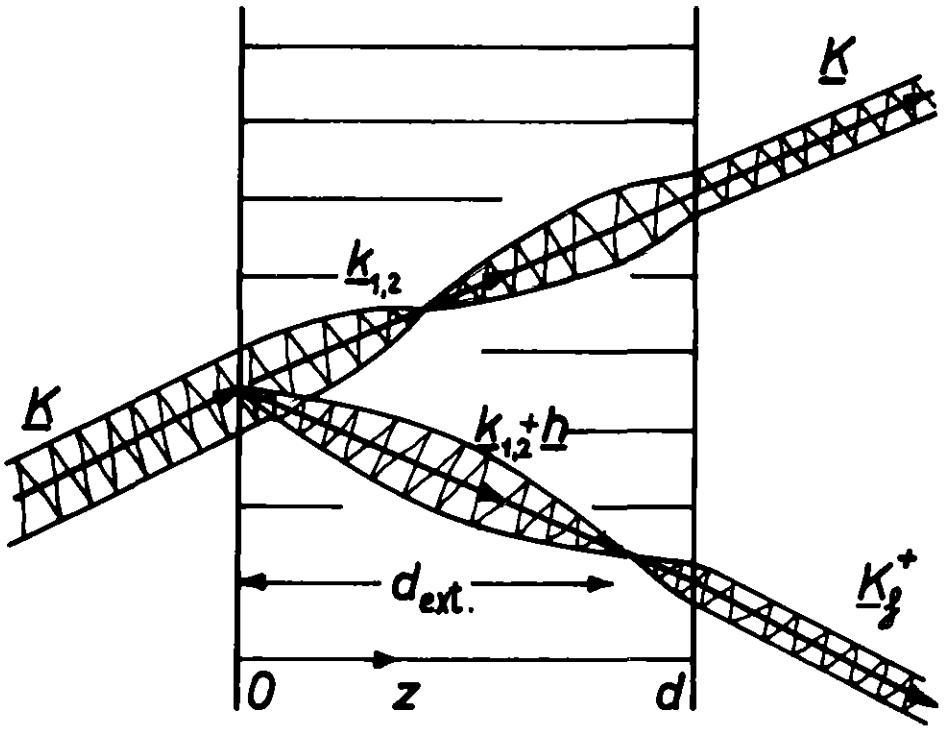

Fig. 22b

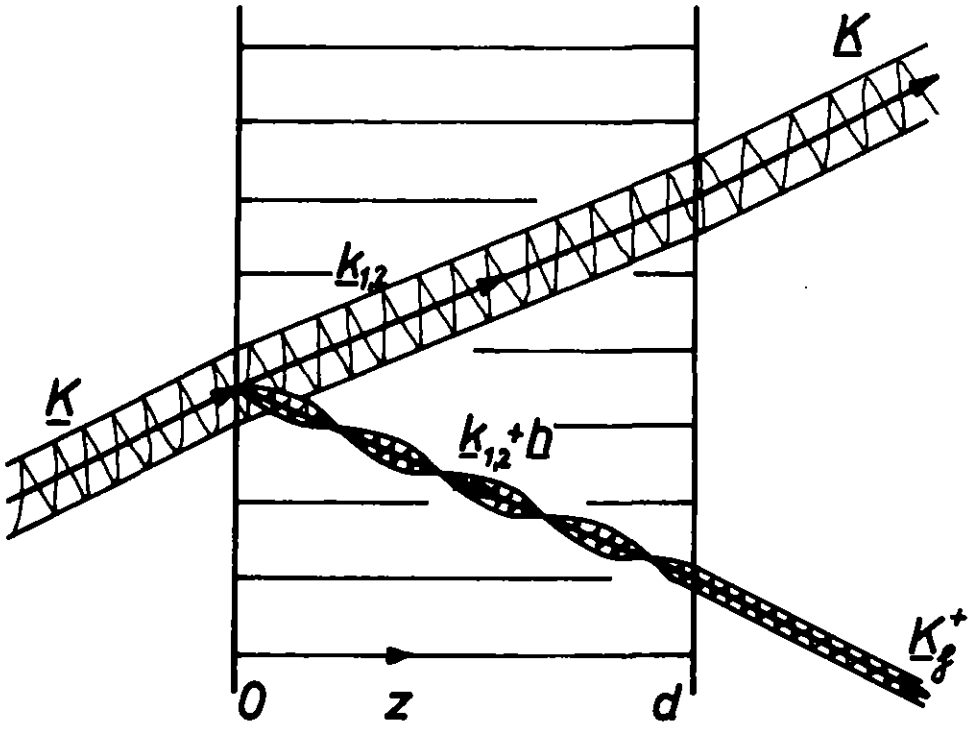

Fig. 22 Wave fields in the symmetrical Laue case
a) W = o exact Bragg condition
b) $|W| \gg |$ kinematical case

Fig. 23 Wave vectors in symmetrical Bragg case

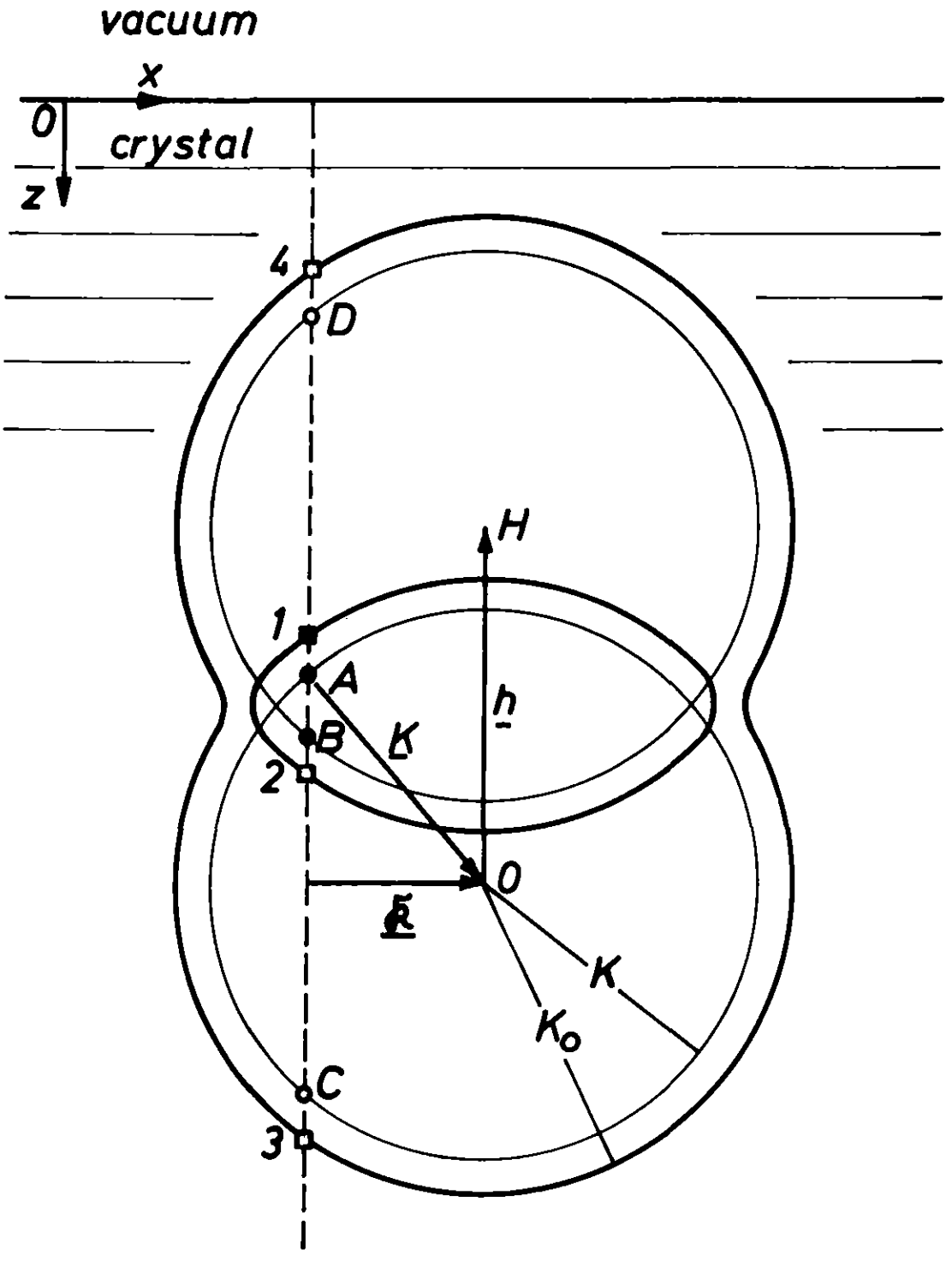

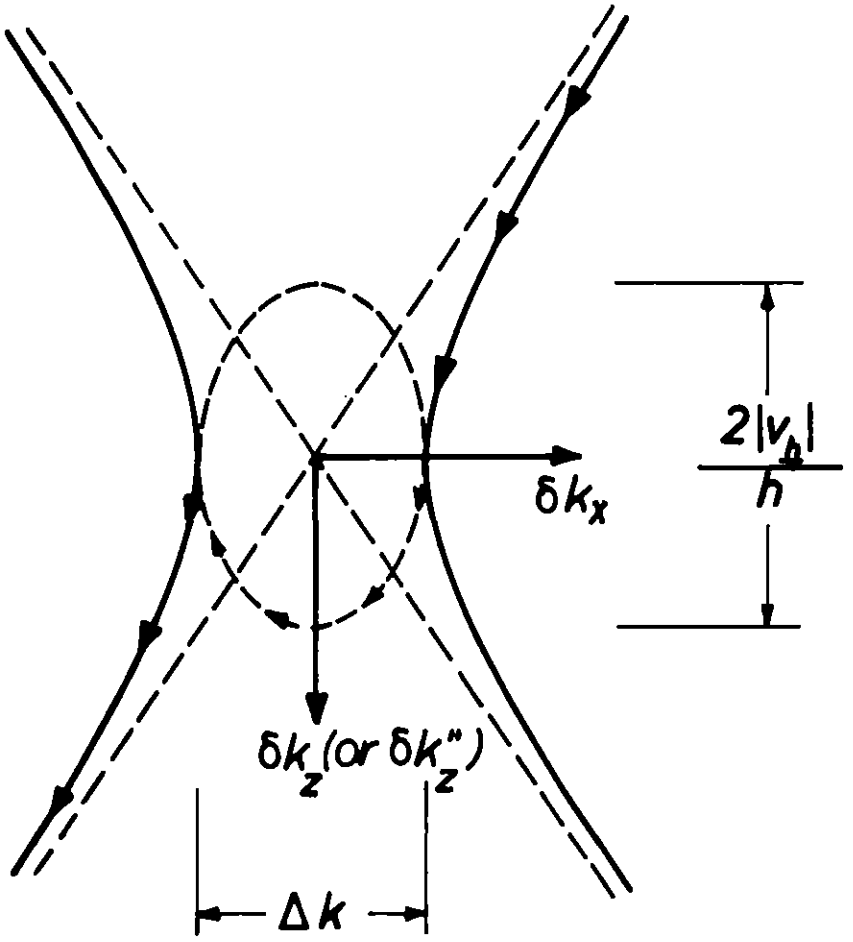

Fig.24

Fig. 24 Variation of $\underline{k}$ in the Bragg case
_____ k_z real, - - - - k_z complex

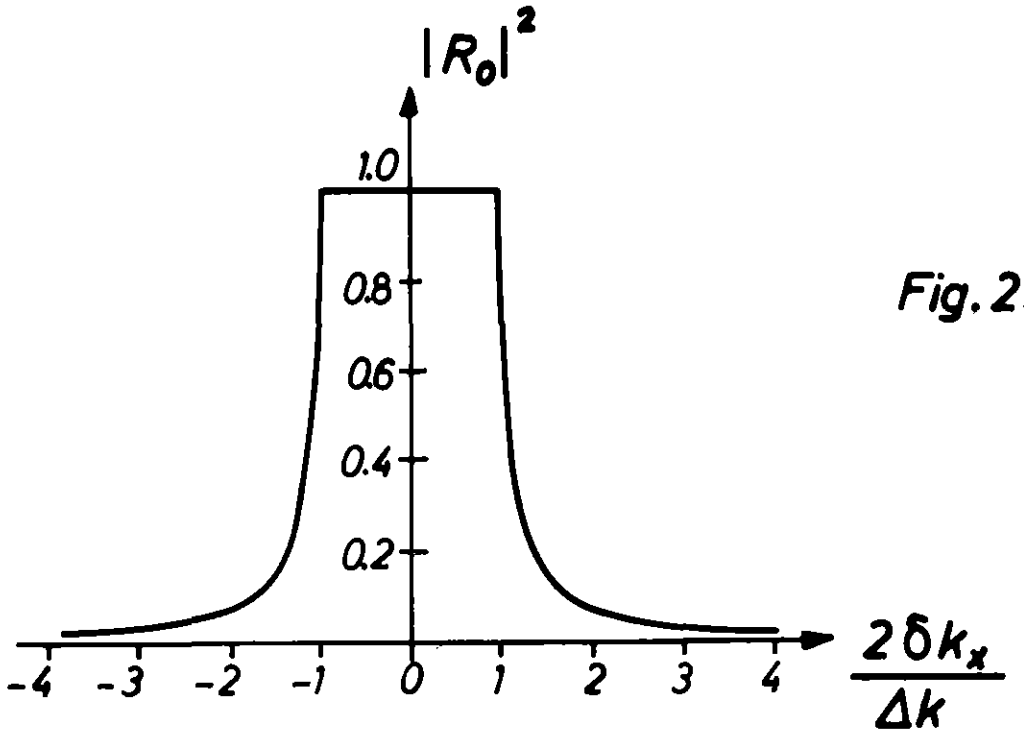

Fig. 25a

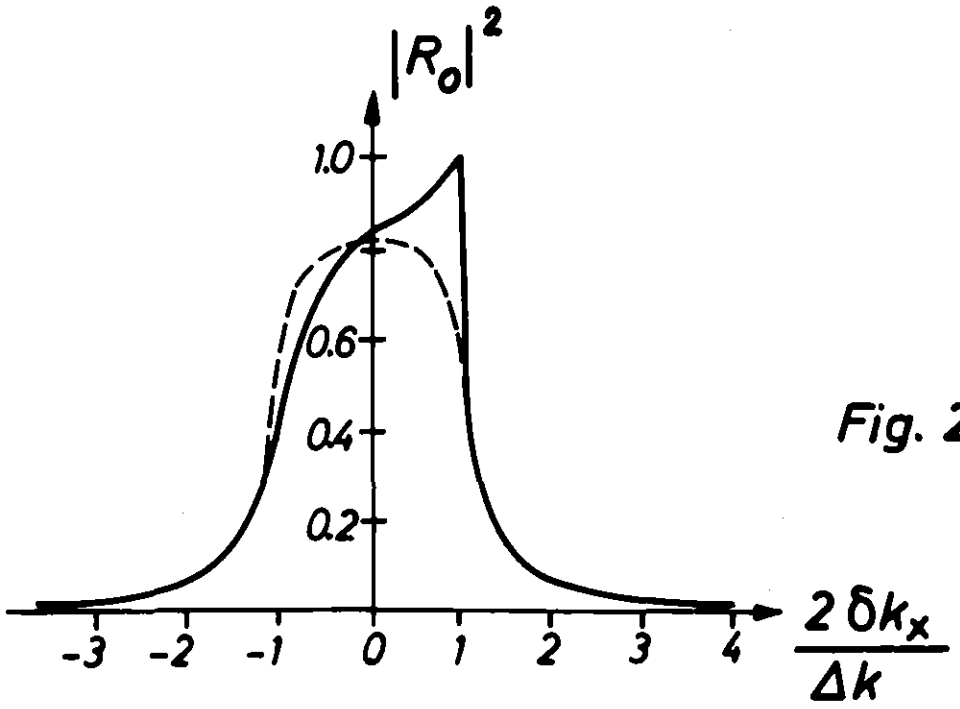

Fig. 25b

Fig. 25 Reflection coefficient $|R_o|^2$
a) without absorption
b) with absorption (——— $\nu_o'' = \nu_{\underline{h}}''$; – – – – $\nu_{\underline{h}}'' = o$)

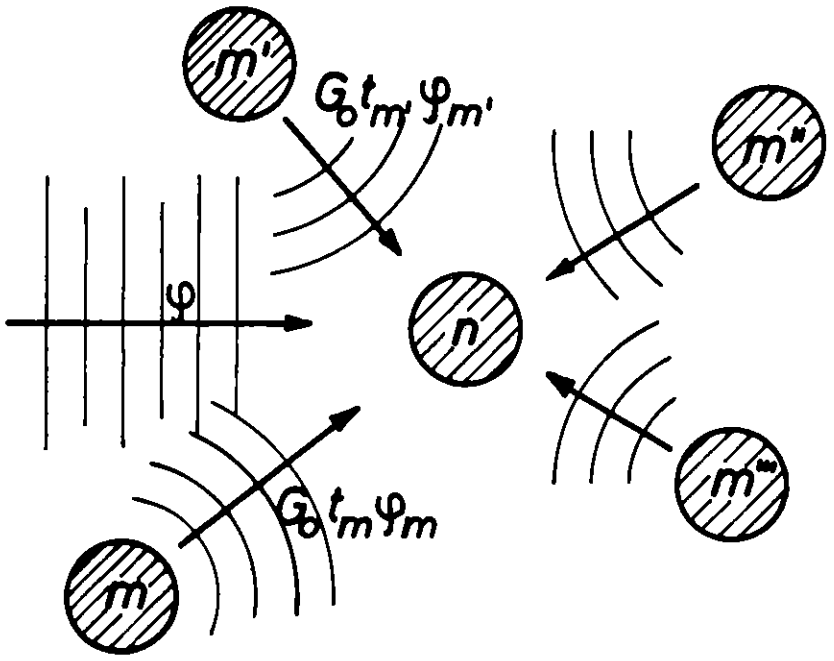

Fig. 26

Fig. 26 Contributions to the effective incident wave φ_n

Fig.27a

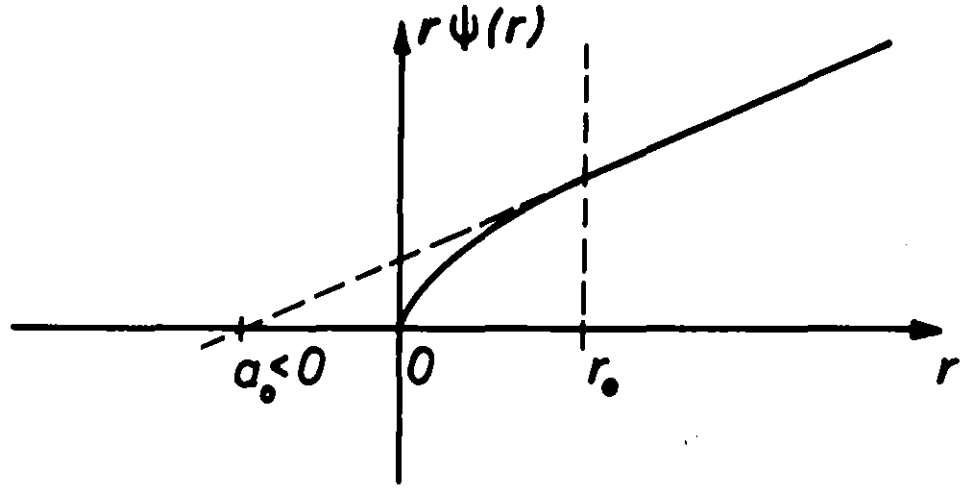

Fig.27b

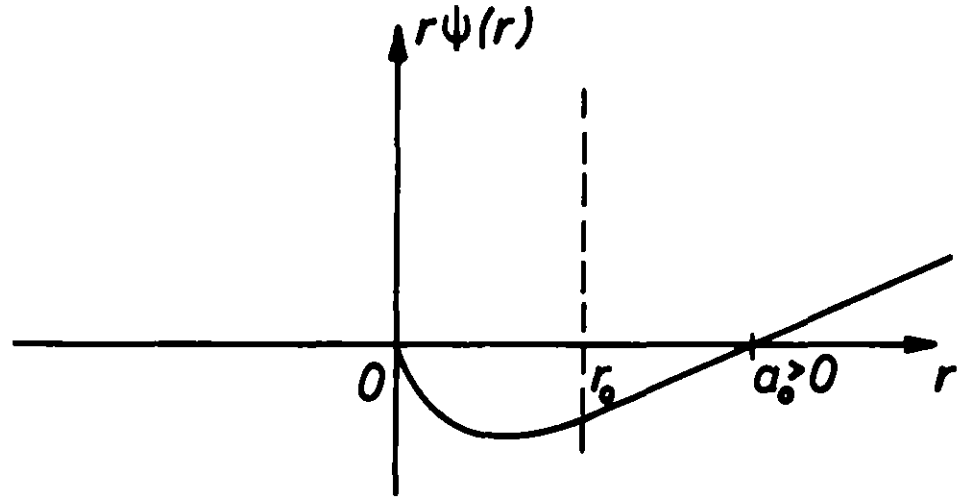

Fig.27c

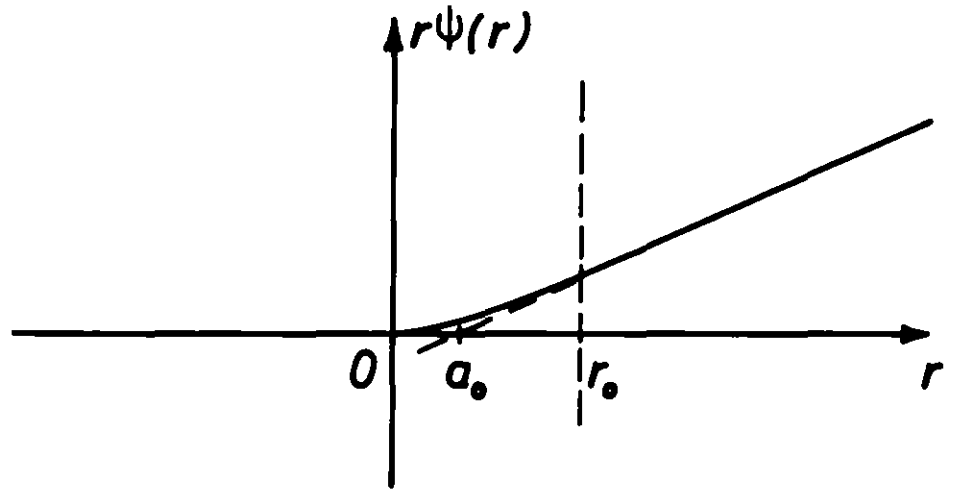

Fig. 27 Scattering length a_o
a) for an attractive potential without bound state ($a_o<o$)
b) for an attractive potential with one bound state($a_o>o$)
c) for a repulsive potential ($o \leq a_o \leq r_o$)

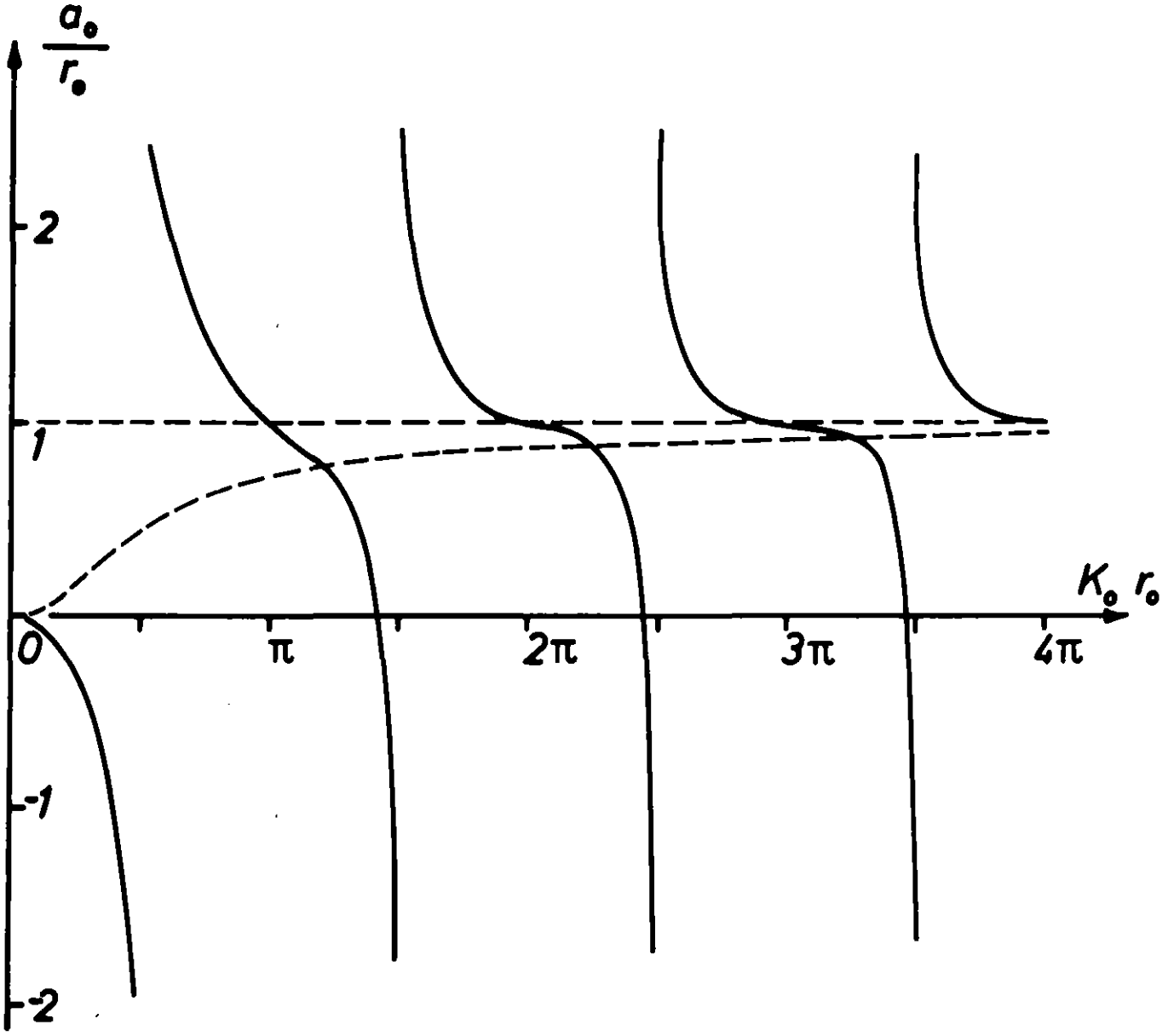

Fig. 28

Fig. 28 Scattering length a_0 for a potential well (attractive potential $-V_0 < 0$: full lines repulsive potential $-V_0 > 0$: dashed lines)

Fig. 29

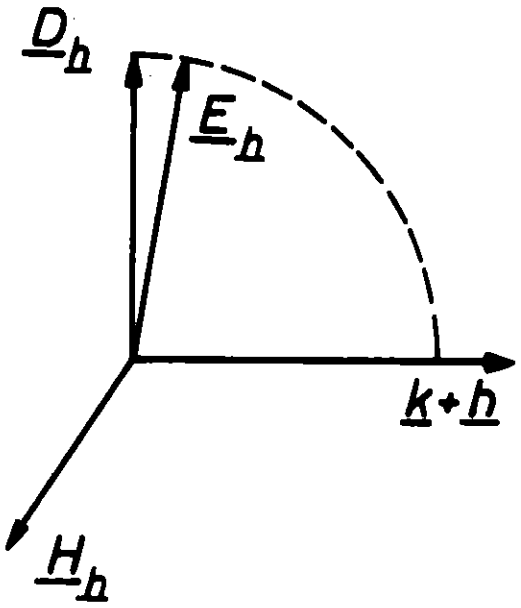

Fig. 29 Direction of the field vectors $\underline{D}_h$, $\underline{E}_h$ and $\underline{H}_h$

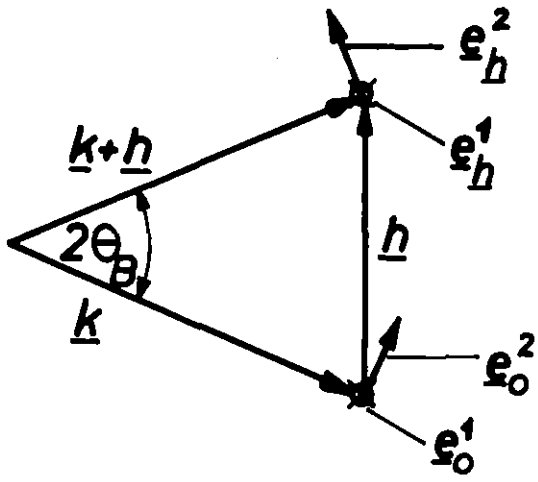

Fig.30a

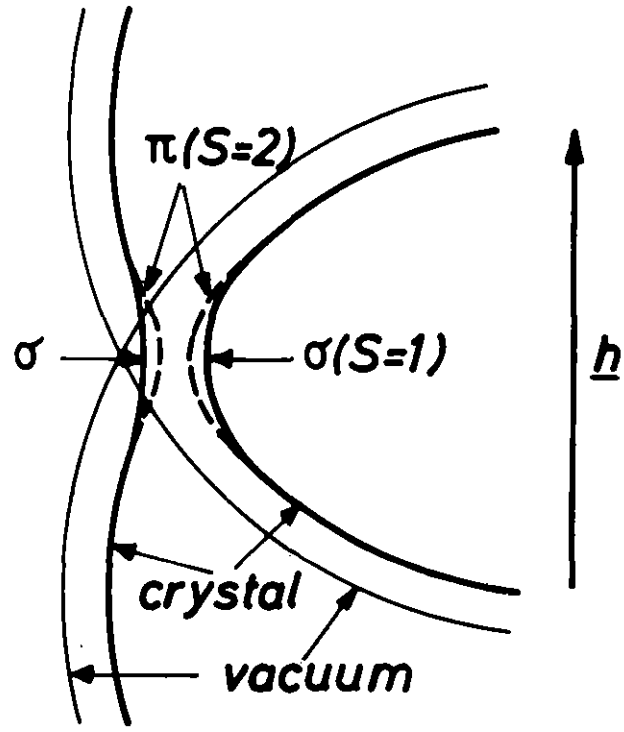

Fig.30b

Fig. 30a Direction of polarisation vectors
($\underline{e}_o^1 = \underline{e}_h^1$ are normal to the plane of drawing)

Fig. 30b Dispersion surfaces for σ and π polarisation